EVALUATION OF FATIGUE CRACKING IN I-65 MOBILE DELTA CROSSING BRIDGES

Volume I
Floorbeam-Girder Connections

by

J. Michael Stallings
Thomas E. Cousins
Richard K. Rotto
Charles B. Reid

sponsored by

The State of Alabama Highway Department
Montgomery, Alabama

February 1993

ACKNOWLEDGEMENT

The material contained herein was obtained in connection with a research project, "Evaluation of Fatigue Cracking in I-65 Mobile Delta Crossing Bridges" (ST2019-16), conducted by the Highway Research Center at Auburn University. The research project was sponsored by the State of Alabama Highway Department. The traffic control, test load vehicles, bridge inspection vehicles and operators were provided by the Alabama Highway Department's Ninth Division and Maintenance Bureau. The interest, cooperation, and assistance of many personnel from the Alabama Highway Department is gratefully acknowledged.

DISCLAIMER

TABLE OF CONTENTS

LIST OF TABLES

LIST OF FIGURES

SUMMARY

The I-65 Mobile Delta Crossing Bridges constitute a six mile section of interstate highway over the Mobile River delta plains located approximately 20 miles north of Mobile, Alabama. A major portion of the bridges are A588 weathering steel plate girder spans. The plate girder spans are a two girder system with a large number of three and four span continuous sections. The bridges were constructed in the early 1980's and were opened to traffic in 1983. Alabama Highway Department bridge inspectors discovered distortion-induced fatigue cracks at six floorbeam-girder connections at pier supports along the plate girder spans in 1990.

One objective of the project was to evaluate the stress conditions and potential for future fatigue cracking at additional floorbeam-girder connections along the bridges through field testing. Field measurements were made at floorbeam connections at pier supports and at connections for the first and second floorbeams away from the piers. All field measurements reported here were made at connections where fatigue cracks had not yet initiated. The test data indicated that two of the six connections tested at pier floorbeam locations experienced distortion-induced stress ranges large enough to cause fatigue cracking. The distortion-induced stress ranges at the other four pier floorbeam connections were very low. The results indicate that significantly different stress conditions exist at the pier floorbeam connections along the bridges. No pattern was

identified for easy identification of the locations that are most prone to have fatigue cracking in the future.

Field measurements were made at two connections at the first floorbeam away from pier supports. Both of the connections experienced stress ranges large enough to result in fatigue cracking. Measurements at two connections at the second floorbeam away from pier supports indicated that fatigue cracking is not likely to occur at that type connection.

Another objective of the project was to evaluate the performance of a positive attachment retrofit designed by the Alabama Highway Department for use in repairing floorbeam-girder connections with distortion-induced cracking. The performance was evaluated by comparing stress ranges and displacements in connections before and after the retrofit was installed. The retrofit was found to be an effective repair method. At one test location where distortion-induced stress ranges were high before the retrofit was installed, the distortion-induced stress ranges and out-of-plane displacement of the floorbeam connection plate were reduced by 70 percent.

CHAPTER ONE
INTRODUCTION

BACKGROUND

The I-65 Mobile Delta Crossing Bridges constitute a six mile section (northbound and southbound) of interstate highway over the Mobile River delta plains located approximately 20 miles north of Mobile, Alabama. The bridges consist of three basic types: precast concrete spans, steel plate girder spans, and a steel tied arch span. The bridges were constructed in the early 1980's and were opened to traffic in 1983. A traffic history (total of northbound and southbound vehicles) for the bridges is given in Table 1. Alabama Highway Department (AHD) bridge inspectors discovered fatigue cracks at six locations along the steel plate girder spans at floorbeam-girder connections in late 1990. The purpose of the project reported here was to evaluate the conditions that created the fatigue cracks through field tests of the bridges. Based on the results of the field tests, recommendations regarding repair and maintenance of the bridges are presented in this report.

BRIDGE DESCRIPTION

The steel plate girder bridges of interest span three different river channels. These are three and four span continuous sections with total lengths of 450 and 500 feet, respectively. The sections are comprised of two steel plate girders with three intermediate stringers and transverse floorbeams. All the steel in the bridges is A588 weathering steel. The top flange of the girders and stringers support

Table 1. Mobile Delta Crossing Bridges' Traffic History

Year	Average Daily Traffic	Percent Commercial Vehicles	Percent Heavy Vehicles	Number Heavy Vehicles
1991	13020	26	85	2877
1990	12220	26	85	2701
1989	11300	28	85	2689
1988	10490	30	85	2675
1987	10150	30	85	2588
1986	9940	30	85	2535
1985	8530	34	85	2465
1984	8410	34	85	2430
1983	8120	35	85	2416

the concrete deck. The stringers span continuously across the top of the transverse floorbeams which are spaced 25 feet on center. The floorbeam-girder connection is made of a vertical connection plate welded to the girder web and bolted to the floorbeam (see Figure 1). At the floorbeam to girder connection over the pier there is a web stiffener plate on the outside of the girder. Horizontal cross-bracing is provided near the girder bottom flange by T-sections arranged in a "X" configuration between floorbeams.

LOCATIONS AND EXTENT OF CRACKING

The floorbeam-girder connection plates (and stiffener on the outside face of the web) are welded to the girder web and compression flange and tight fit against the tension flange. The weld between the connection plate and girder web terminates a short distance away from the tension flange of the girder. The area between the end of the weld and the tension flange is commonly referred to as the web gap. Because the connection plate is not welded to the tension flange, the web gap is subjected to out-of-plane distortion of the girder web resulting from end rotation of the floorbeam (see Figure 2). As traffic crosses the floorbeam, the end of the floorbeam rotates causing the top of the connection plate to be pulled inward and producing the out-of-plane distortion of the web gap. Fatigue cracks were found in this type region at the end of the connection plate-web weld and along the toe of the girder web-flange weld. An elevation of the girder web at the top of the floorbeam connection plate is shown in Figure 3 to illustrate the

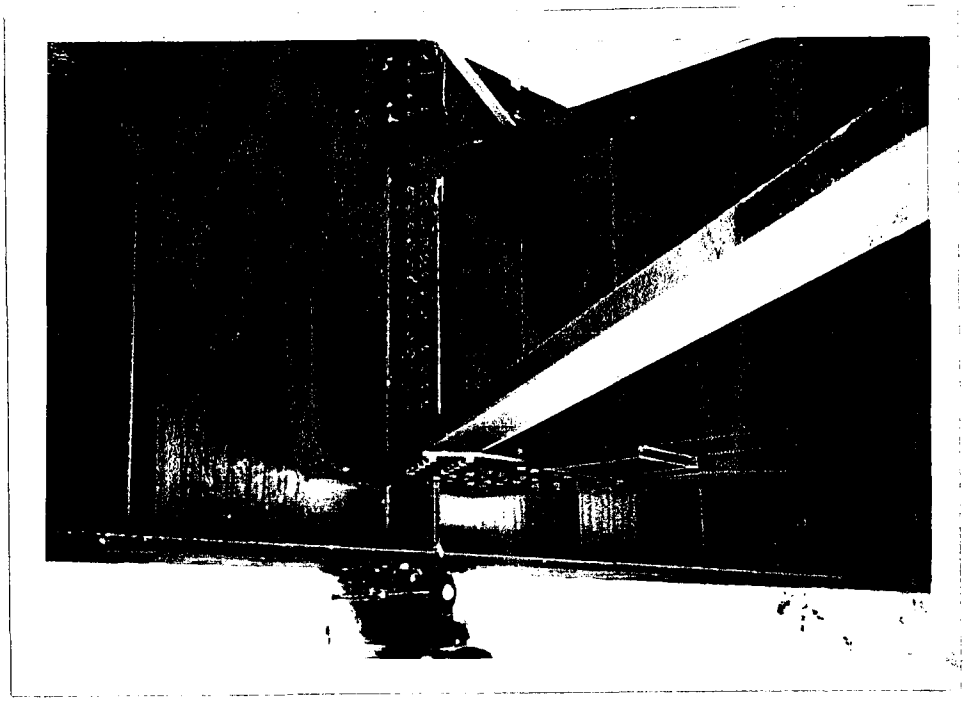

Figure 1. Floorbeam-Girder Detail at a Girder Support

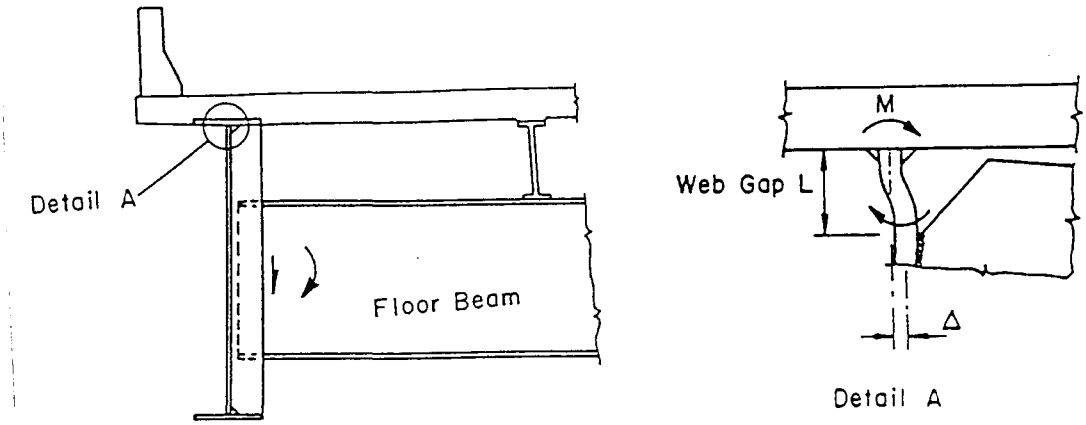

Figure 2. Illustration of Out-of-Plane Behavior in Web Gap Region (from Fisher et al. 1990)

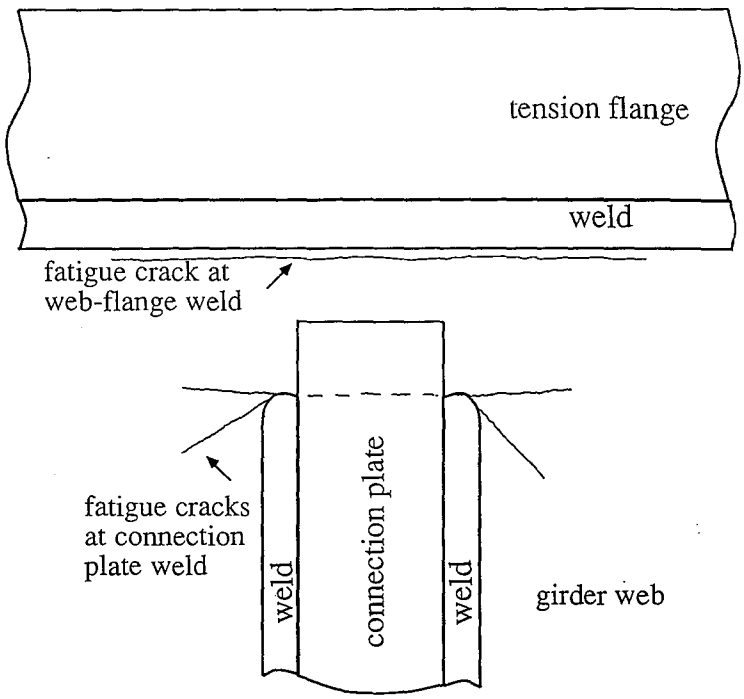

Figure 3. Typical Crack Found at Floorbeam Connection Plate Details

locations of typical cracks.

Cracking was found at a total of six connection plates. All the cracks occurred at floorbeam details over pier locations. Five of the locations with cracks were under the southbound lanes. Three of the cracks were located in the girder on the slow lane side of the bridge, the outside, while the other two occurred on the inside girder. A total of 192 locations on the bridges have this type of connection detail. There are up to four times as many (768) additional locations where distortion-induced cracking at floorbeam-girder connections may eventually occur. These locations are at floorbeam-girder connections away from the girder supports.

RIGID ATTACHMENT REPAIR

The fatigue cracks created special concern due to the fact that the main girders are fracture critical members. As a result, the AHD developed the retrofit detail shown in Figures 4 and 5 to arrest crack growth at the five cracked locations. The retrofit detail shown in Figures 4 and 5 is referred to as "rigid attachment" or "positive attachment" because the floorbeam connection plate is rigidly attached to the tension flange of the girder. The purpose of the retrofit is to reduce out-of-plane displacement at the top of the connection plate, so that the associated stresses are no longer large enough to cause cracks to form. The retrofit is being considered for possible use at all 192 similar locations at girder supports as preventative maintenance.

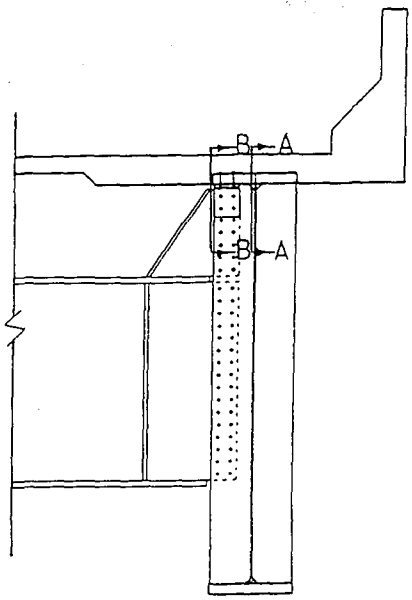

FLOORBEAM CONNECTION

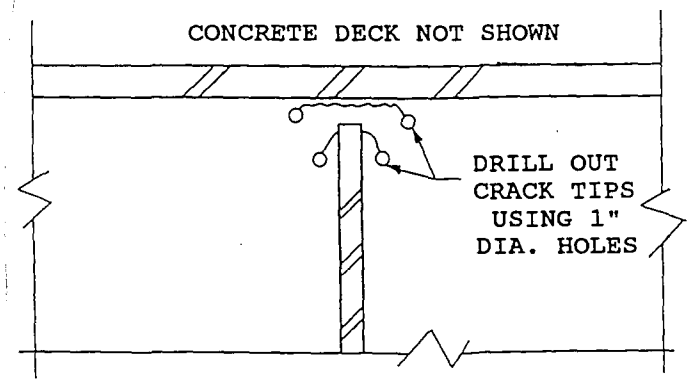

SECTION A

Figure 4. Positive Attachment Retrofit Detail

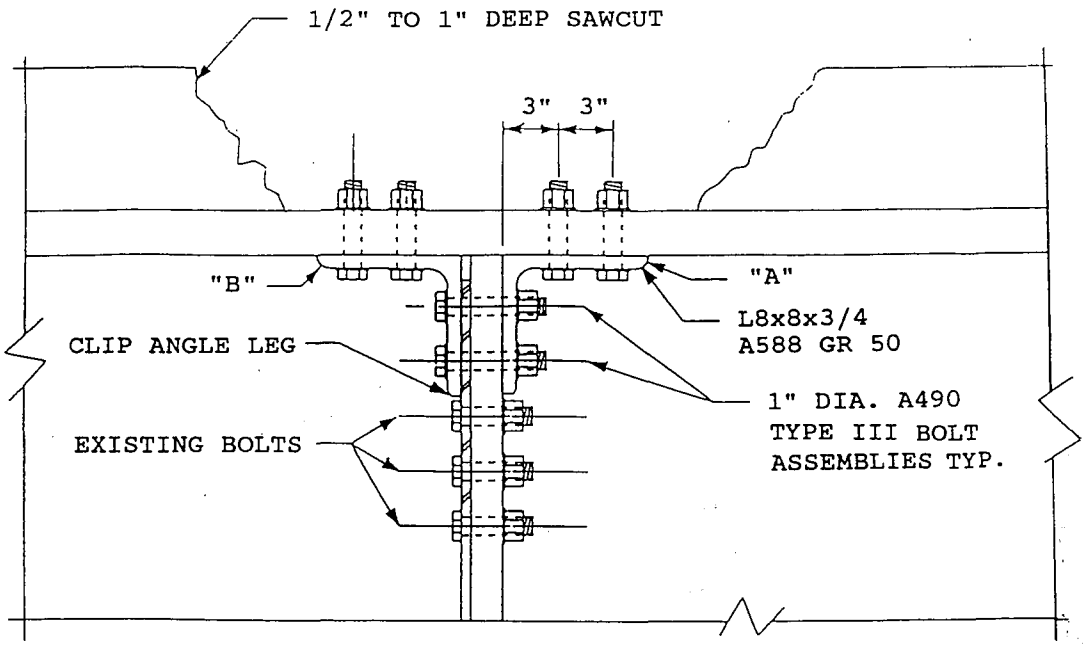

SECTION B

NOTES:
1) REMOVE CONCRETE DECK.
2) DRILL HOLES IN FLANGE FOR ANGLES "A" AND "B".
3) BOLT ANGLE "A" TO FLANGE.
4) MATCH DRILL HOLES IN CONNECTION PLATE WITH ANGLE "A".
5) BOLT ANGLE "B" TO FLANGE.
6) MATCH DRILL HOLES IN CONNECTION PLATE WITH ANGLE "B".
7) BOLT ANGLES "A" AND "B" TO CONNECTION PLATE. STOP TRAFFIC WHILE BOLTING THE ANGLES TO THE CONNECTION PLATE.
8) REPLACE CONCRETE DECK.

Figure 5. Positive Attachment Retrofit Detail (Section B from Figure 4)

PROJECT OBJECTIVES

Use of the rigid attachment retrofit at 192 locations represented a significant expense. The AHD concluded that the effectiveness of the repair needed investigation. Auburn University was contracted to evaluate the effectiveness of the retrofit through field testing. The specific objectives of the portion of AHD Research Project ST 2019-15 as reported here was to provide answers to the following questions:

1) Is the retrofit illustrated in Figures 4 and 5 an effective means of preventing initiation and propagation of out-of-plane distortion induced web cracks in the plate girder spans?
2) Are out-of-plane distortion induced fatigue cracks likely to occur in the future at floorbeam-girder connections not at supports, and will positive attachment be required to stop the propagation of such cracks?

In addition to providing answers to the above specific questions, answers to other related questions were developed from the results of the project. A recommended plan for repairing distortion induced web cracks in the bridges is presented in the final chapter of this report. The plan does not require immediate use of the rigid attachment retrofit detail at all floorbeam-girder connections.

METHODOLOGY AND SCOPE OF REPORT

The project objectives were met by use of field tests performed during the summer of 1991 and spring of 1992. Field measurements were made to determine the magnitudes of

the out-of-plane displacements and distortion-induced stresses at typical floorbeam-girder connections. Measurements were made with loading from trucks of known weight and with loading from the normal truck traffic crossing the bridges. Measurements were made at floorbeam-girder connections at the girder supports and at floorbeam locations not at a support. These measurements were compared to results of laboratory tests performed by other researchers to assess the potential for future fatigue cracking at similar connections along the bridge. Measurements were made at four floorbeam-girder connections before and after the positive attachment retrofit shown in Figures 4 and 5 was performed. These measurements provided direct comparisons for evaluating the effectiveness of the rigid attachment retrofit detail.

A review of the field and laboratory investigations by others related to out-of-plane distortion induced cracking is presented in Chapter Two of this report. Descriptions of the test locations, instrumentation, and data acquisition and reduction methods used for the I-65 bridges are described in Chapters Three, Four, and Five. The test results and analyses of the test results are given in Chapter Six, Seven, and Eight. Conclusions and Recommendations are presented in Chapter Nine.

CHAPTER TWO
LITERATURE REVIEW

FATIGUE CRACKING AT FLOORBEAM CONNECTION PLATES

Before the advent of welded bridge structures, rivets were used as the primary attachment mechanism. During that era, no evidence suggested that considerations of out-of-plane behavior was necessary in designing bridge structures. Engineers believed that designing bridge girders for the primary traffic loading in the plane of the web was reasonable and sufficient. As bridge designers began incorporating welded details, the previously used behavior models were assumed valid (Fisher et al. 1979). Because fatigue cracking is a long term process, a number of years passed before any evidence of fatigue cracking due to out-of-plane displacements was found in welded steel bridges. The magnitudes and effects of out-of-plane displacements were not discovered until the 1970's (Fisher 1978).

Out-of-plane displacements at floorbeam-girder connections create distortion-induced cyclic stresses that have caused fatigue cracks in a number of bridges. The distortion-induced stresses are secondary stresses that occur as a result of cyclic bending of transverse members such as floorbeams and diaphragms. These secondary stresses are not calculated or explicitly accounted for in the AASHTO design procedures.

The attachment of a transverse floorbeam to the girder is typically made through a connection plate which is bolted

to the floorbeam and welded to the girder web. It is common practice that the connection plate be fitted and welded to the compression flange. Prior to the late 1980's the connection plate was commonly either fitted against the tension flange or cut short leaving a gap between the end of the connection plate and tension flange. The connection plate was commonly cut short of the tension flange to alleviate the need for exact measurements on the connection plate which in turn allows for easy installation. The connection plate was generally not welded to the tension flange because the weld would reduce the fatigue strength of the girder (Lee et al. 1986). As a result of distortion-induced fatigue cracking problems, the current common design practice is to rigidly attach the connection plate to the tension flange by welding.

Fatigue cracking due to out-of-plane displacements at floorbeam connection plates have been detected in both simple and continuous span bridges as discussed by Fisher et al. (1979, 1990). In simple span bridges, this type cracking commonly occurs at the supports near the bottom (tension) flange. Distortion-induced cracks generally occur in continuous span bridges at or near the girder supports in the negative moment region near the top (tension) flange. The same type of reverse curvature distortion in the web gap region that occurs at floorbeam connection plates can be induced at diaphragm connection plates by the relative vertical deflection of parallel girders causing end rotations of the diaphragms. Laboratory tests by Fisher et al. (1978,

1990) suggest that cyclic stresses greater than 10 ksi in web gaps produce crack growth in bridge structures. Field tests reported by Fisher (1987) indicate that this magnitude of cyclic stress can be produced by out-of-plane displacements of the web gap as small as 0.001 inch.

LABORATORY TESTS

To date, only three series of full scale laboratory tests have been conducted which investigated out-of-plane displacement induced fatigue cracks and retrofit procedures. The first such laboratory tests were reported by Fisher et al. (1979). In these tests built up girders with vertical connection plates welded to the girder webs were laid horizontally on pedestals and subjected to cyclic loads causing out-of-plane displacements. Figure 6 shows a schematic of the test set up. The control parameter for this series of tests was the magnitude of the out-of-plane displacements. The variables for the tests were the number of cycles until fatigue cracks initiated and the length of the web gaps. The web gaps used for these tests were 1.25, 2.5, 5, 10, and 20 times the web thickness. The magnitude of the out-of-plane displacement was varied from 0.0005 to 0.1 inches.

The results from these tests showed that at very short gap lengths, less than 5 times the web thickness, the behavior of the gap region is difficult to predict because high shear and bending stresses are developed in the web gap. With these short gaps, very erratic behavior was observed.

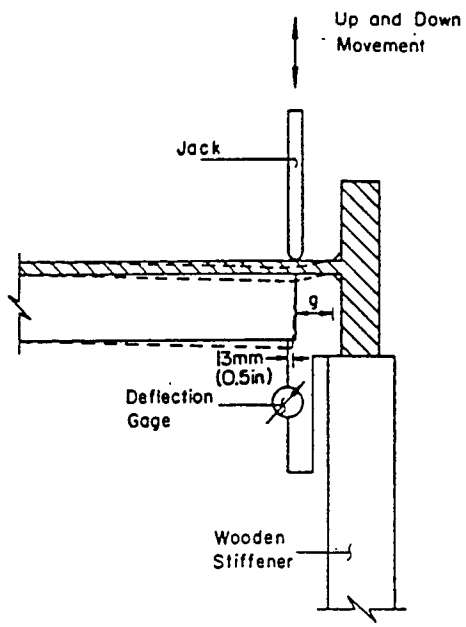

Figure 6. Out-of-Plane Bending Test Setup (from Fisher et al. 1979b)

As the gap length was increased the behavior of the web gap was more compatible with the flexural response.

The out-of-plane displacement testing was discontinued when the details experienced 10 to 20 million cycles without detectable cracks. Analysis of the test data suggests that no fatigue cracks would occur at a gap length of 5 times the web thickness or greater if the out-of-plane displacement did not exceed 0.007 inches. Likewise, the values for 10 and 20 times the web thickness were 0.003 and 0.01 inches respectively.

Once the test girders experienced cracking, 1/2 inch diameter retrofit holes were drilled at the crack tips. The retrofitted girders were then subjected to in-plane loading only. This condition simulated field conditions when cracks have developed from shipping and handling and the girders were not subjected to out-of-plane deflections. In-plane cyclic stress range at the level of the holes varied between 6.1 ksi and 14 ksi. Between 0.97 and 5.25 million cycles of stress were applied with no detectable crack growth at the retrofit holes.

One question not examined in these initial laboratory tests was the effect of continued out-of-plane displacements once cracks have been retrofitted by drilling holes at the crack tip. This question was addressed by the second and third series of laboratory tests conducted by Keating and Fisher (1987) and Fisher et al. (1990).

The tests reported by Keating and Fisher (1987) were performed on one diaphragm-girder connection. The web gap at

the end of the diaphragm connection plate was subjected to high variable amplitude distortion-induced stress ranges and in-plane bending stress ranges. A sketch of the test setup is given in Figure 7. The variable amplitude loading was applied by controlling the in-plane bending loading to produce an effective in-plane stress range at the web gap of 7 ksi. Less than 12% of the in-plane stress ranges exceeded 12 ksi. At an in-plane bending stress of 12 ksi the distortion-induced strain in the web gap before cracking occurred corresponded to a stress 20% higher than the nominal yield strength of the steel. After cracking occurred, the magnitude of the in-plane bending stress and out-of-plane distortion was kept constant during subsequent testing.

A number of fatigue cracks formed in the web gap and were repaired by using hole drilling alone. A history of the cracking is shown in Figure 8. After the hole at Stage IV was drilled, the diaphragm was removed so that the web gap was subjected only to in-plane bending. The test results indicate that at high levels of out-of-plane distortion hole drilling alone is not an effective repair.

The third laboratory investigation of distortion-inducted cracking was reported by Fisher et al. (1990). In that study, test girders were subjected to combined in-plane and out-of-plane loading. A schematic of the test set up is shown in Figure 9. In the setup the "driving" rod, connected to the transverse connection plate, induced the out-of-plane loadings and the loads "P" induced the in-plane loading. The clamped strut was attached to the girder

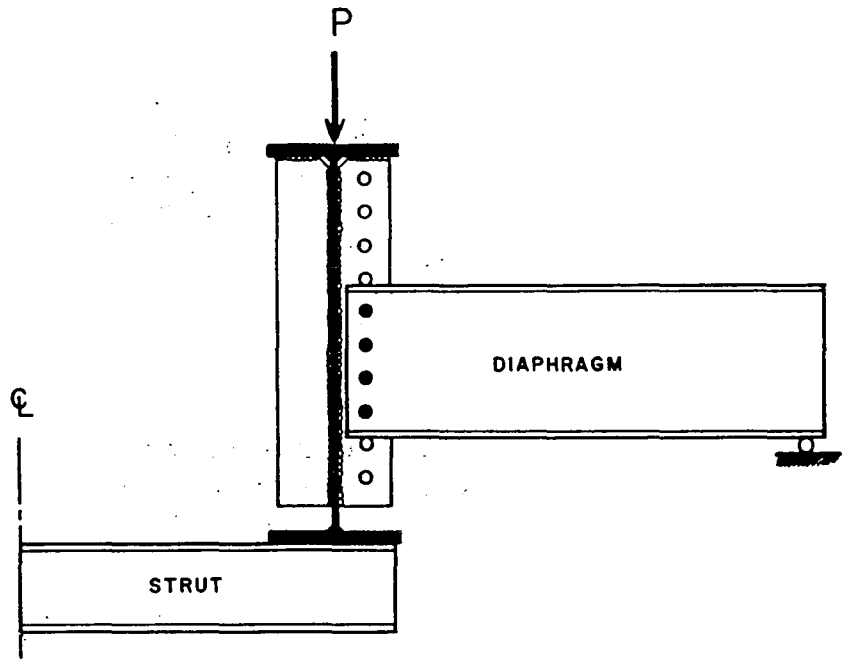

Figure 7. Test Setup for Distortion-Induced Web Gap Fatigue Cracking (from Keating and Fisher 1987)

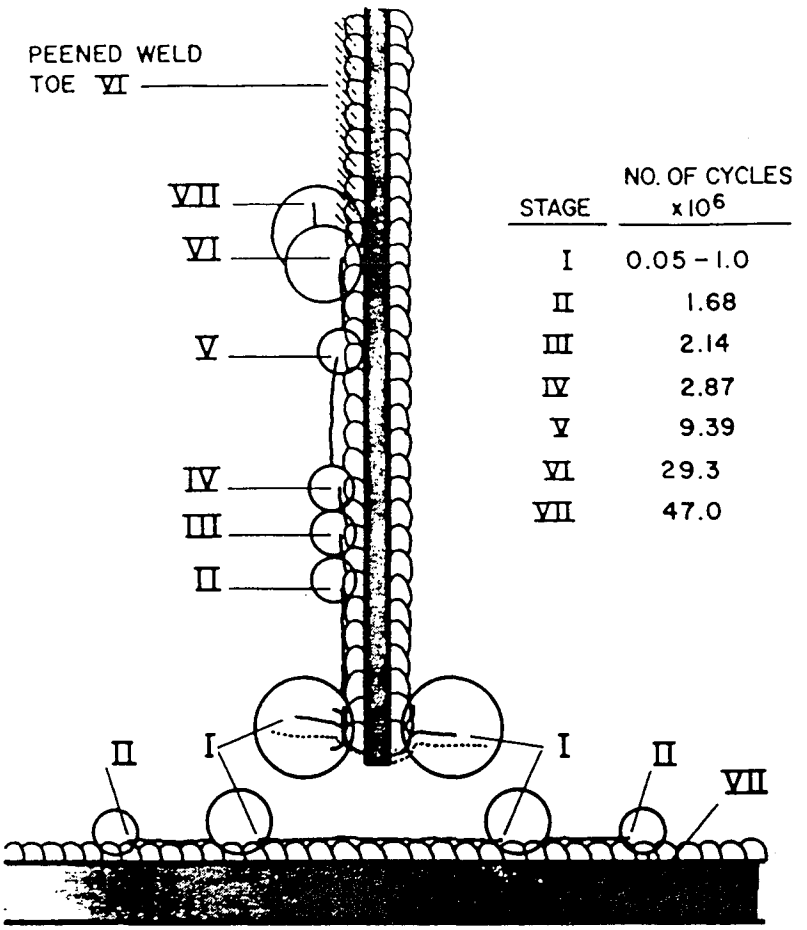

Figure 8. History of Web Gap Fatigue Cracking (from Keating and Fisher 1987)

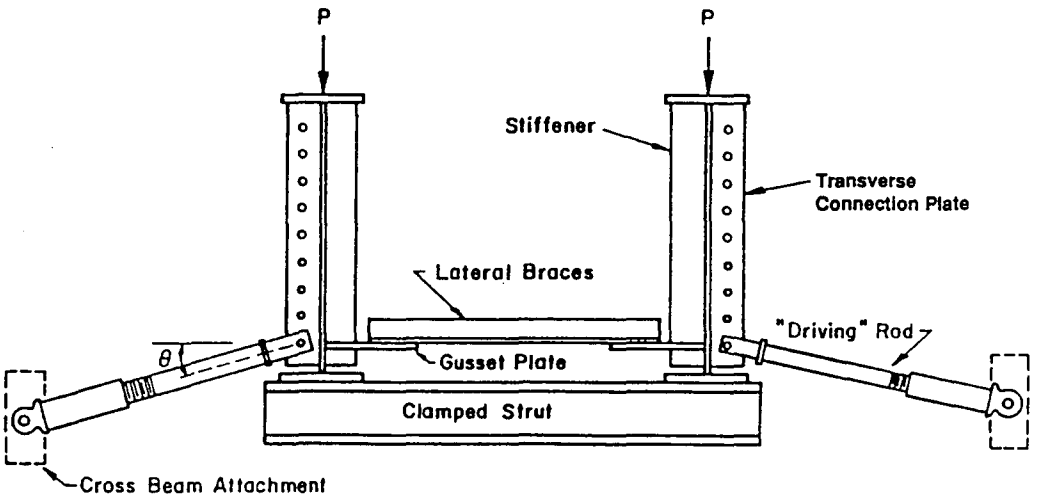

Figure 9. Out-of-Plane Bending Test Setup for Third Series of Tests (from Fisher et al. 1990)

flanges to simulate concrete deck in an actual bridge. The attachment restricted the girder flange from translation and rotation. The web gaps at the bottom of the vertical connection plates on the test girders had lengths of 1.5 and 3 inches. The web gaps of various specimens were subjected to cyclic in-plane bending stress ranges of either 6 or 12 ksi. The stress ranges from out-of-plane bending varied from 6.2 ksi to 32.5 ksi. The out-of-plane bending stress ranges were monitored by strain gages mounted at the web gaps.

Once a crack in the web gap exceeded 2 inches a retrofit procedure was performed. The retrofits were performed using one of the following three techniques: drilling holes at the crack tips, increasing the web gap length by removing part of the vertical connection plate, or providing a direct attachment between the connection plate and the girder flange. After the retrofit was completed, testing was continued to assess the effectiveness of the retrofit procedure.

Drilling holes at crack tips alone was found to be effective under certain conditions for cracks that had initiated at the end of the connection plate weld, propagated into the web, and turned perpendicular to the in-plane bending stress. Hole drilling arrested growth of this type crack when the distortion induced stress range was less than 15 ksi and the in-plane bending stress range was less than 6 ksi. The retrofit hole diameters were chosen to satisfy

$$\frac{\Delta K}{\sqrt{\rho}} < 4\sqrt{\sigma_y} \qquad [1]$$

where ρ in the hole diameter; ΔK is the stress intensity factor range; and σ_y is the yield stress in ksi. The stress intensity factor range in Equation [1], $\Delta K = S_r\sqrt{\pi a_r}$, is for the in-plane flexural stress range with a crack length a_r defined by Figure 10.

Based on the test results Fisher et al. (1990) recommended that hole drilling alone could be used to repair web gap cracks at diaphragm connections in multigirder bridges. However, it was also pointed out that past experiences indicated that hole drilling alone was not effective at floorbeam-girder connections. Hole drilling alone was not recommended at floorbeam-girder connections.

Increasing the web gap rendered the web gap zone more flexible and significantly reduced the crack growth rate. The web gap was increased by cutting away the connection plate along the connection plate-web weld toe so that only the welds and a small portion of plate segment remained. It was suggested that the web gap length be increased to 20 times the web thickness, or a minimum of 12 inches, when this retrofit option is used. In addition to increasing the gap length, drilling holes at the crack tips was suggested for best results. However, only a small number of tests were performed on this type repair, and a repair procedure was not recommended. Caution was advised because removal of an excessive amount of the connection plate could significantly increase the out-of-plane distortion.

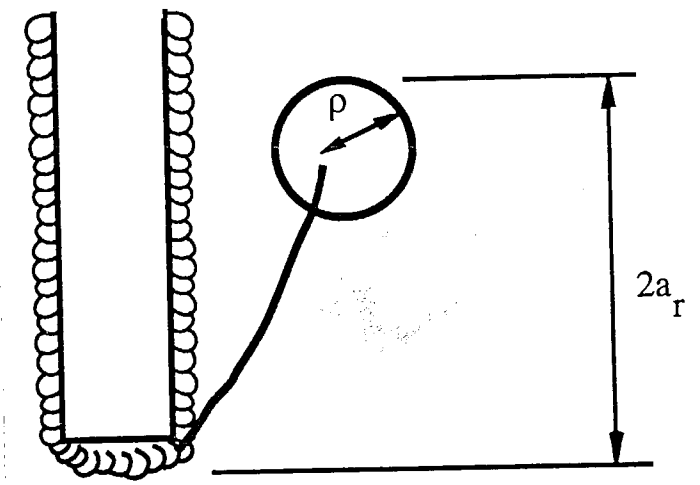

Figure 10. Defined Crack Length, a_r (from Fisher et al. 1990)

The final retrofit method, positive attachment, provided the greatest resistance to fatigue cracking due to out-of-plane displacement. The retrofit was performed without drilling holes at the crack tip. Laboratory tests indicated that for web gap stress ranges over 15 ksi, a positive attachment similar to the detail in Figures 4 and 5 reduced or arrested fatigue cracking. It was speculated that if both positive attachment and hole drilling retrofits were performed at cracked web gaps, complete arrestment of the cracks would result.

INSTRUMENTATION

Details susceptible to distortion-induced cracking have been instrumented in field and laboratory tests with strain gages for determining both primary (in-plane) and secondary (distortion-induced) stresses. Primary stresses have been measured with gages installed on flanges and webs of girders, while secondary stresses have been measured with gages located in the web gap region. The combined results were used to determine the structural behavior of the detail. The following discussion incorporates a summary of the instrumentation reported by Fisher (1978), Fisher et al. (1987), Fisher et al. (1990), and Lee et al. (1986).

In general, between 8 and 30 gages were installed to determine the primary and secondary stresses at a cross-member detail, one girder only. Fisher et al. (1990) reported instrumenting both girders of the details with 40 to 60 gages. In most cases discrete gages were used, but strip gages have also been employed.

The primary flexural behavior of the girders and cross members was determined with gages located on the flanges aligned parallel to the axis of the member. A single gage was usually placed on one or both flanges of a girder. Similarly, gages were placed on transverse members as well. For floorbeams, gages were placed on the flanges. Where truss diaphragms were instrumented, gages were placed on select web members and on the top and bottom chords as well.

Secondary stresses have been measured with a number of gages installed in the web gap region. Several arrangements have been utilized by past tests. Particular arrangements used depend on the web gap configuration. For fitted connection plate details, gages have been installed along the side of the connection plate near the tension flange. However, for details in which the web gap area was large enough gages were sometimes installed in the actual web gap.

Regardless of the location of the gages with respect to the connection plate, similar arrangements were used. Figure 11 shows typical gage arrangements employed in the web gap region. For discrete gages one to six gages were aligned vertically. For gages located alongside the connection plate, a horizontal distance of 1/2 to 1 inch separated the gages from the plate surface. The gage in an arrangement nearest to the flange usually measured 3/16 to 3/4 inches from the flange surface. When two gages were used, a distance of approximately 1/4 to 1/2 an inch separated the two locations (case a). Sometimes rather than two gages vertically aligned, a horizontal and a vertical gage would be

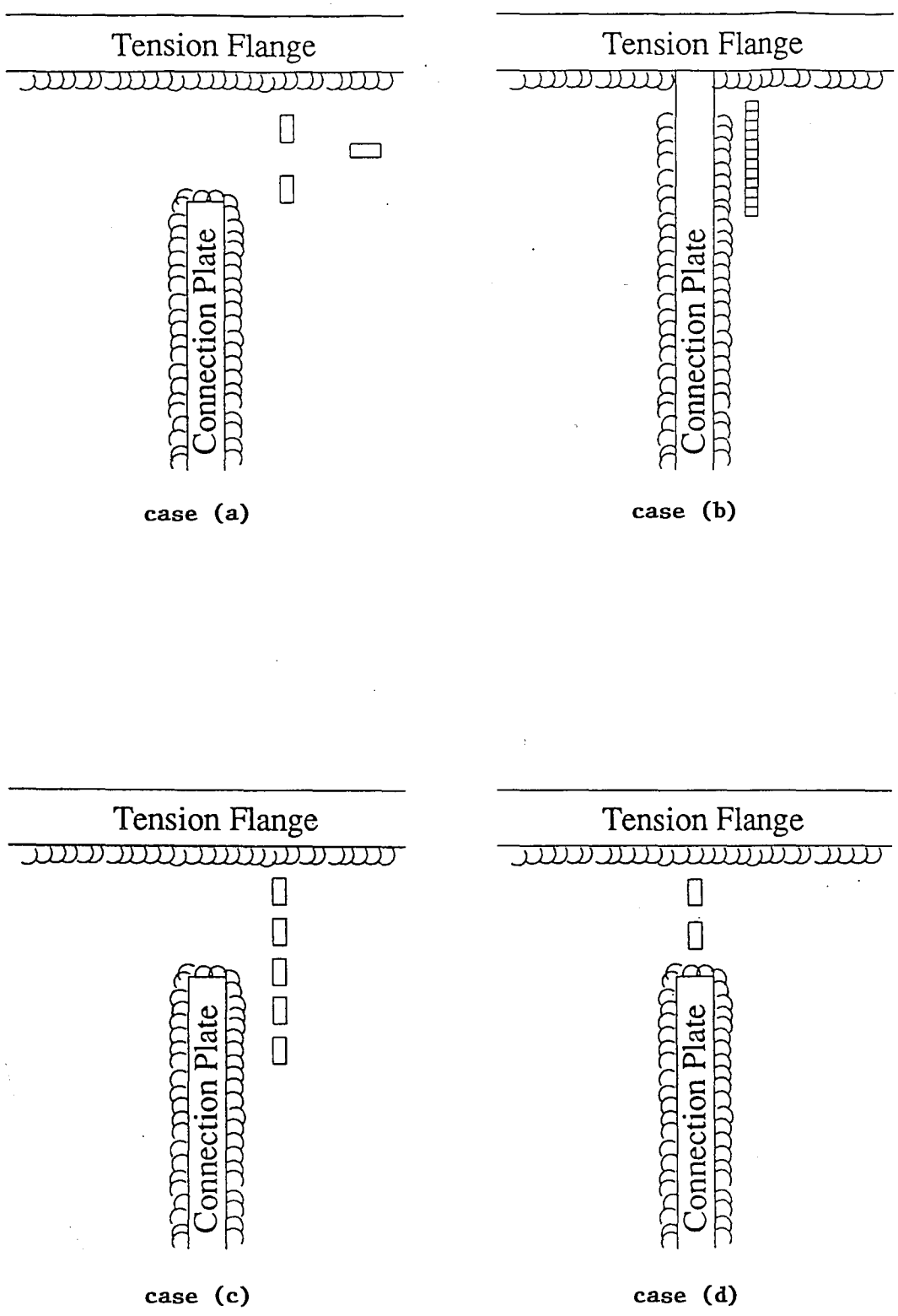

Figure 11. Typical Web Gap Region Gage Arrangements

installed. Also, instead of discrete gages, strip gages were sometimes installed (case b). In addition to the vertical arrangement of gages, horizontal gages were sometimes placed at distances between 2.5 to 5 inches off of the connection plate surface (case a).

CYCLE COUNTING METHODS

After variable amplitude data have been recorded from field tests, it is then necessary to determine the effective stress range. In some past studies, this step has been included in the recording process of the data acquisition system itself. The method chosen to determine the stress range magnitudes has been shown for general structural/mechanical cases to affect the predicted fatigue damage considerably. As a result, this topic alone has been addressed in a number of different papers from a variety of engineering disciplines. Table 2 shows a number of different cycle counting methods known to exist. Further explanation of the various methods are given by the references shown.

When selecting a method, the stress or strain versus time response must be considered. For complex responses considerable thought must be given to the restrictions of the particular counting method used. The greatest difference in the methods lies in the treatment of secondary cycles or cycles within a cycle. Several of the methods listed have been reported to be inconsistent or invalid. In particular, the histogram, zero-crossing, level-crossing count, range-mean count, and the range count method have all shown poor correlation in comparison with constant amplitude test

Table 2. Cycle Counting Methods

Counting Method Name	References
Histogram method	D
Zero-crossing peak count method	B, C
Level-crossing count method	C
Range mean count method	B, C
Mean-crossing peak count method	B, C
Power spectral density approach	E
Range count method	B, C, D
Ordered overall range method	E
Range pair method	B, C
Peak-to-peak method	B
Rainflow count method	A, B, E

A = Downing and Socie (1982)
B = Fisher et al. (1989)
C = Schijve (1963)
D = Wetzel (1971)
E = Wetzel (1977)

results, for one reason or another. In contrast, reports have shown that the ordered overall range, range-pair count, peak-to-peak, and the rainflow count methods yield reasonably consistent results.

The peak-to-peak and rainflow methods have been used most often for fatigue of highway bridges (Fisher et al. 1989). In the peak-to-peak method, one or more cycles can be counted. For only one stress cycle the range for an event is represented by the difference between the maximum and the minimum peaks. Additional stress cycles are then selected in a decreasing order of magnitude. Figure 12 shows a graphic representation of the peak to peak method for one stress cycle. In the figure, distance D-G represents the peak-to-peak stress range. The rainflow cycle counting procedure is more complex. A detailed discussion of the procedure as well as source code for the rainflow method is given by Downing and Socie (1982). Fisher et al. (1989) compared the two methods and concluded that they yield similar results for field test data. Due to its simplicity, the peak-to-peak method is more appealing for cases where the accuracy of the results are comparable to more complex methods.

EFFECTIVE STRESS RANGE

A primary goal of field tests is to determine the effective stress range (equivalent constant amplitude stress range) at a critical location where cracks have initiated, or are expected to initiate. Generally, it is not possible to place strain gages at the most critical spot because of the geometry of the critical areas. Hence, gages are placed a

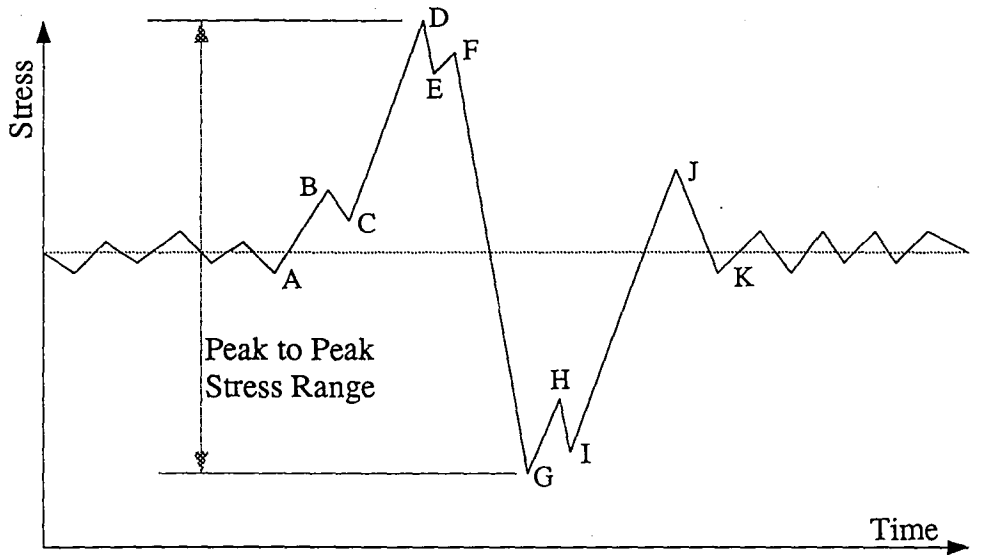

Figure 12. Illustration of Peak-to-Peak Method

short distance away from the critical locations. Stresses measured at gage locations must be extrapolated to the critical location before the effective stress range at the critical location can be determined. In most cases this has been accomplished using a linear extrapolation (Fisher 1978, Fisher et al. 1987). However, finite element analysis has also been used (Lee et al. 1986). Studies have shown that due to the steep stress gradient found in the web gap, the stresses at the weld toe can be 2 to 3 times greater than outside this area (Fisher et al. 1987).

Two different methods exist and are currently being used to determine an equivalent constant amplitude stress range from variable amplitude stress range data. These are the root-mean-square method (RMS) and Miner's effective stress range, also called the root-mean-cubed method (RMC). Both of the methods can be represented by

$$S_r = \left[\sum_{i=1}^{k} \frac{(n_i S_{ri}^b)}{N} \right]^{\frac{1}{b}} \qquad [2]$$

where k is the total number of stress ranges; i is the current stress range, n_i is number of stress cycles at the ith stress range, S_{ri}; and N is the total number of cycles. The value of b indicates which method the equation represents. For the Miner's effective stress range, b is related to the slope of a log-log plot for constant amplitude fatigue life data. For most structural details b equals 3,

therefore Miner's effective stress range uses a value of 3 for b. The root-mean-square method uses a value of 2 for b.

Both methods have shown good correlation with experimental data (Fisher 1978, Yamada and Albrecht 1976, Fisher et al. 1989). Miner's effective stress range tends to give a larger result than the root-mean-square method (Fisher et al. 1989). It is also more theoretically based (Yamada and Albrecht 1976). On the other hand, the root-mean-square method has been reported to show slightly better correlation to test data but results in a less conservative value (Fisher et al. 1989). In conclusion, both methods have been widely used. However, because the Miner's effective stress range produces a more conservative estimate than the RMS method, it is more commonly used for making bridge fatigue life estimates.

CHAPTER THREE
TEST LOCATIONS

All field tests referred to in this report were performed during the months of August and September of 1991 and March of 1992. The tests were performed on sections with plate girders and transverse floorbeams in order to determine the effectiveness of the positive attachment retrofit (Figures 4 and 5). Four separate locations along the bridges were selected for testing. The locations were identified according to the designation of the pier nearest the instrumented details. The four test locations were S7-5, S7-9, S5-2, and S7-12. For this notation, the "S" denotes southbound bridge piers. The locations of each of these test sites along the six mile elevated section are illustrated in Figure 13.

The plate girders with transverse floorbeam configurations exist in both three and four span continuous sections. Test locations S7-9 and S7-12 were located on three span continuous structures. The other two sites, S7-5 and S5-2, were located on four span continuous structures. The position of each test site along the continuous girders are illustrated in Figure 14.

Two girder depths, 84 and 96 inches, occur along the bridges considered here. The girder depth at locations S7-5 and S5-2 are 84 inches. The other two locations, S7-9 and S7-12, are 96 inch deep girders.

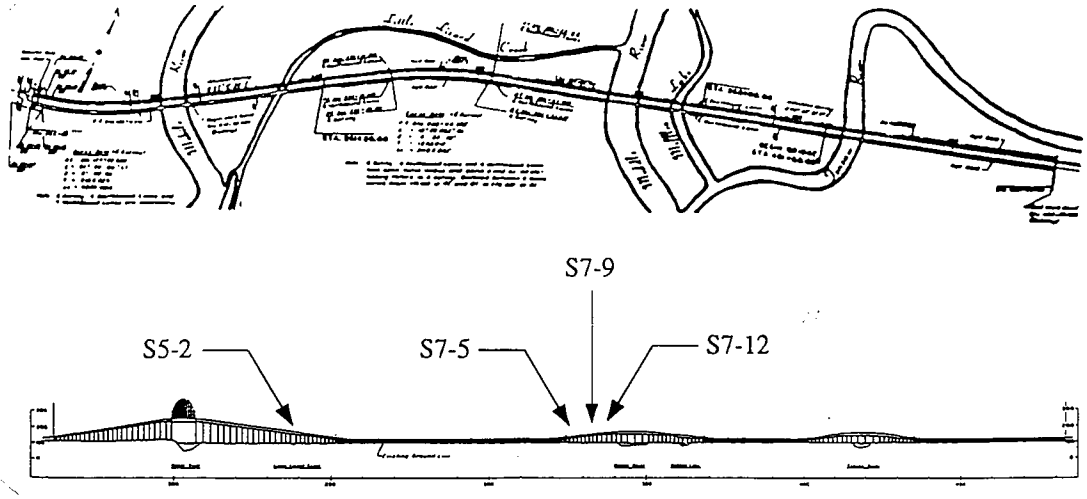

Figure 13. Four Test Locations on Mobile Delta Crossing Bridges

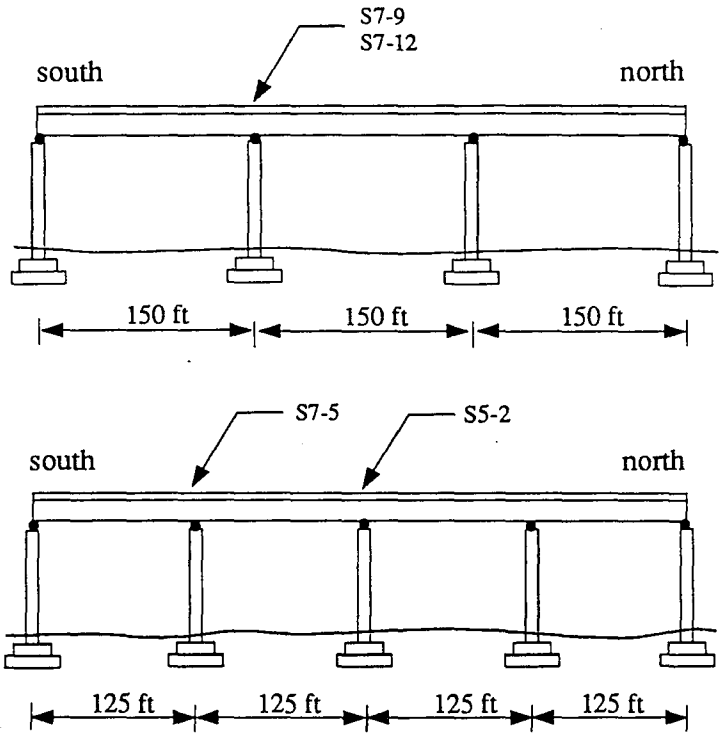

Figure 14. Position of Test Piers on the Continuous Spans

A typical cross-section illustrating the transverse floorbeam is shown in Figure 15. Figure 16 identifies the location of the web gap regions. For each girder depth, two different testing arrangements were utilized. Using the first arrangement, implemented at piers S7-5 and S7-9, measurements were made at floorbeam-girder connections at piers. Displacements and stresses were measured near the web gap detail at both ends of the floorbeam. In addition, stresses were measured at locations along the floorbeam, plate girder, and stringer flanges.

The other two locations, S5-2 and S7-12, were tested to determine if the two previously mentioned test sites were representative of all piers. A modified arrangement was employed at these locations which allowed the investigation of out-of-plane distortions at floorbeam details away from the piers. This was accomplished by instrumenting the floorbeam-girder connections at the pier and at the first and second floorbeams south of the pier. Using this second type of arrangement, measurements were made on one side (girder) of the bridge only.

Since more than one floorbeam was instrumented at sites S5-2 and S7-12, it was necessary to adopt a notation that would differentiate between the different floorbeams. The following notation was used. The floorbeam located at the pier was referred to as floorbeam number one (FB1). Similarly, floorbeam number two (FB2) referred to the first floorbeam south of the pier. And lastly, floorbeam number

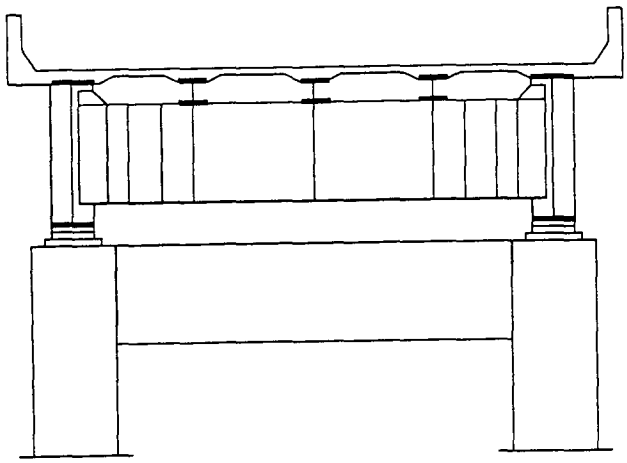

Figure 15. Cross-Section of Bridges Illustrating Transverse Floorbeam

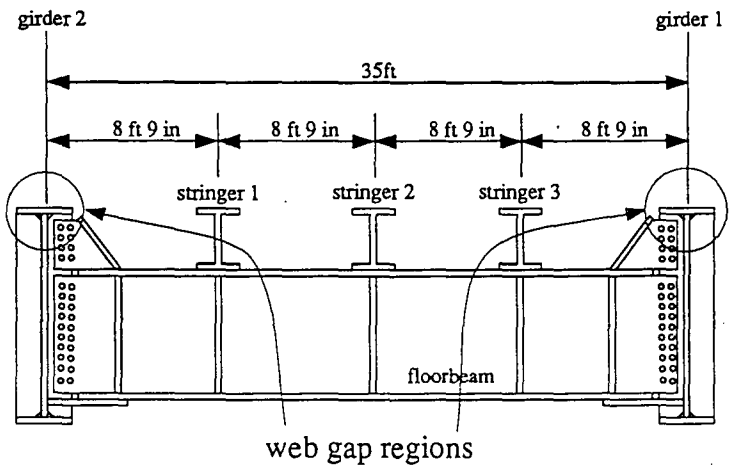

Figure 16. Location of Web Gap Regions on Cross-Section

three (FB3) represented the second floorbeam south of the pier. This notation is used throughout this report.

Field test were performed at all four locations prior to the retrofit in order to assess the stress and displacement behavior of the structures in their original state. Two of the sites, S7-5 and S7-9, were also tested after the retrofit was installed. For these two locations, the initial field tests served a dual purpose. In addition to determining the behavior of the structures in their original state, the field tests were also used to provide baseline conditions for evaluating the effectiveness of the retrofit.

Due to the nature of the construction process, the dimensions of the web gap regions at the four test locations were not identical. The web gap itself is defined as the distance from the flange surface to the toe of the connection plate welds as shown in Figure 17. This distance in particular varies substantially between gap details. The weld sizes also vary. The actual characteristics of the web gaps at the different test locations were measured in the field. The variable dimensions, defined in Figure 17, are listed in Table 3. The girder notation 1 and 2 represents the west (slow lane side) and east girders on the bridges. The dimensions of the plate girders for each test location are listed in Table 4. Listed are the dimensions of the top flange plate, the bottom flange plate, and the web plate.

Table 3. Web Gap Geometric Properties

Location	Variable Dimensions[a] (in.)					
	A	B	C	D	E	F
	(a) Girder 1, Floorbeam 1 at S7-5					
Inside[b]	1.5	1.625	1.125	0.5	1.563	0.5
Outside[c]	0.5	1.25	1.0	0.5	1.563	0.375
	(b) Girder 2, Floorbeam 1 at S7-5					
Inside	1.5	1.5	1.25	0.5	1.5	0.375
Outside	0.5	1.75	1.125	0.5	1.563	0.5
	(c) Girder 1, Floorbeam 1 at S7-9					
Inside	1.625	1.625	1.0	0.5	1.813	0.5
Outside	1.125	1.125	1.125	0.625	1.75	0.5
	(d) Girder 2, Floorbeam 1 at S7-9					
Inside	1.375	1.625	1.0	0.625	1.813	0.5
Outside	1.75	1.5	1.125	0.625	1.75	0.5
	(e) Girder 1, Floorbeam 1 at S5-2					
Inside	0.875	1.5	1.25	0.625	1.75	0.5
Outside	1.125	1.375	1.0	0.5	1.25	0.375
	(f) Girder 2, Floorbeam 1 at S5-2					
Inside	0.75	1.0	0.875	0.375	1.25	0.5
Outside	0.875	0.75	1.0	0.375	1.25	0.375
	(g) Girder 1, Floorbeam 2 at S5-2					
Inside	1.0	0.875	1.25	0.5	0.5	0.375
	(h) Girder 1, Floorbeam 3 at S5-2					
Inside	1.0	1.125	1.25	0.5	0.5	0.25
	(i) Girder 1, Floorbeam 1 at S7-12					
Inside	1.75	1.625	1.0	0.625	1.75	0.5
Outside	1.375	1.375	0.5	0.625	1.75	0.5
	(j) Girder 2, Floorbeam 1 at S7-12					
Inside	1.625	1.75	1.25	0.625	1.75	0.5
Outside	1.375	1.375	1.75	0.625	1.75	0.375
	(k) Girder 2, Floorbeam 2 at S7-12					
Inside	1.625	1.625	1.25	0.5	0.5	0.375
	(l) Girder 2, Floorbeam 3 at S7-12					
Inside	1.625	1.625	1.25	0.375	0.5	0.25

[a]Web gap variable dimensions defined in Figure 17.
[b]Inside face of girder.
[c]Outside face of girder.

Table 4. Plate Girder Dimensions

Floorbeam	Top Flange Plate	Bottom Flange Plate	Web Plate
	(a) Test Location S7-5		
FB1	2 1/4" x 20"	2 1/4" x 20"	7/16" x 84"
FB2	1 1/2" x 20"	1 1/2" x 20"	7/16" x 84"
FB3	1" x 14"	1 1/2" x 20"	3/8" x 84"
	(b) Test Location S5-2		
FB1	1 5/8" x 20"	1 5/8" x 20"	7/16" x 84"
FB2	1 5/8" x 20"	1 5/8" x 20"	7/16" x 84"
FB3	1" x 12"	1 1/8" x 20"	3/8" x 84"
	(c) Test Location S7-9		
FB1	2 1/2" x 20"	2 1/2" x 20"	7/16" x 96"
FB2	1 3/4" x 20"	1 3/4" x 20"	7/16" x 96"
FB3	1 1/8" x 20"	1 7/8" x 20"	3/8" x 96"
	(d) Test Location S7-12		
FB1	2 1/2" x 20"	2 1/2" x 20"	7/16" x 96"
FB2	1 3/4" x 20"	1 3/4" x 20"	7/16" x 96"
FB3	1 1/8" x 20"	1 7/8" x 20"	3/8" x 96"

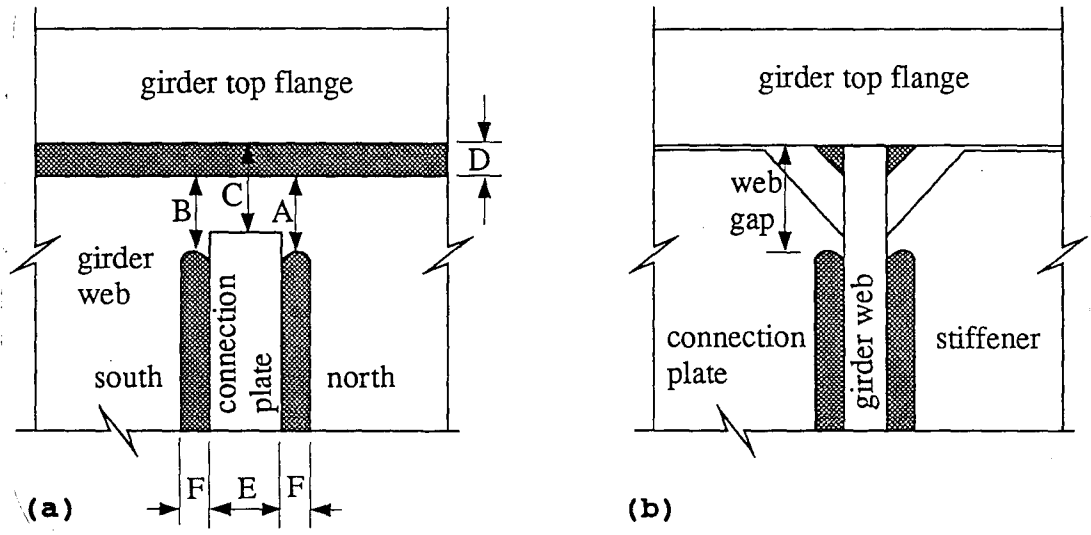

Figure 17. Typical Web Gap Region: (a) Elevation of Inside Face of Girder; (b) Section View

CHAPTER FOUR
INSTRUMENTATION AND DATA ACQUISITION

WORKING ENVIRONMENT

Due to the nature and location of the bridges, the underside of the structures were only accessible by bridge maintenance equipment operated from the bridge deck. In order to decrease the equipment usage, time, and man power, as well as increase the efficiency of preparing the test sites, work platforms were installed under the bridges by the AHD (see Figure 18). Two reusable platforms, composed of structural steel members and aluminum planks, were installed prior to the beginning of the field work at the first two test sites. The platforms were bolted around the pier cap and were to be used at all four test sites. The majority of the instrumentation and all of the data collection was conducted from these platforms. The two separate platforms provided an effective allocation of man power and eliminated down time between site relocation.

Access to and from the platforms was accomplished using two different pieces of equipment owned and operated by the AHD. One piece of equipment, shown in Figure 19, was a bucket and boom truck (Reach-All). The other was a bridge inspection platform. In addition to providing access to and from the platforms, both pieces of equipment were also used on occasion to assist in the instrumentation of areas not accessible from the platforms.

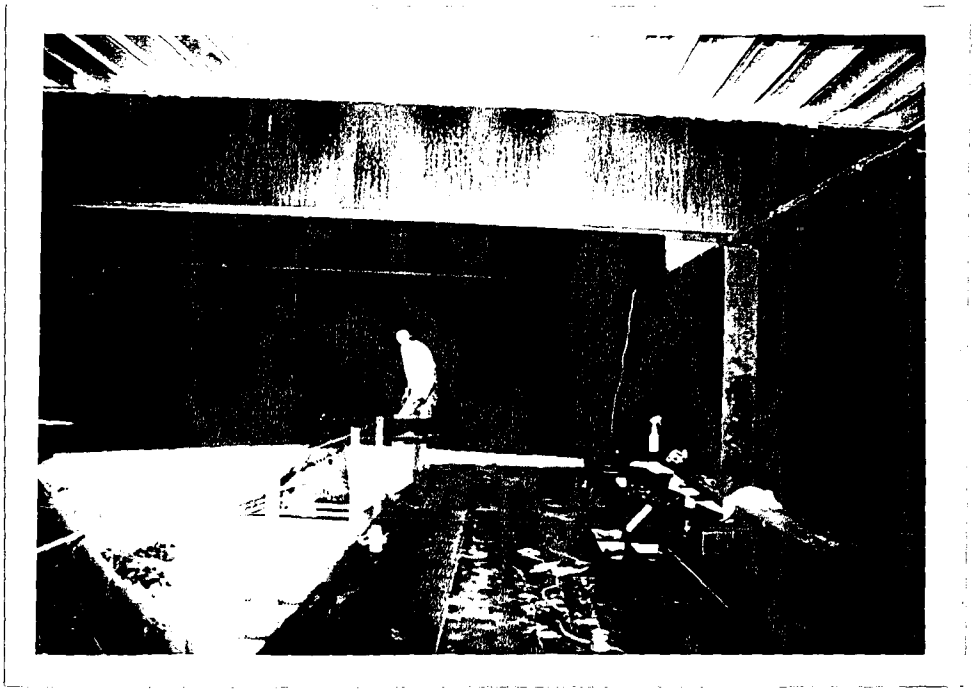

Figure 18. Work Platform

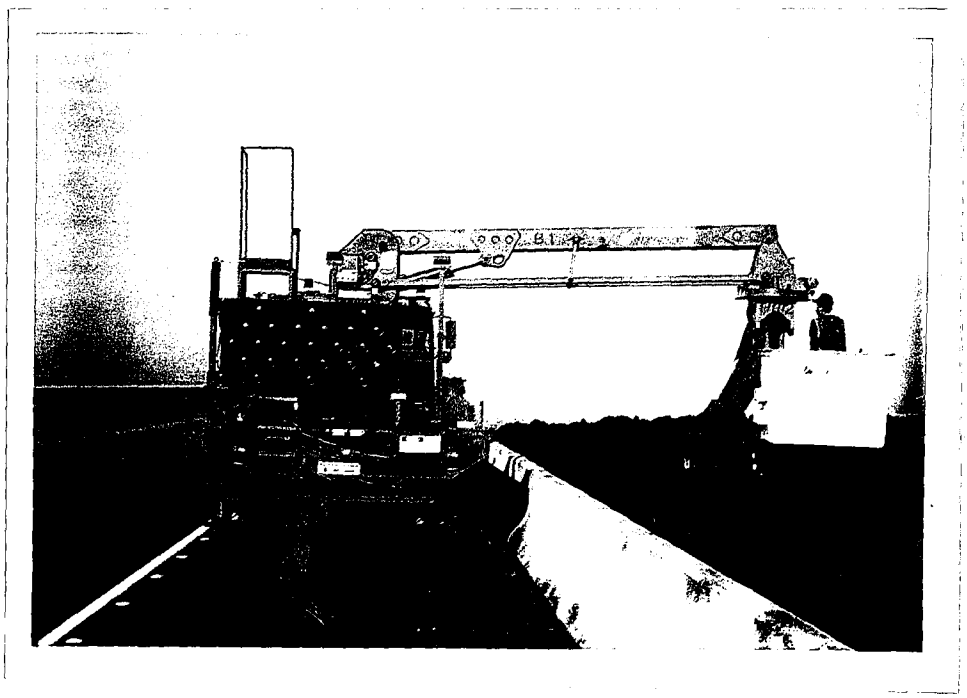

Figure 19. Reach-All Truck

INSTRUMENTATION

The typical transducers used were electrical resistance strain gages for measuring surface strains on the girders and floorbeams and linear variable differential transformers (LVDTs) for measuring the out-of-plane displacement of the floorbeam-girder connection plate. The strain gages were self temperature compensating foil gages with polyamide encapsulation and preattached leads. All the gages had a nominal resistance of 120 ohms and nominal gage factor of 2. The gages were manufactured by BLH Electronics, Inc.

The strain gages and LVDTs were all connected to the data acquisition system by shielded cable. This was done to reduce the affects of electrical noise on the data.

To expedite the connection and disconnection process as well as to enable reuse of the shielded cable, cinch connectors were installed near the gage locations using five-minute epoxy. The distance between the gages and the cinch connectors was bridged with light gage two lead stranded wire.

Roughly 40 transducers, strain gages and LVDTs, were used at each site for the initial field tests conducted before the retrofit. Four areas in the vicinity of a tested floor beam to girder connection were instrumented with strain gages: the web gap, the stringer flanges, the floorbeam flanges, and the girder flanges. Typically, gages with a 3/8 in. gage length were installed in the latter three areas, all flange locations, and gages with a 1/8 in. gage length were

installed on girder web locations. Some deviations from this pattern resulted from stock shortages causing some 1/8 in. gages to be used at flange locations.

Figure 20 shows the typical locations and the numbering scheme for gages installed in the web gap region. The numbering scheme illustrated in Figure 20 easily identifies the location of gages in the web gap; however, it alone can not differentiate between a gage on the inside of a plate girder versus a gage on the outside of a plate girder. As a result, the following notation was adopted to unmistakably identify any gage at a particular test location. An "I" in the gage name represented a gage on the inside of the plate girder. Similarly, an "O" defined a gage on the outside of the plate girder. Furthermore, an "N" within the gage name represented a gage on the northern side of the floorbeam or connection plate while an "S" represented a gage on the southern side. Lastly, the girders themselves were named. The plate girder on the west side of the bridges, or the slow lane side of the bridge, was referred to as girder one. This was noted within the gage name as the number one in parenthesis or (1). Similarly, the eastern girder was referred to as girder two (written (2)). An example of this notation would be (2)ON1. This would describe the gage in the number one position on the outside of girder two north of the connection plate.

After the field pre-retrofit tests had been completed at locations, S7-5 and S7-9, a modified version of the web gap

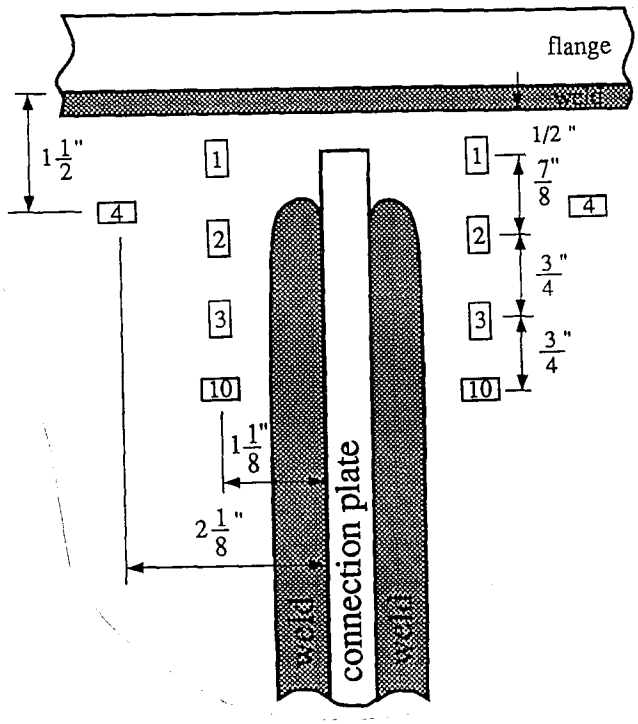

Figure 20. Numbering and Locations of Strain Gages on Girder Web

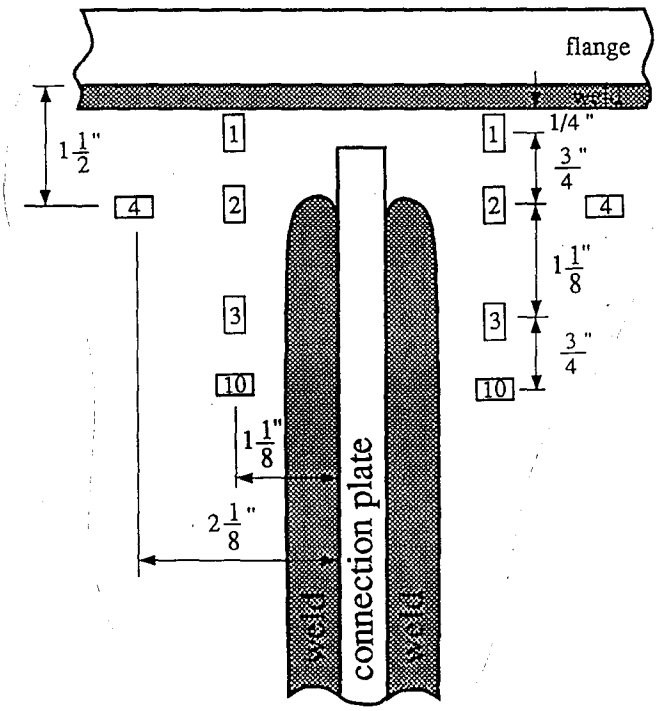

Figure 21. Numbering and Modified Locations of Strain Gages on Girder Web

gaging arrangement was introduced to be used at some connections at the remaining test locations, S5-2 and S7-12. For this modified scheme, illustrated in Figure 21, only the number one and two gages changed locations. The number one gage was moved vertically from 0.5 in. to 0.25 in. below the web-flange weld and the number two gage was placed at 0.75 in. below the number one gage. The other gages remained in their original locations.

Both the top and bottom flanges of the plate girders were instrumented in order to determine the in-plane bending strains. Typically, one 3/8 in. gage was used on each flange. The gage was centered between the web and the outer edge of the flange 18 inches from the connection plate (Figure 22). The tension and compression flange gages were identified by the numbers eight and nine, respectively.

Figure 23 illustrates the gage locations used on floorbeams. A total of six gages were typically used, three centered on the top flange and three centered between the web face and the edge on the bottom flange. These gages were designated as FB2, FB4, FB5, FB6, and FB8. In addition, Figure 23 illustrates the locations of gages on the stringers. They are denoted as S1, S2, and S3.

Tables 5 through 10 list the gages installed at each test location. In these tables, an asterisk denotes a gage in a modified position as illustrated in Figure 21.

All displacements were measured with GCD-121-250 Linear Variable Differential Transformers manufactured by Lucas

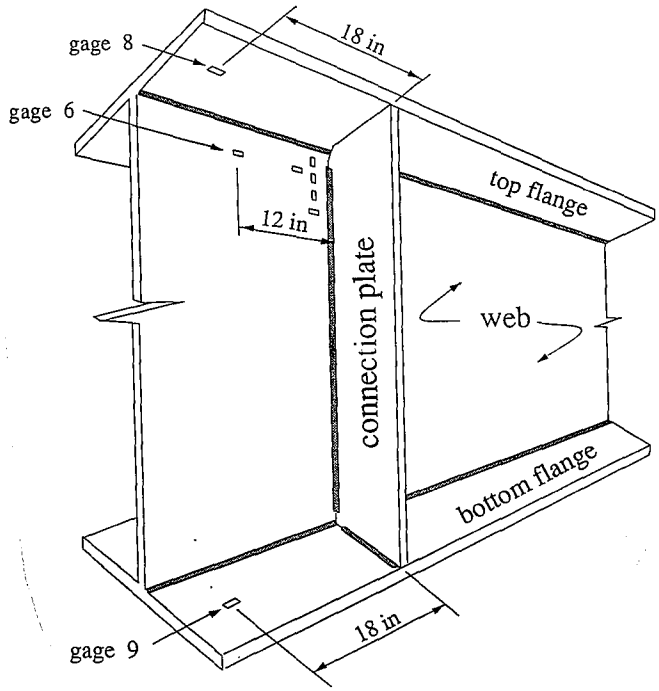

Figure 22. Numbering and Locations of In-Plane Bending Gages On Girder

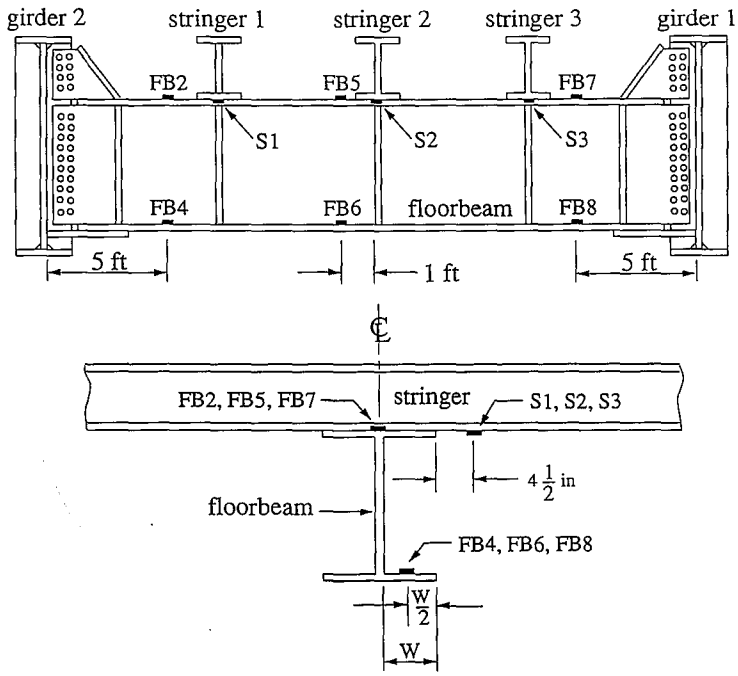

Figure 23. Numbering and Locations of Strain Gages on Floorbeam and Stringers

Table 5. Gages Installed at S7-5 Before Retrofit

Location	Gage Number[a]								
	1	2	3	4	6	8	9	10	
(a) Gages on Girder 1 at Floorbeam 1									
Inside, South	S[b]	S	S	S	S	L[c]	L		
Outside, South	S	S	S	S		L			
Inside, North	S	S		S					
Outside, North									
(b) Gages on Girder 2 at Floorbeam 1									
Inside, South	S	S	S	S	S	L	L		
Outside, South	S	S	S	S		L			
Inside, North	S	S	S	S					
Outside, North									

(c) Gages on Floorbeams and Stringers

Location	Gage Number[a]								
	FB2	FB4	FB5	FB6	FB7	FB8	S1	S2	S3
Floorbeam 1	L	L	L	L	L	L			

[a]Gage numbering defined in Figures 20 through 23.
[b]S = FAE-12-12-S6EL, 1/8 in. gage length.
[c]L = FAE-37-12-S6EL, 3/8 in. gage length.

Table 6. Gages Installed at S7-9 Before Retrofit

Location	Gage Number[a]								
	1	2	3	4	6	8	9	10	
(a) Gages on Girder 1 at Floorbeam 1									
Inside, South	S[b]	S	S	S	S	L[c]	L	S	
Outside, South	S	S	S	S					
Inside, North	S	S	S	S				S	
Outside, North									
(b) Gages on Girder 2 at Floorbeam 1									
Inside, South	S	S	S	S	S	L	L	S	
Outside, South	S	S	S	S					
Inside, North	S	S	S	S				S	
Outside, North									

(c) Gages on Floorbeams and Stringers

Location	Gage Number[a]								
	FB2	FB4	FB5	FB6	FB7	FB8	S1	S2	S3
Floorbeam 1	L	L	L	L	L	L	S	S	S

[a]Gage numbering defined in Figures 20 through 23.
[b]S = FAE-12-12-S6EL, 1/8 in. gage length.
[c]L = FAE-37-12-S6EL, 3/8 in. gage length.

Table 7. Gages Installed at S5-2

Location	Gage Number[a]								
	1	2	3	4	6	8	9	10	
(a) Gages on Girder 1 at Floorbeam 1									
Inside, South	S[b]	S		S		L[c]	L	S	
Outside, South	S	S						S	
Inside, North	S							S	
Outside, North	S								
(b) Gages on Girder 1 at Floorbeam 2									
Inside, South	S*	S*		S		L	L	S	
Outside, South	S*	S*							
Inside, North	S*							S	
Outside, North	S*								
(c) Gages on Girder 1 at Floorbeam 3									
Inside, South	T*	T*		T		L	T	T	
Outside, South	T*	T*							
Inside, North	S*							S	
Outside, North	T*								
(d) Gages on Girder 2 at Floorbeam 1									
Inside, South						L	L		
Outside, South									
Inside, North									
Outside, North									

(e) Gages on Floorbeams and Stringers

Location	Gage Number[a]								
	FB2	FB4	FB5	FB6	FB7	FB8	S1	S2	S3
Floorbeam 1					S	S	L	L	L
Floorbeam 2					S	S			
Floorbeam 3					L	L			

[a]Gage numbering defined in Figures 20 through 23.
[b]S = FAE-12-12-S6EL, 1/8 in. gage length.
[c]L = FAE-37-12-S6EL, 3/8 in. gage length.
*Gage installed in modified position.

Table 8. Gages Installed at S7-12

Location	Gage Number[a]								
	1	2	3	4	6	8	9	10	
(a) Gages on Girder 1 at Floorbeam 1									
Inside, South						S[b]	S		
Outside, South									
Inside, North									
Outside, North									
(b) Gages on Girder 2 at Floorbeam 1									
Inside, South	S	S		S		S	S	S	
Outside, South	S	S							
Inside, North	S*	S*						S	
Outside, North	S*	S*							
(c) Gages on Girder 2 at Floorbeam 2									
Inside, South	S*	S*		S		S	S	S	
Outside, South	S*	S*							
Inside, North	S*							S	
Outside, North	S*								
(d) Gages on Girder 2 at Floorbeam 3									
Inside, South	S*	S*		S		S	S	S	
Outside, South	S*	S*							
Inside, North	S*							S	
Outside, North	S*								

(e) Gages on Floorbeams and Stringers

Location	Gage Number[a]								
	FB2	FB4	FB5	FB6	FB7	FB8	S1	S2	S3
Floorbeam 1	S	S					S	S	S
Floorbeam 2	S	S							
Floorbeam 3	S	S							

[a]Gage numbering defined in Figures 20 through 23.
[b]S = FAE-12-12-S6EL, 1/8 in. gage length.
[c]L = FAE-37-12-S6EL, 3/8 in. gage length.
*Gage installed in modified position.

Table 9. Gages Installed at S7-5 After Retrofit

Location	Gage Number[a]								
	1	2	3	4	6	8	9	10	
(a) Gages on Girder 1 at Floorbeam 1									
Inside, South	S[b]	S				L[c]	L	S	
Outside, South	S								
Inside, North	S	S						S	
Outside, North	S								
(b) Gages on Girder 2 at Floorbeam 1									
Inside, South	S	S				L	L	S	
Outside, South	S								
Inside, North	S	S						S	
Outside, North	S								
(c) Gages on Floorbeams and Stringers									
Location	Gage Number[a]								
	FB2	FB4	FB5	FB6	FB7	FB8	S1	S2	S3
Floorbeam 1	L	L	L	L	L	L			

[a]Gage numbering defined in Figures 20 through 23.
[b]S = FAE-12-12-S6EL, 1/8 in. gage length.
[c]L = FAE-37-12-S6EL, 3/8 in. gage length.

Table 10. Gages Installed at S7-9 After Retrofit

Location	Gage Number[a]								
	1	2	3	4	6	8	9	10	
(a) Gages on Girder 1 at Floorbeam 1									
Inside, South	S[b]	S				L[c]	L	S	
Outside, South	S								
Inside, North	S	S						S	
Outside, North	S								
(b) Gages on Girder 2 at Floorbeam 1									
Inside, South	S	S				L	L	S	
Outside, South	S								
Inside, North	S	S						S	
Outside, North	S								

(c) Gages on Floorbeams and Stringers

Location	Gage Number[a]								
	FB2	FB4	FB5	FB6	FB7	FB8	S1	S2	S3
Floorbeam 1	L	L	L	L	L	L	S	S	S

[a]Gage numbering defined in Figures 20 through 23.
[b]S = FAE-12-12-S6EL, 1/8 in. gage length.
[c]L = FAE-37-12-S6EL, 3/8 in. gage length.

Schaevitz, Inc. The devices were roughly 7.5 inches in length and had a dynamic measurement range of approximately plus and minus 0.25 inches. The purpose of the LVDTs was to measure the out-of-plane displacement of the connection plate in the web gap region. This was accomplished by anchoring the LVDTs with aluminum angles to the stay-in-place forms used to cast the concrete deck and measuring the displacement of the connection plate at approximately half an inch below the tension flange surface. Figure 24 shows the arrangement of the apparatus at pier locations. Figures 25 and 26 show the arrangement of the LVDTs at the first (FB2) and second (FB3) floorbeams south of the pier respectively.

All strain gages were installed in the following manner. The surface was first ground with an electrical grinder. Three types of grinders were used to accomplish this. A hand held pencil bit grinder was used first. Afterwards, a disk grinder with 60 and 120 grit disks was used to smooth the surface. On occasion, a belt grinder was also used to touch up the corner of the web gap at points where the disk grinder could not reach. After the grinding was completed, the surface was hand sanded with 200 and 400 grit sand paper. Once the surface was prepared, cross hairs were marked on the surface with a ball point pen at the desired locations. The surface was then degreased and cleaned with methyl ethyl ketone (MEK) and gauze pads.

Gages were initially prepared for installment on a clean aluminum plate. After cleaning the gages with MEK, they were

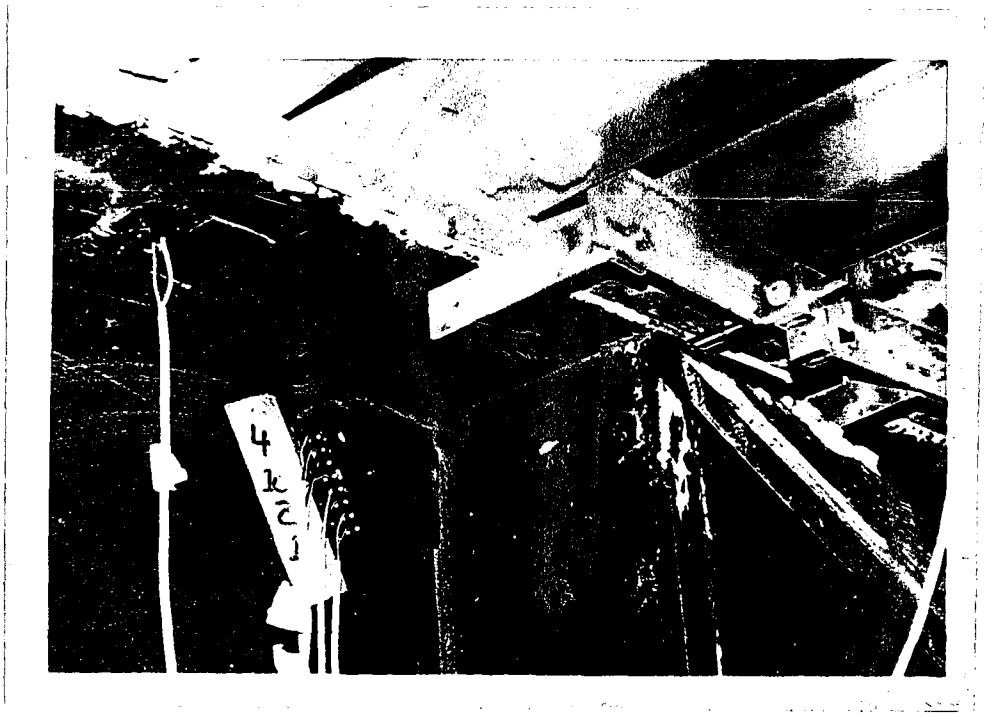

Figure 24. LVDT Arrangement at Pier Floorbeam

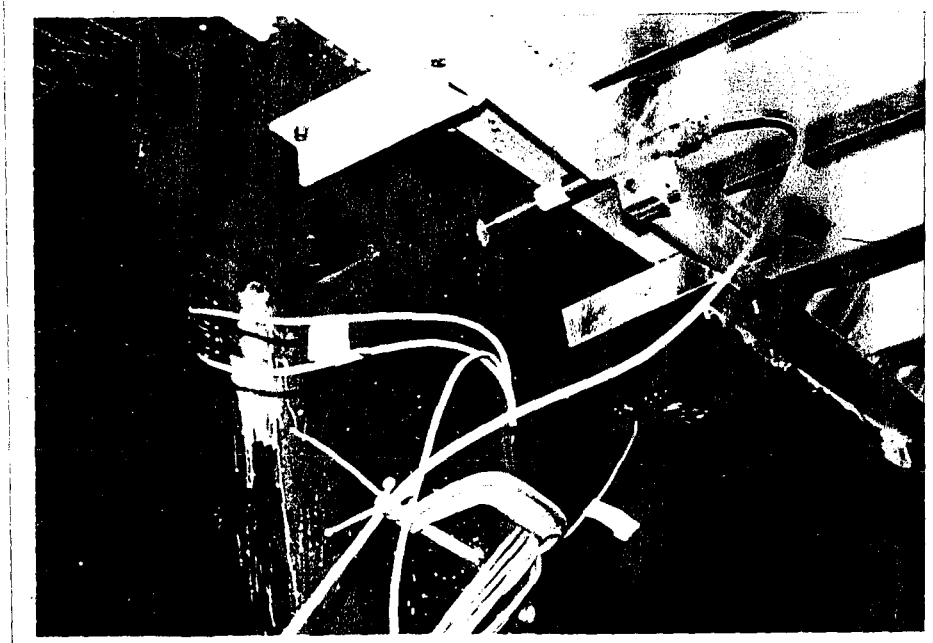

Figure 25. LVDT Arrangement at First Floorbeam South of Pier

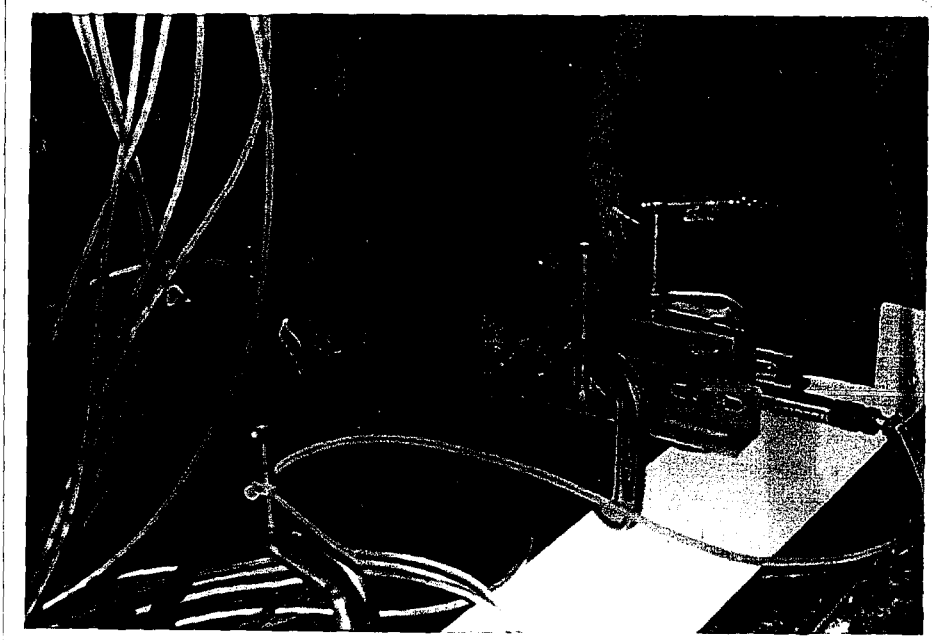

Figure 26. LVDT Arrangement at Second Floorbeam South of Pier

transferred from the aluminum plate to the appropriate mounting location using cellophane tape. By adjusting the tape, the gages were aligned with the location marks and glued to the surface using a Permabond 910 Adhesive Kit manufactured by BLH Electronics, Inc. After the glue dried, the tape was peeled off and moisture removed from the surface with freon purge. The gages were then temporarily protected with drafting tape. Afterwards, connection wires were soldered to the gage wires and then connected to the cinch connectors.

The final step of the installation process was to waterproof the gage. This was accomplished with either wax, putty, or an adhesive backed neoprene pad. Typically, the entire instrumentation process for a test location was completed within a three to four day period.

DATA ACQUISITION

All field test data was collected (during this portion of the project) with a MEGADAC 2200C dynamic data acquisition system with cassette recorder (Technical Manual 1988). The unit, manufactured by OPTIM Electronics Corporation, is capable of recording data from multiple channels at an overall rate of 20,000 samples per second. A maximum of forty-three channels were utilized in the project reported here. Forty strain gage channels were provided through five screw terminal blocks (STBs) with eight channels each. The STBs enabled easy connection and disconnection of the strain gage cables to and from the acquisition system. The LVDTs

were connected to the data acquisition system and an external power supply with special connectors developed for the project. All data was recorded and stored on DC 300A data cartridge tapes. An IBM AT personal computer equipped with a compatible software package OPUS2000 (Technical Manual 1988) was used to drive the MEGADAC. Communication between the computer and the data acquisition system was provided by RS-232 interface.

Previous field testing experience with the MEGADAC data acquisition system indicated problems were likely when recording data under humid conditions. Therefore, it was necessary that an environmental chamber be developed to protect the computer and data acquisition system from the heat and humidity common in the Mobile Delta. The resulting chamber, shown in Figure 27, provided protection against the harsh field conditions and could furthermore be broken down into three sections for easy transport under the bridge. The chamber included a 4500 BTU air conditioner to provide the environment necessary for proper operation of the equipment. The AT computer was mounted on an isolation platform which provided protection from harmful vibration.

All electrical equipment housed in the environmental chamber was powered by a portable AC generator. Figure 28 shows one of the two eight horsepower generators used on the project. Hangers were fabricated and bolted to the generator frames to enable the units to be hung over the side of the bridge during field testing. By hanging the generators over

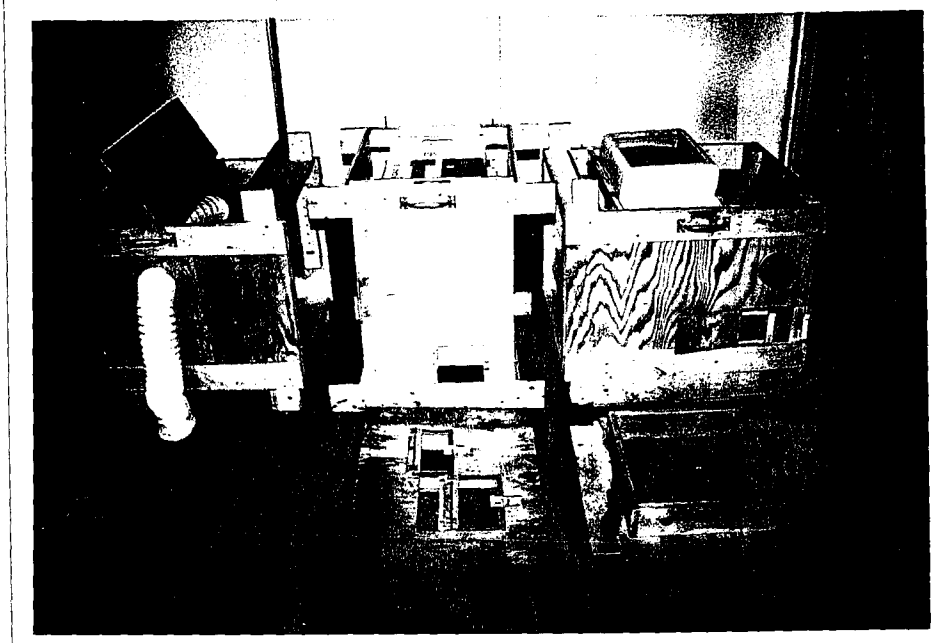

Figure 27. Environmental Chamber

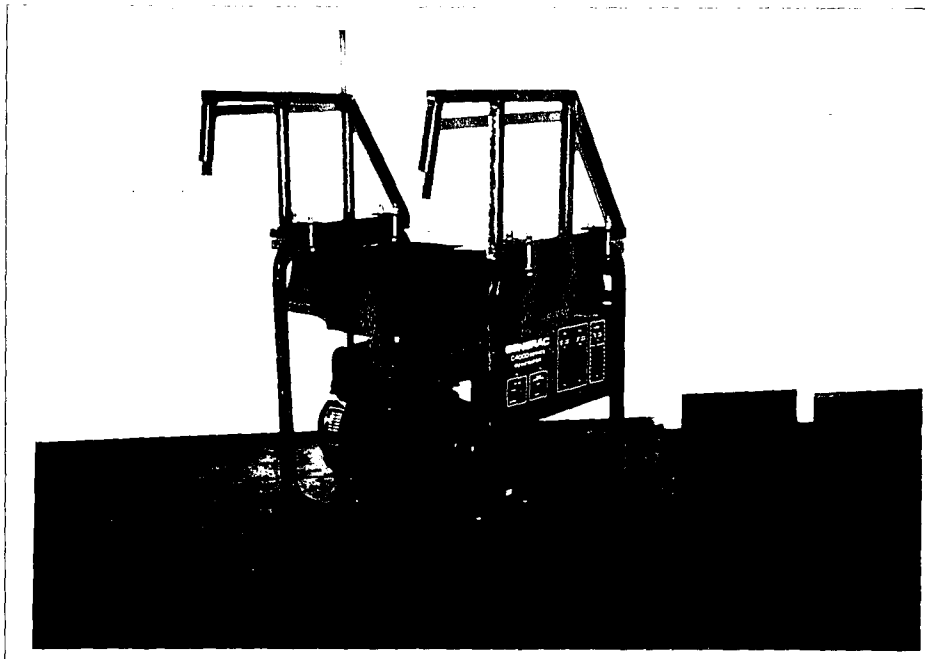

Figure 28. Generator with hangers Attached

the side of the bridge, it was possible to completely clear the bridge deck during testing so that normal traffic patterns were not affected.

CHAPTER FIVE
DATA COLLECTION AND REDUCTION

The initial field tests, conducted prior to the retrofit at all four test locations were performed during August and September of 1991. The post retrofit field tests conducted at locations S7-5 and S7-9 were performed during March of 1992. All testing conducted during these months occurred between the hours of 7:00 am and 5:00 pm Monday through Friday. Typically, the entire field test for a particular location including instrumentation was completed within two weeks. The site preparation and instrumentation for a test location usually lasted three to five days. The remaining time spent at each location was used for the data collection. The following sections discuss the different types of data collected during testing.

Once a test site was instrumented, the data acquisition system was setup on the pier platform. Afterwards, all the transducer cables were connected to the cinch connectors at the gage locations and to the STBs at the data acquisition system. Once this was accomplished, a sample run was performed. This procedure consisted of recording one or more random truck crossings selected at random from the traffic and observing the measured results of all the transducers. The main purpose of this operation was to identify defective gages and short circuits which would warrant repair. The general behavior of the structure was also assessed at this

time. Furthermore, individual gage magnitudes were recorded to help identify possible future gage malfunctions.

Each field test was performed in the following manner. First, data was collected under controlled conditions for trucks of known weights and lane positions. Tests of this type were referred to as calibration tests. Upon completion of the calibration test, data was collected under uncontrolled or random traffic conditions. This type of testing involved trucks of unknown weight traveling within the normal traffic stream. Data recorded in this manner was referred to as random truck data. The approach, methodology, and procedure for both the calibration and random tests are discussed in detail below.

CALIBRATION TESTS

The calibration tests were performed for two main reasons. First, the tests enabled the structural response of the details to be investigated under known loading conditions. And second, they provided a means for determining relationships between stress range magnitudes and truck weights for select locations.

The calibration test for each location lasted approximately three hours. Two different test trucks, one with three axles and one with five axles, were used to induce the loadings during these tests. For most cases, a dump truck and a lowboy were used as the three and five axle trucks. These two trucks, supplied by the AHD, were used for all calibrations except at S7-9 before retrofit. For this

calibration, the dump truck was not available the day of testing, and a three axle sand spreader was substituted. The axle dimensions for each truck are shown in Figure 29. Figure 29 also defines variables A through E representing the different truck axles. The test trucks were loaded and weighted on AHD scales prior to each calibration test. Tables 11 through 16 lists the axle weights of each truck for the various calibration tests.

In order to compare the strains and displacements between girders one and two, symmetrical loading conditions were necessary. However, the existing traffic lanes on the bridges (two traffic lanes and one emergency lane) were not symmetrical. An additional fictitious lane was used for the calibration tests that was symmetrical to the inside lane, the fast lane. Figure 30 illustrates the three different lane positions utilized. The three lanes were called lanes A, B, and C. The fictitious lane was referred to as lane A. Lane B was the outside or slow lane, and, lane C was the inside or fast lane. All of the lanes were physically identified on the deck with spray paint. Dashed lines, running the length of the span, located the wheel positions for the three lanes. The test trucks were driven with either the left wheels centered over the line for lane C, or the right wheels centered over the line for lane A and the line for lane B.

During the calibration tests, traffic control was provided by the AHD. At least one lane remained open to

Table 11. Calibration Truck Weights for S7-5 Before Retrofit

Truck[a]	Side[b]	Axle A (lbs)	Axle B (lbs)	Axle C (lbs)	Axle D (lbs)	Axle E (lbs)	Total (lbs)	Legal (lbs)
D.T.	L	4,800	10,200	10,200	----	----		
	R	4,900	10,800	10,500	----	----	51,400	60,000
L.B.	L	4,900	8,300	8,100	8,900	8,600		
	R	5,400	9,200	8,900	9,700	9,600	81,600	80,000

[a]D.T. = Dump Truck; L.B. = Lowboy.
[b]L = Left (drivers) side; R = Right side.

Table 12. Calibration Truck Weights for S7-9 Before Retrofit

Truck[a]	Side[b]	Axle A (lbs)	Axle B (lbs)	Axle C (lbs)	Axle D (lbs)	Axle E (lbs)	Total (lbs)	Legal (lbs)
D.T.	L	4,900	7,900	7,800	----	----		
	R	4,800	8,700	8,300	----	----	42,400	60,000
L.B.	L	4,800	8,000	7,600	9,300	9,300		
	R	5,000	9,300	9,100	9,900	9,600	81,900	80,000

[a]D.T. = Dump Truck; L.B. = Lowboy.
[b]L = Left (drivers) side; R = Right side.

Table 13. Calibration Truck Weights for S5-2 Before Retrofit

Truck[a]	Side[b]	Axle A (lbs)	Axle B (lbs)	Axle C (lbs)	Axle D (lbs)	Axle E (lbs)	Total (lbs)	Legal (lbs)
D.T.	L	4,700	9,800	10,200	----	----		
	R	5,300	11,100	11,400	----	----	52,500	60,000
L.B.	L	4,800	7,600	7,100	8,800	8,800		
	R	4,000	8,600	8,800	9,600	10,600	78,700	80,000

[a]D.T. = Dump Truck; L.B. = Lowboy.
[b]L = Left (drivers) side; R = Right side.

Table 14. Calibration Truck Weights for S7-12 Before Retrofit

Truck[a]	Side[b]	Axle A (lbs)	Axle B (lbs)	Axle C (lbs)	Axle D (lbs)	Axle E (lbs)	Total (lbs)	Legal (lbs)
D.T.	L	5,900	10,200	9,900	----	----		
	R	5,600	9,500	9,300	----	----	50,400	60,000
L.B.	L	4,900	9,400	9,200	9,700	9,700		
	R	4,100	7,400	6,700	9,000	8,500	77,600	80,000

[a]D.T. = Dump Truck; L.B. = Lowboy.
[b]L = Left (drivers) side; R = Right side.

Table 15. Calibration Truck Weights for S7-5 After Retrofit

Truck[a]	Side[b]	Axle A (lbs)	Axle B (lbs)	Axle C (lbs)	Axle D (lbs)	Axle E (lbs)	Total (lbs)	Legal (lbs)
D.T.	L	5,100	10,300	9,500	----	----		
	R	5,500	9,900	10,300	----	----	50,600	60,000
L.B.	L	4,900	8,300	8,500	8,800	9,100		
	R	5,100	8,900	8,500	8,800	9,200	80,100	80,000

[a]D.T. = Dump Truck; L.B. = Lowboy.
[b]L = Left (drivers) side; R = Right side.

Table 16. Calibration Truck Weights for S7-9 After Retrofit

Truck[a]	Side[b]	Axle A (lbs)	Axle B (lbs)	Axle C (lbs)	Axle D (lbs)	Axle E (lbs)	Total (lbs)	Legal (lbs)
D.T.	L	5,100	10,300	9,500	----	----		
	R	5,500	9,900	10,300	----	----	50,600	60,000
L.B.	L	4,900	8,300	8,500	8,800	9,100		
	R	5,100	8,900	8,500	8,800	9,200	80,100	80,000

[a]D.T. = Dump Truck; L.B. = Lowboy.
[b]L = Left (drivers) side; R = Right side.

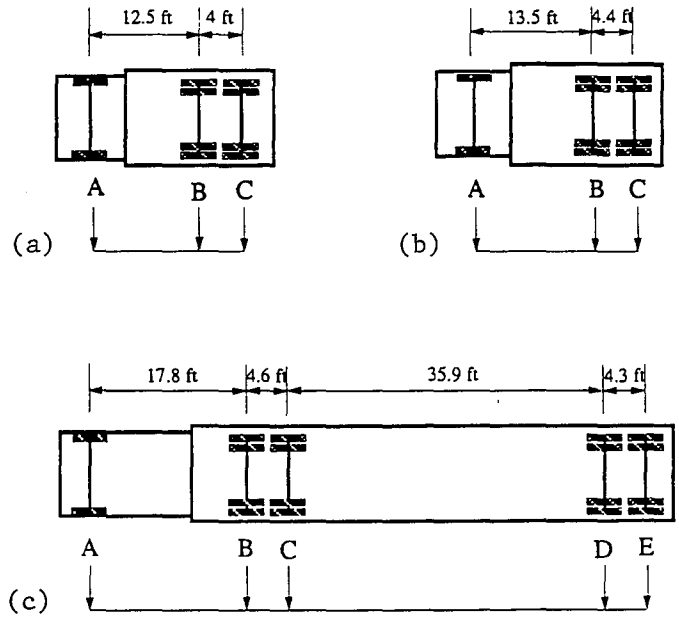

Figure 29. Trucks Used for Calibration Tests: (a) Dump Truck; (b) Sand Spreader; (c) Lowboy

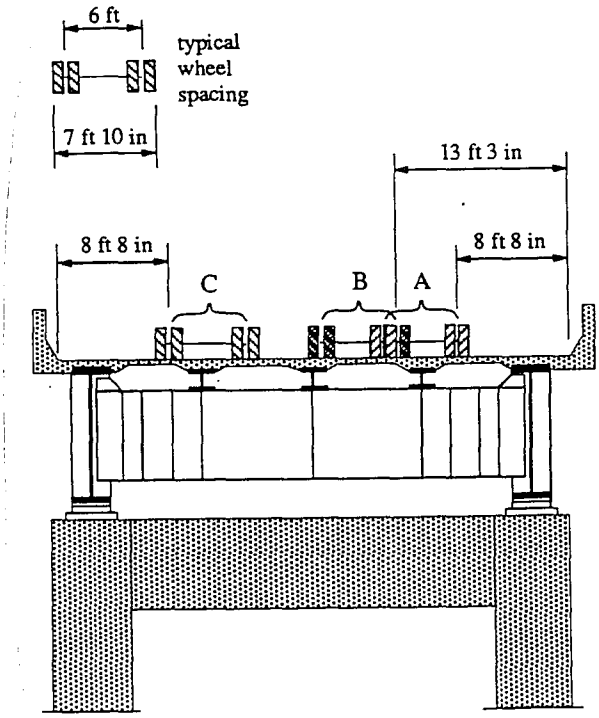

Figure 30. Test Lanes A, B, and C used for Calibration Tests

traffic at all times. Table 17 shows a typical sequence of events for a calibration test.

Four basic operations were performed during the calibration tests. These included balance intervals, static tests, crawl runs, and fast runs. The first type of data, balance data, consisted of recording measurements over a short duration of time (2 seconds) with no vehicular activity on the continuous span. The purpose here was to establish the zero live load state. The second type of operation was the static test. This test consisted of parking the test truck over the floorbeams as shown in Figures 31 and 32 and recording data for a short time (2 seconds) while no vehicular traffic was on the continuous span. The positioning of the five axle truck was accomplished by aligning the rear axle of the front tandem over the floorbeam. For the three axle trucks the front axle of the rear tandem was aligned over the floorbeam. Static tests were performed in each of the three test lanes.

The purpose of the crawl and fast runs was to determine the response at the test locations under dynamic loading. A comparison of the two tests enabled assessment of the impact effects. Crawl runs were made in each of the three test lanes. During the crawl runs, a 15 mph speed was maintained by the trucks over the length of the continuous span. Slower speeds were desirable, but not possible because of the relatively long period of time required for the calibration truck to cross the span. Since one lane was

Table 17. Typical Event Sequence for Calibration Tests

Event	Truck	Lane	Traffic Control
Balance	------	-	Lane C Open
Crawl	Dump Truck	A	Lane C Open
Static	Dump Truck	A	Lane C Open
Crawl	Dump Truck	B	Lane C Open
Static	Dump Truck	B	Lane C Open
Balance	------	-	Lane C Open
Crawl	Lowboy	A	Lane C Open
Static	Lowboy	A	Lane C Open
Crawl	Lowboy	B	Lane C Open
Static	Lowboy	B	Lane C Open
Balance	------	-	Lane C Open
Balance	------	-	Lane B Open
Crawl	Dump Truck	C	Lane B Open
Static	Dump Truck	C	Lane B Open
Balance	------	-	Lane B Open
Crawl	Lowboy	C	Lane B Open
Static	Lowboy	C	Lane B Open
Balance	------	-	Lane B Open
Fast Run	Dump Truck	B	No Traffic Control
Fast Run	Lowboy	B	No Traffic Control
Fast Run	Dump Truck	B	No Traffic Control
Fast Run	Lowboy	B	No Traffic Control
Fast Run	Dump Truck	C	No Traffic Control
Fast Run	Lowboy	C	No Traffic Control
Fast Run	Dump Truck	C	No Traffic Control
Fast Run	Lowboy	C	No Traffic Control

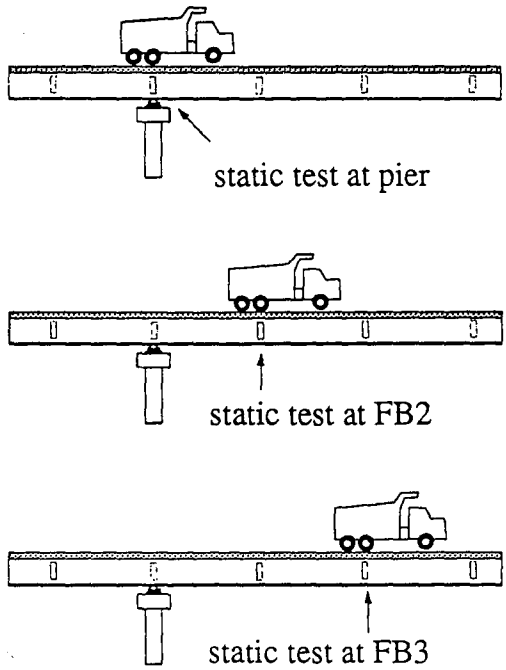

Figure 31. Dump Truck Positions Over Floorbeams During Static Tests

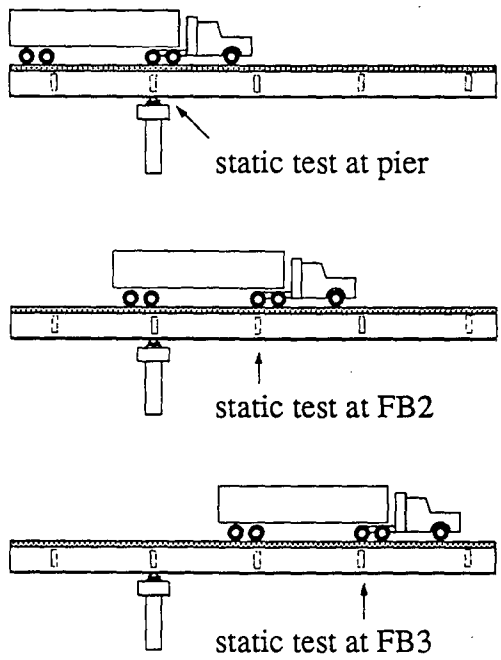

Figure 32. Lowboy Positions Over Floorbeams During Static Tests

open to traffic at all times, it was not possible to find long time periods when other vehicles would not cross the span with the test truck. For fast runs, the trucks were driven at normal traffic speeds, usually between 55 and 70 miles per hour. Each truck made two or three fast runs in lanes B and C. Fast runs were not made in lane A because of safety considerations.

RANDOM TRUCK TESTS

The calibration tests provided data for known truck weights and positions. It was also important to study the behavior of the connection plate details under normal traffic loading. This required the determination of effective constant amplitude stress ranges at the critical locations. To determine these accurately, data for a large number of truck passes was required. Initial plans for the project called for recording 1000 random trucks at each test location. However, due to time restrictions, this number was decreased. The number of random truck crossings that were recorded at the four test sites are given in Table 18.

All data acquisition equipment was situated on the pier cap platform underneath the bridge during random truck testing. The only equipment not located under the bridge was the portable generators. The generators were hung over the guardrail so as to be out of the field of vision of on-coming traffic. No equipment or traffic control was permitted on the bridge during these tests. The purpose was to ensure that the speeds and lane positions of the random

Table 18. Number of Random Truck Crossings Recorded at Each Test Location

Test Site	Number of Truck Records
S7-5 Before Retrofit	788
S7-9 Before Retrofit	740
S5-2 Before Retrofit	795
S7-12 Before Retrofit	773
S7-5 After Retrofit	333
S7-9 After Retrofit	364

trucks followed the normal traffic patterns. One or two people were located under the bridge to monitor the equipment during testing.

A self triggering process was used to activate data recording during random truck testing. The data acquisition system continuously scanned a selected gage for strains that exceeded a prescribed limit. When the limit was exceeded, the system recorded data for a period of time from approximately 2 seconds before to 4 seconds after the limit was exceeded. The resulting record was approximately six seconds in length with the majority of the truck response occurring between 2 and 4 seconds. The gage limits were defined so as to prevent electronic noise and strains from light vehicles from triggering the system. Typically, a vehicle with a strain range over 15 to 20 microstrain in a number one gage in the web gap was required to activate the system.

DATA REDUCTION

All data were collected and stored directly onto magnetic tapes. Approximately 24 tapes were required to store the data for all four field tests. Since the data was stored on tapes, it was necessary to down-load the data to diskettes before the results could be plotted and reduced. The down-loading process required communication with the MEGADAC. The same IBM AT computer that controlled the data acquisition system during testing was used for this process as well.

The initial step of the down-loading process consisted of transferring a portion of the data to the computer's hard disk. Due to software and hardware limitations, only ten trucks were down-loaded at a time. Afterwards, the trucks were transferred to high density diskettes using the DOS backup command.

Several 386 and 486 personal computers, equipped with Opus software (Technical Manual 1988), were used to retrieve the strain ranges from the raw data. The counting method used to determine the strain ranges from the strain histories was the peak-to-peak method. Selection of this method was based on the findings of the literature review. By definition, using the peak-to-peak method, the strain range was defined as the absolute difference between the maximum and minimum values. Each truck crossing created one strain range. Using this method, all strain ranges were extracted directly from plots on the computer monitor screen. A stress range was obtained by multiplying the strain range by a modulus of elasticity of 29,000 ksi. The random strain ranges were combined using Equation 2 to determine a Miner's effective stress range at the critical locations.

Figure 33 shows a strain history response of the (2)OS1 gage at S7-5 for a typical random truck crossing prior to the retrofit. Because the data were recorded at a high sampling rate, 400 samples per second, in a digital format the plot of raw data was complicated by electronic noise. To extract values accurately from the plots, the data were

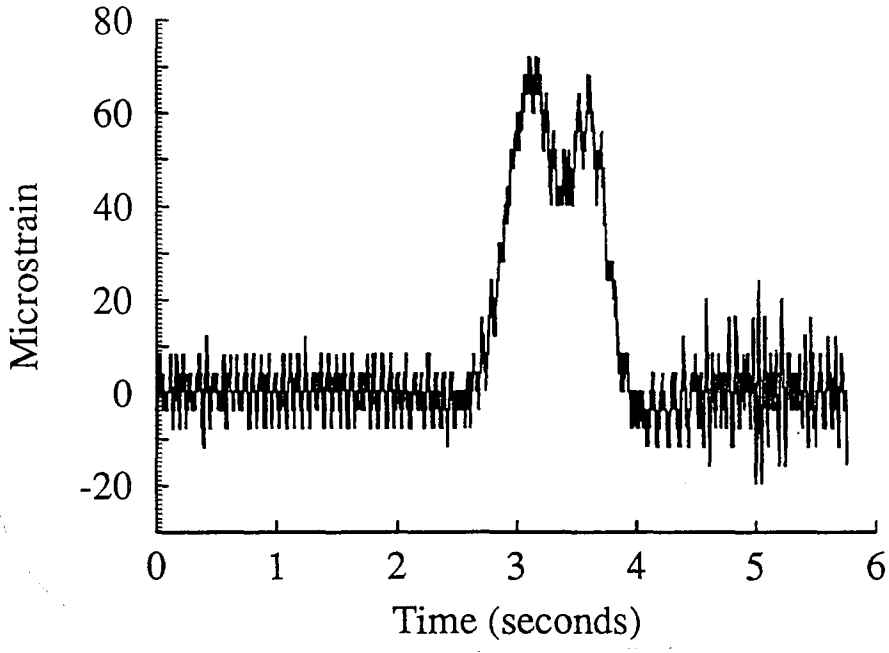

Figure 33. Typical Truck Crossing Record (400 Samples/Second)

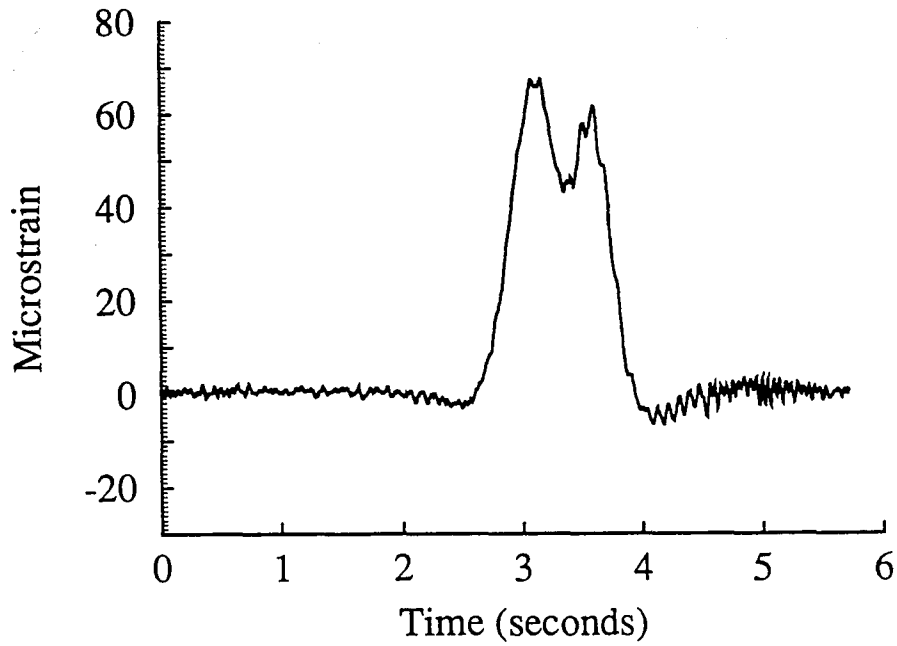

Figure 34. Truck Crossing Shown in Figure 34 Compressed by Averaging Every 25 Scans

compressed. The compression process essentially replaced a predefined number of scans with the average magnitude of the group. For most data, a group size of 25 scans was used. A comparison of Figures 33 and 34 illustrates the effects of the averaging process. Figure 34 shows the same response shown in Figure 33 except that the data was compressed by averaging every 25 scans.

The balance and static test data were reduced by averaging over a larger number of scans than the other types of data. Since these types of measurements result in a constant value, the accuracy of the measurements was enhanced by the averaging process. The resulting data was also considerably easier to work with.

CHAPTER SIX
RESULTS AT PIER FLOORBEAM CONNECTIONS

BEHAVIOR AT TEST LOCATIONS

Tests were performed at two 84 inch girder locations and two 96 inch girder locations. The two 84 inch girder depth locations were S7-5 and S5-2. The two 96 inch girder depth locations were S7-9 and S7-12. At locations S7-5 and S7-9, testing was conducted both before and after the rigid attachment retrofit. At the other locations, S5-2 and S7-12 testing was only conducted before the retrofit. Comparisons of field test data indicated that the general behavior between the different test sites was similar. However, some characteristic differences were evident between the in-plane and out-of-plane behavior. The behavioral differences were most evident in the duration and character of the strain response to a truck crossing.

The response duration was typically longer for in-plane gages than for out-of-plane gages. For example, the in-plane strain record, particularly from flange gages, indicated a measurable response for trucks traveling from one end of the continuous structure to the other. The gages registered either tension or compression depending on where the truck was located along the span. This general response was also influenced by the dynamic response of the system to the moving load. The dynamic effect originated when the truck

rolled onto the first span of the continuous structure and continued after the truck left the structure before damping out. Gages for which this behavior was most obvious were the bottom flange gages on both the plate girders and the stringers.

Figure 35 illustrates the general in-plane behavior using the outside (slow lane side) girder bottom flange gage for both test trucks at test locations S7-5 and S5-2. The effects of vehicle position can be seen in the static strain line (dashed line). The dashed line is an approximation of the strain without dynamic effects that would be observed if the truck moved very slowly across the span. The dynamic effect of truck crossing the structure is exemplified by the cyclic movement of the strain history about the static strain line.

The out-of-plane bending gages, located in the web gaps, experienced short response durations. These gages were primarily affected by trucks located in the proximity of the test location. Trucks in this region caused a downward deflection in the stringers which resulted in bending of the floorbeam. This in turn caused rotations at the ends of the floorbeam to occur which created an out-of-plane distortion in the web gap. At all locations tested, the LVDTs showed that the instrumented connection plates in the web gaps moved inward (towards the center line of the bridge). Also, the out-of-plane displacements measured with the LVDTs were the best indicators of the amount of distortion experienced in

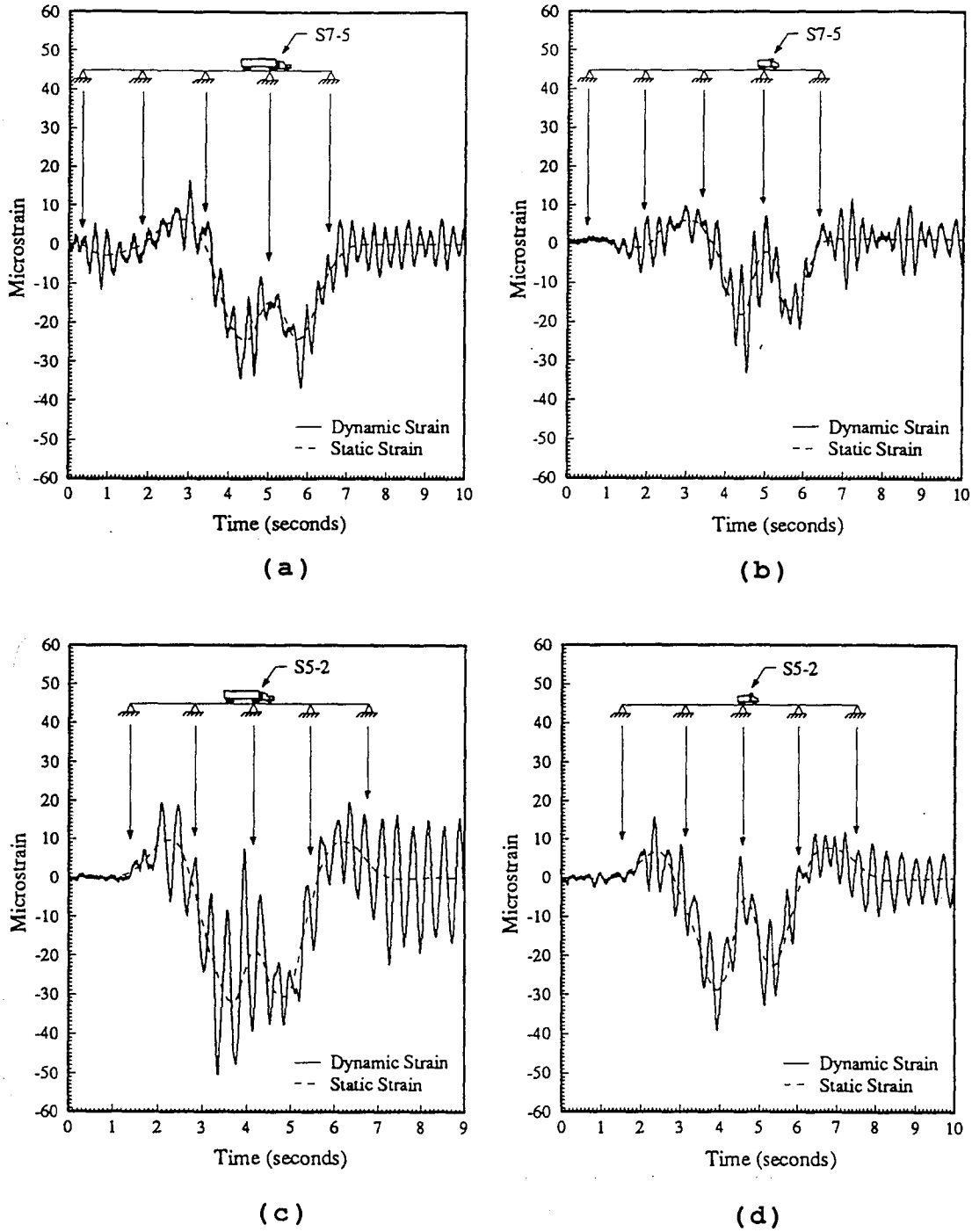

Figure 35. Bottom Flange Strain measured on the Outside Girder at Pier (a) S7-5 for Lowboy in the Outside Lane at 60 mph, (b) S7-5 for Dump Truck in the Outside Lane at 58 mph, (c) S5-2 for Lowboy in the Outside Lane at 65 mph, (d) S5-2 for Dump Truck in the Outside Lane at 60 mph

the web gap regions. The out-of-plane displacement as measured by LVDTs is used in Figure 36 to illustrate the general out-of-plane behavior. The test runs shown in Figure 36 are the same test runs used for Figure 35.

A comparison between Figure 35 and 36 illustrates the characteristic differences between the in-plane and out-of-plane behavior as mentioned above. Figure 35 shows that the in-plane strains reached their largest magnitudes when trucks were located near the middle of the spans adjacent to the test pier. Figure 36 shows that the out-of-plane displacements peaked when the trucks were located directly over the test location. Plots similar to Figure 36, except showing out-of-plane bending strain instead of out-of-plane deflection, showed that strains peaked as well when the trucks were located directly over the test location. The sustained vibration created by the moving load is also much less apparent in the out-of-plane response (Figure 36) than in the in-plane response (Figure 35).

In-Plane Strains at Web Gap

The in-plane strains illustrated in Figure 35 were measured on the girder's compression flange. In-plane strains near the tension flange at the web gap were generally much smaller in magnitude. In-plane strains were measured at each of the pier floorbeam test locations on the girder tension flange (No.8 gage) and on the web adjacent to web gaps (No.4 gages). Small differences between strains measured on the webs and tension flanges indicate that the

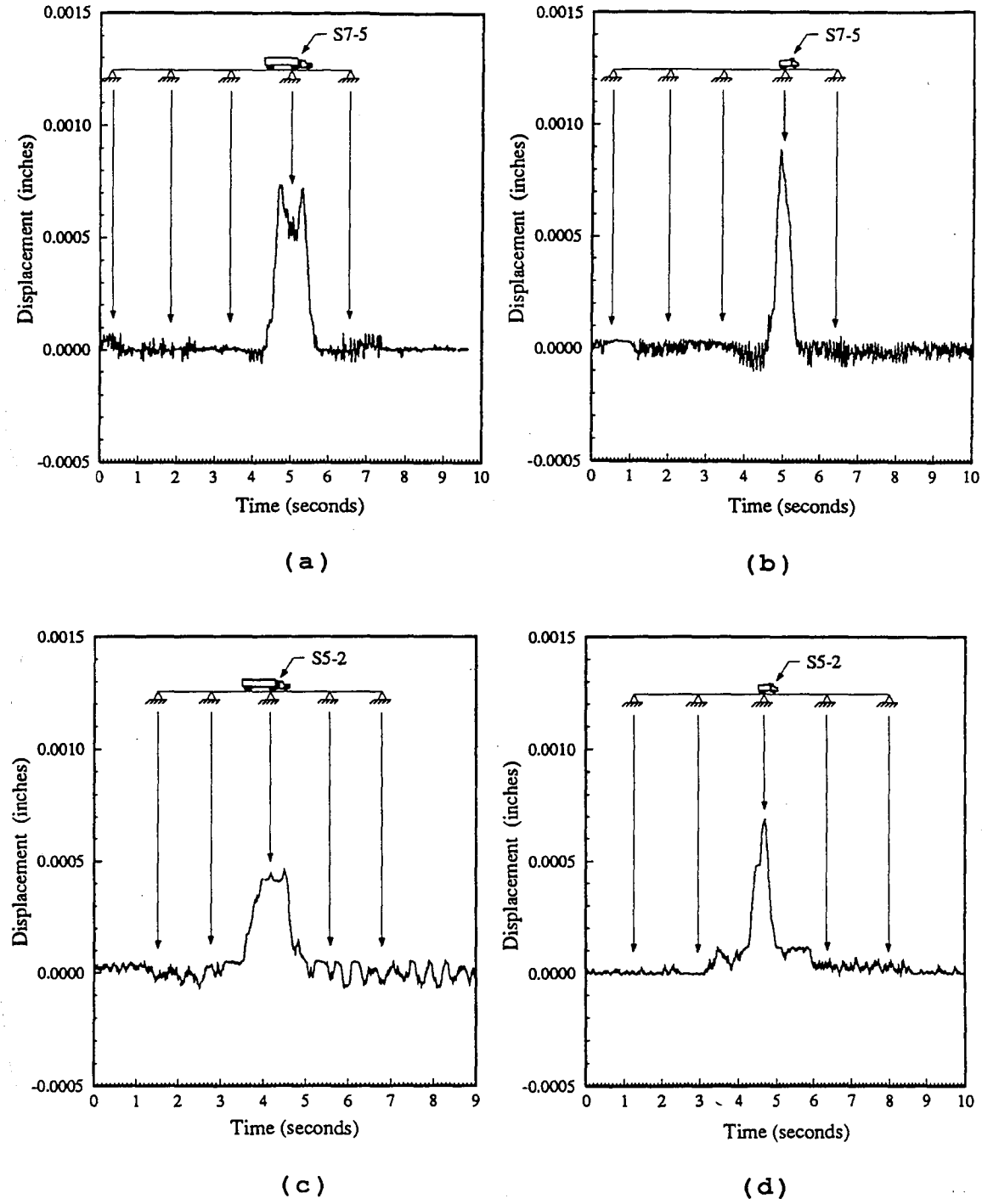

Figure 36. Web Gap Displacement Measured on the Inside Girder at Pier (a) S7-5 for Lowboy in the Outside Lane at 60 mph, (b) S7-5 for Dump Truck in the Outside Lane at 58 mph, (c) S5-2 for Lowboy in the Outside Lane at 65 mph, (d) S5-2 for Dump Truck in the Outside Lane at 60 mph

strains at the girder web gages were somewhat affected by the out-of-plane bending. However, both the girder web and girder tension flange gages indicated that the in-plane bending strains were very small at the web gap. The maximum stress range measured on the tension flange and web near the web gap was approximately 0.4 ksi, and the stress ranges were typically only 0.2 ksi. The low stress ranges experienced at these locations were due to the fact that the gages were located near the neutral axis of the composite girder.

Connection Plate Rotation

A question of interest was whether the floorbeam connection plates were rotating about a vertical axis as trucks crossed the bridge. Either strain gages (No. 10 gages) or an LVDT was installed at the web gaps to detect the amount of rotation experienced by the connection plate. At S7-5, an LVDT was used to measure the rotation at the top of the pier floorbeam connection plate on the outside girder. The measurements indicated that the connection plate was rotating in the direction of traffic flow (downhill). The data indicated rotations on the order of 2.0E-6 radians were occurring. Strain gage readings also indicated a slight rotation of the connection plate at this location. Small rotations at some of the other test locations were detected from differences in response at the No. 10 strain gage locations on opposite sides of the connection plate. However, the effects of the rotations did not appear to be significant at any of the test locations.

Impact Effects on Web Gap Strains

Moving truck loads generate a dynamic response as illustrated in Figure 35. The increase in peak strains or stresses that result from a moving truck load as compared to a static truck load is commonly referred to as the impact effect. The magnitude of the impact effect on web gap strains can be determined by comparing peak strains from the crawl and fast run calibration tests. Typical results of these tests are illustrated by Figures 37 through 42. The figures indicate only a moderate impact effect on the web gap strains. Overall, the test results indicate that the increase in web gap strains and out-of-plane displacements as a result of impact was generally less than 20%. In many cases the peak strains and displacements decreased slightly as a result of the dynamic response peak canceling part of the static peak.

WEB GAP STRESSES FROM STATIC TESTS

The static tests provided a means of evaluating the response of the connection plate details at various truck positions. Before the tests were performed, it was suspected that the connections on either end of a floorbeam would respond to truck loads in a reasonably symmetric fashion. For example, if symmetry holds, the strains and displacements at the outside girder resulting from a truck in lane C (Figure 30) should equal the strains and displacements at the inside girder resulting from a truck in lane A. However, the test results indicate that the connections respond to truck

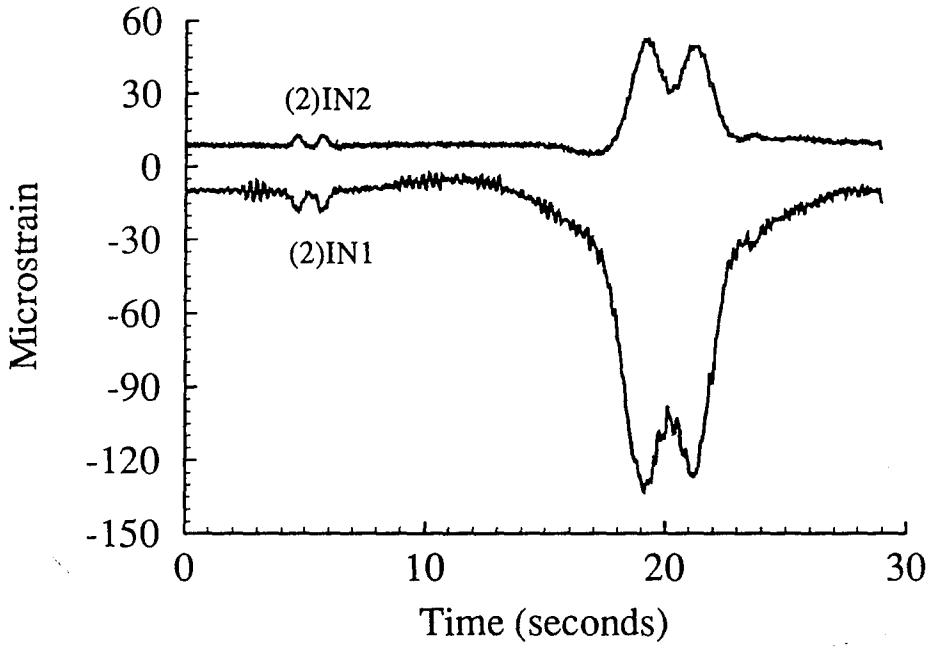

Figure 37. Response of Gages IN1 and IN2 on the Inside Girder at Pier S7-5 During Lowboy Crawl Pass in the Outside Lane

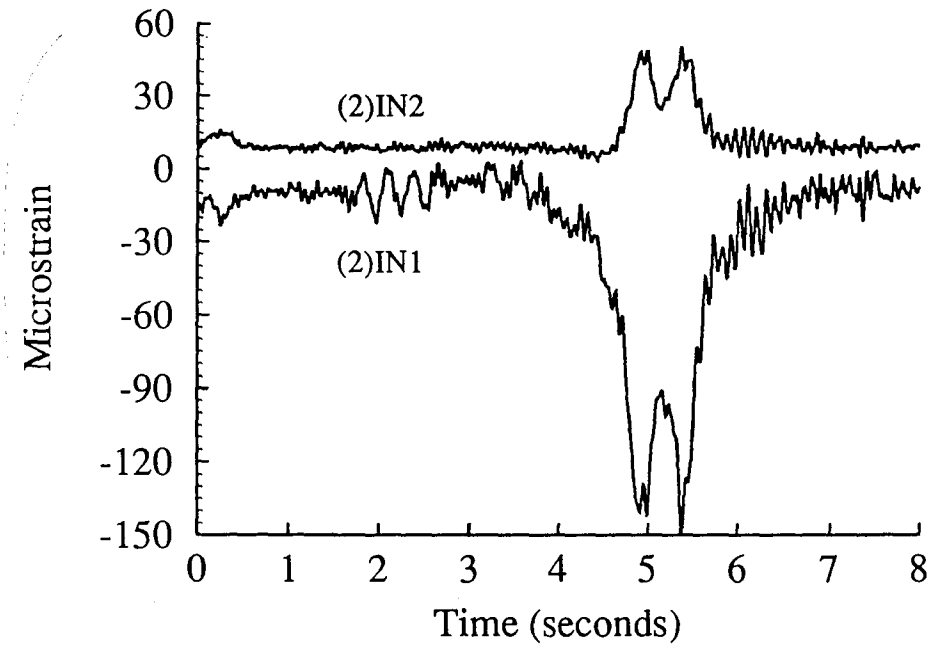

Figure 38. Response of Gages IN1 and IN2 on the Inside Girder at Pier S7-5 During Lowboy Fast Pass in the Outside Lane

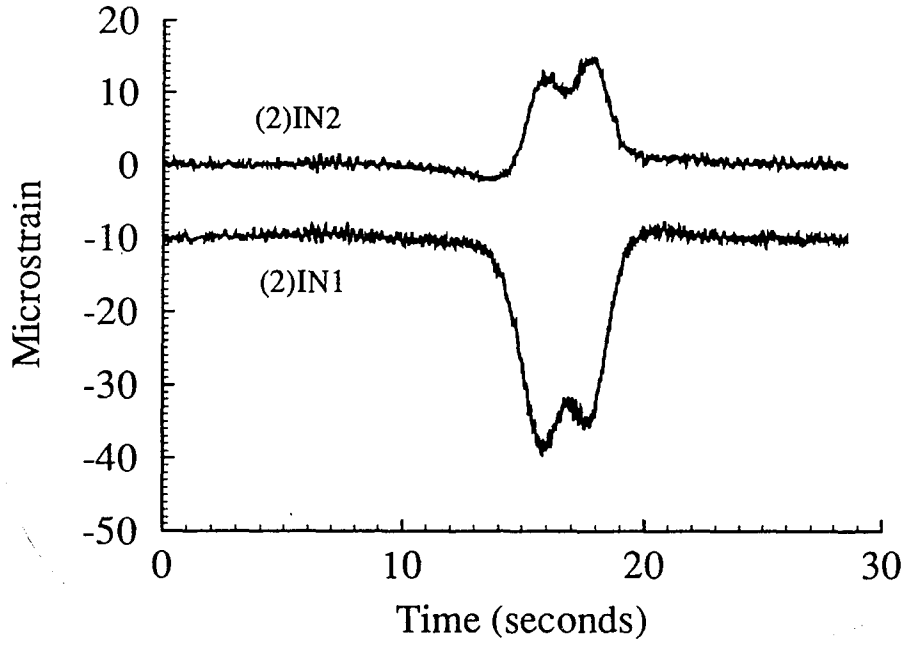

Figure 39. Response of Gages IN1 and IN2 on the Inside Girder at Pier S7-9 During Lowboy Crawl Pass in the Outside Lane

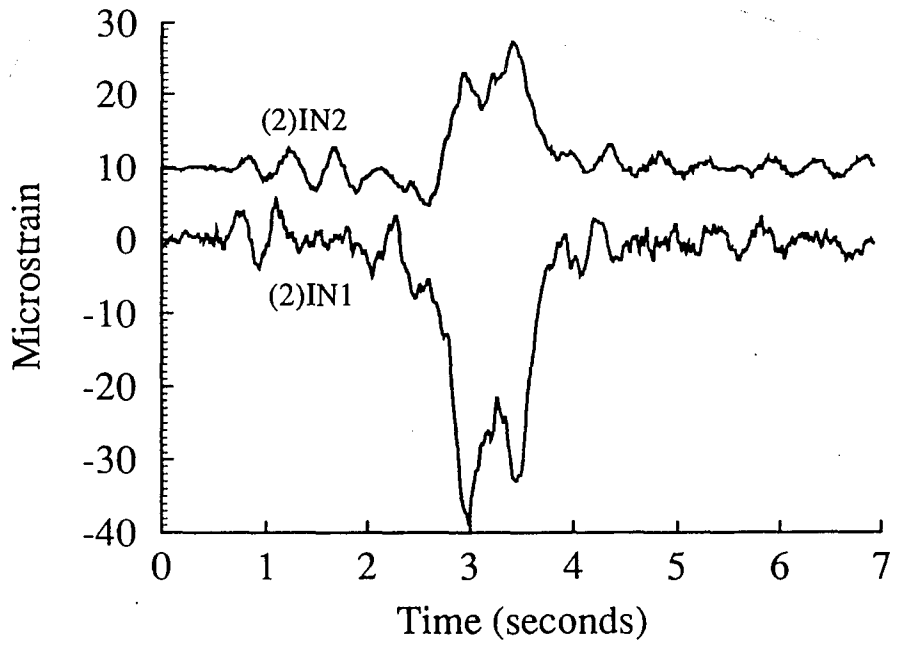

Figure 40. Response of Gages IN1 and IN2 on the Inside Girder at Pier S7-9 During Lowboy Fast Pass in the Outside Lane

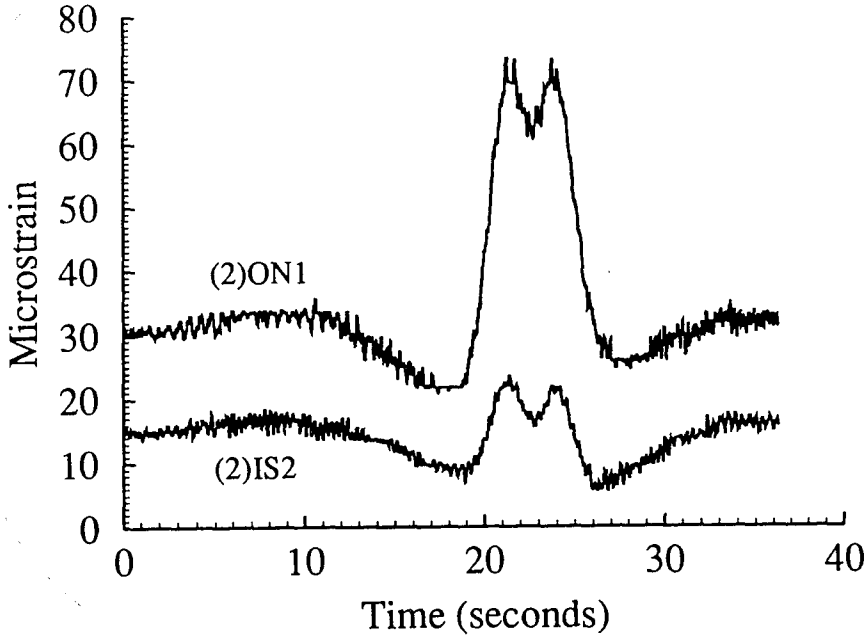

Figure 41. Response of Gages ON1 and IS2 on the Inside Girder at Pier S7-12 During Lowboy Crawl Pass in the Outside Lane

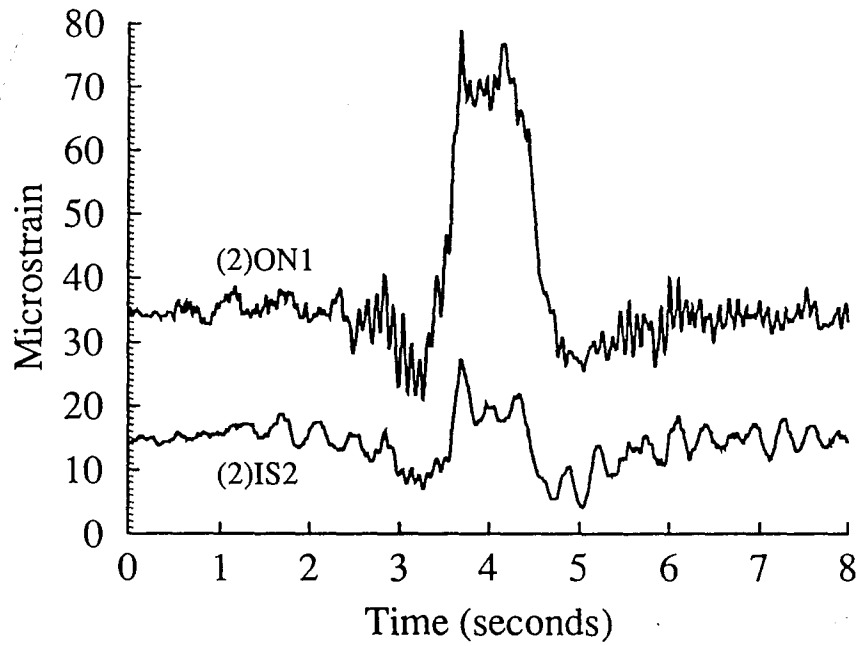

Figure 42. Response of Gages ON1 and IS2 on the Inside Girder at Pier S7-12 During Lowboy Fast Pass in the Outside Lane

loading in a much less predictable fashion. A significant variation in the strains and displacements resulting from apparently similar loadings was observed. This variation is understandable when the effects of all the slight differences in structural geometry on the transfer of loading to the connection are considered.

One objective of performing static tests at each test site was to determine the lane and truck position which created the highest web gap stresses. Stress distribution plots are shown in Figures 43 through 48 to illustrate the results. The figures give a graphical illustration of the web gap geometry and the gage locations to scale. The maximum out-of-plane displacement at the top of the connection plate is also shown in each figure. The figure captions indicate the test case which yielded the largest stresses for each pier floorbeam detail. For all details tested, the highest stresses were produced by a truck in the outside traffic lane (slow lane). The dump truck produced the highest stresses for all pier locations except S7-9. A comparison of the test truck weights reveals that the dump truck weighed slightly more than the front three axles of the lowboy for all cases except at pier S7-9. These results indicate that the web gap stresses are affected more by the weight of a group of closely spaced axles than by the gross vehicle weight. Also, the outside traffic lane apparently produces the highest stresses because the truck loading is

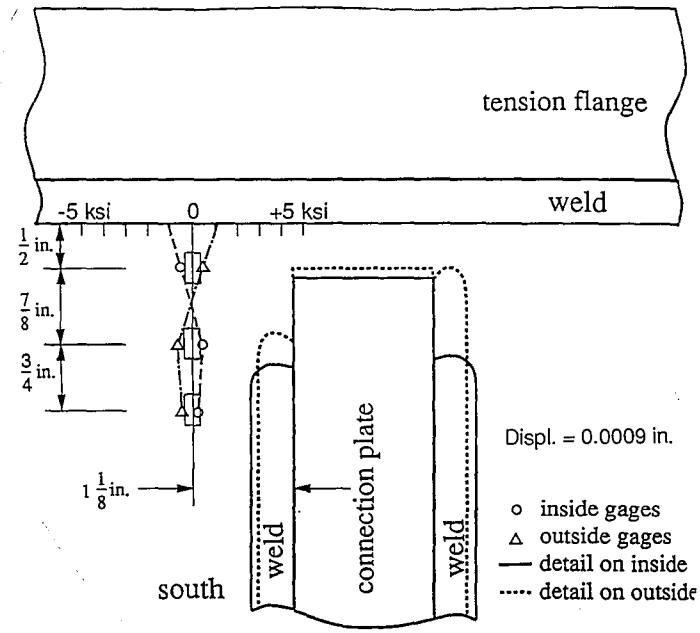

Figure 43. Static Stress Distribution on Outside Girder at Pier S7-5 (84 in. Girder) Before Retrofit with Dump Truck in Outside Lane (Worst Case)

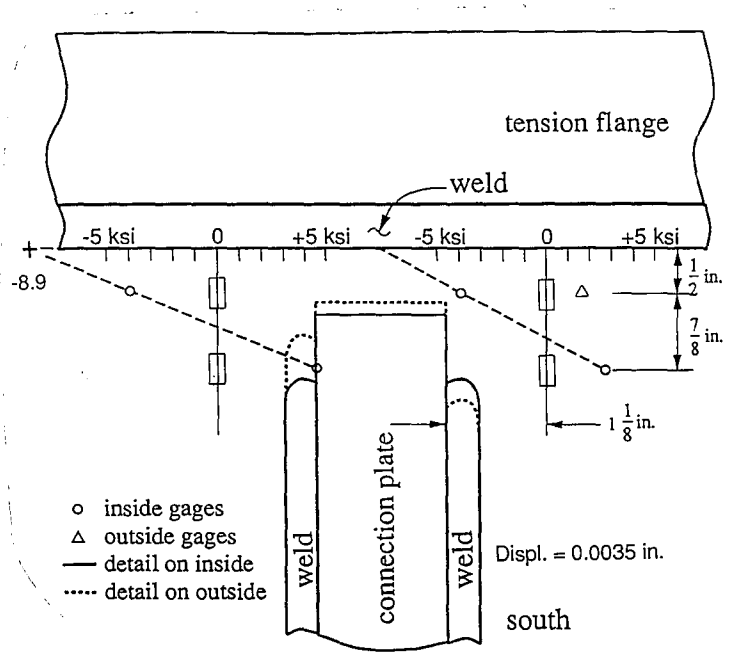

Figure 44. Static Stress Distribution on Inside Girder at Pier S7-5 (84 in. Girder) Before Retrofit with Dump Truck in Outside Lane (Worst Case)

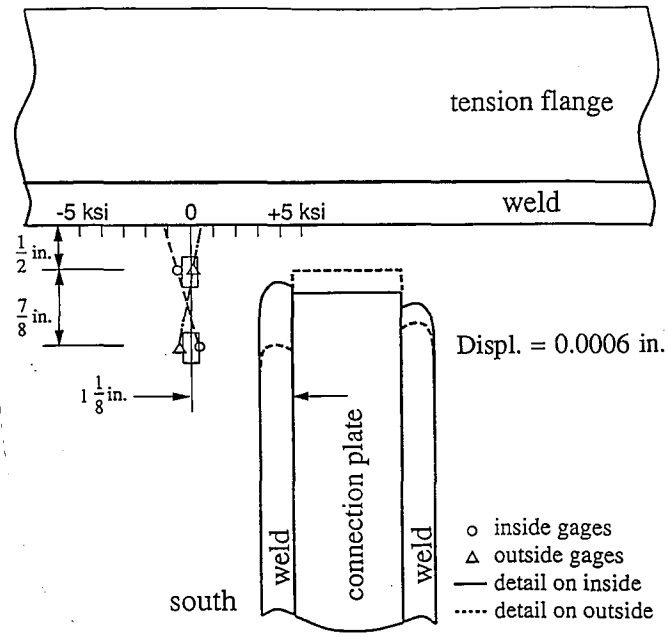

Figure 45. Static Stress Distribution on Outside Girder at Pier S5-2 (84 in. Girder) Before Retrofit with Dump Truck in Outside Lane (Worst Case)

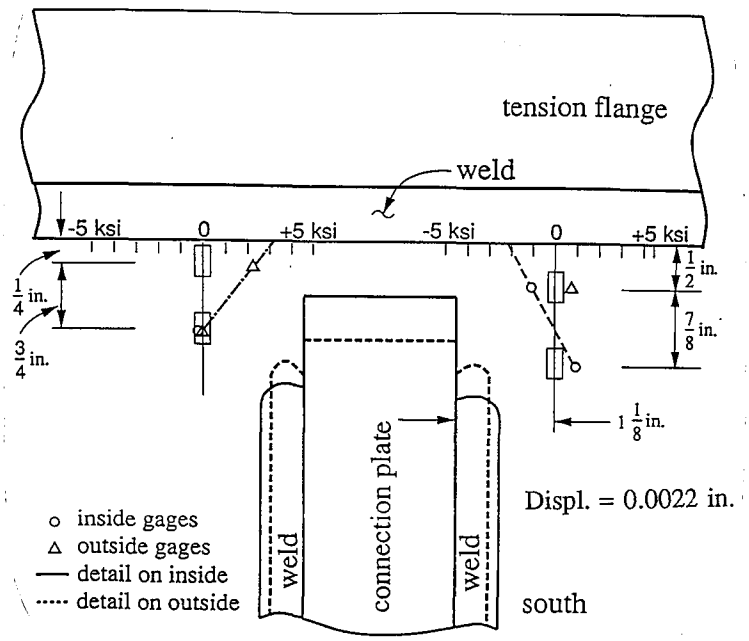

Figure 46. Static Stress Distribution on Inside Girder at Pier S7-12 (96 in. Girder) Before Retrofit with Dump Truck in Outside Lane (Worst Case)

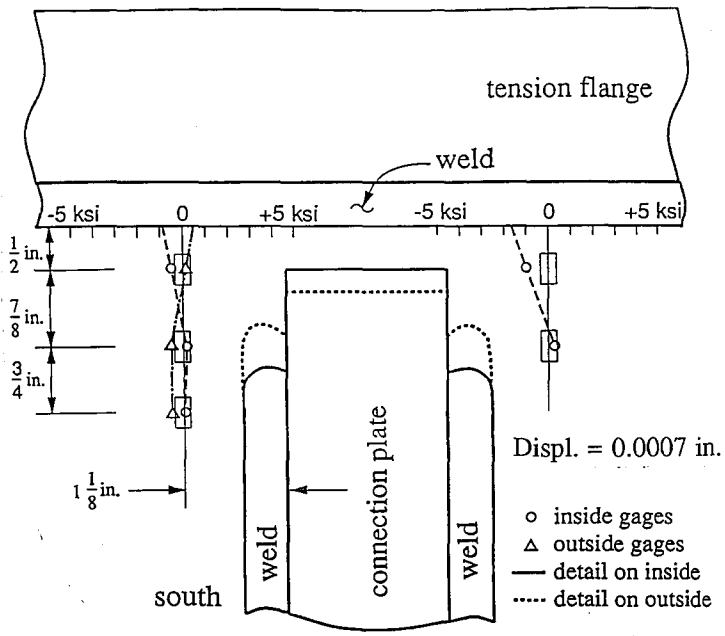

Figure 47. Static Stress Distribution on Outside Girder at Pier S7-9 (96 in. Girder) Before Retrofit with Lowboy in Outside Lane (Worst Case)

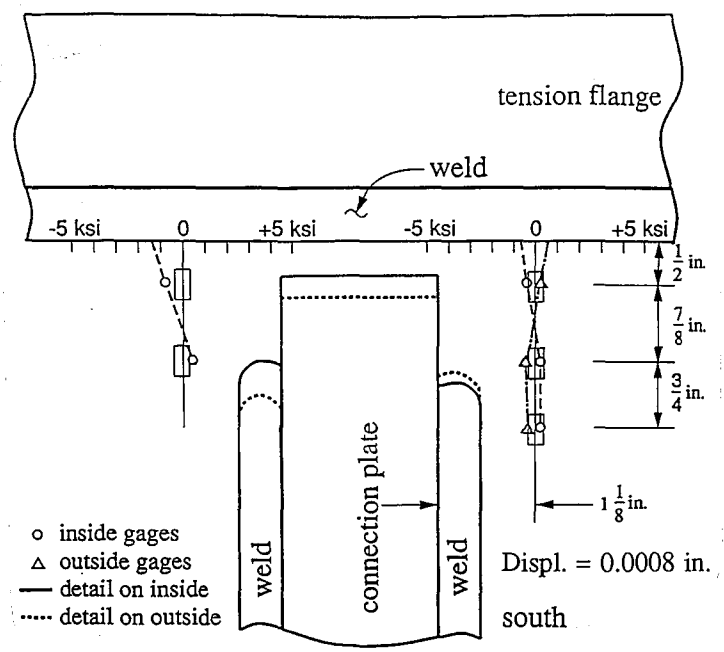

Figure 48. Static Stress Distribution on Inside Girder of Pier S7-9 (96 in. Girder) Before Retrofit with Lowboy in Outside Lane (Worst Case)

near the floorbeam midspan so that the floorbeam end rotations and resulting web distortion are maximized.

EFFECTIVE STRESS RANGES FROM TRUCK TRAFFIC

Effective stress ranges at critical locations were of interest in evaluating the potential for fatigue cracking at the pier floorbeam connection plate details. The end of the connection plate weld on the inside of the girder web and the web-flange weld toe on the outside of the girder were the two critical locations of primary interest. These locations are where the cyclic tensile stresses occur and where fatigue cracks are most likely to initiate. Stress ranges at the critical locations were obtained from the stress ranges at the No. 1 and 2 strain gage locations by linear extrapolation as illustrated for the static test results in Figures 43 through 48. Miner's effective stress ranges (Sre) were then calculated using the individual stress ranges in Equation 2. Sufficient random truck data for calculation of effective stress ranges at the outside web-flange weld were not available in most cases. In those cases, the magnitude of the compressive effective stress range of the web-flange weld on the inside face of the web was considered to be a good estimate of the stress range on the outside face.

A summary of the effective stress range calculations is given in Table 19. Figures 49 through 64 show histograms of the stress range data used for each entry in Table 19 and data at other critical locations. Histogram data for the critical locations and strain gage locations are tabulated in

Table 19. Effective Stress Ranges at Critical Locations for Random Truck Data Before Retrofit

Outside Girder		Inside Girder	
Inside Conn. Plate Weld Sre (ksi)	Inside Web-Flange Weld Sre (ksi)	Inside Conn. Plate Weld Sre (ksi)	Inside Web-Flange Weld Sre (ksi)
S7-5 Pier Floorbeam Details			
+0.5	-0.8(0.9*)	+1.7	-4.3(4.6*)
S5-2 Pier Floorbeam Details			
+0.4	-1.0	N.A.†	N.A.
S7-9 Pier Floorbeam Details			
+0.3	-0.8	+0.4	-0.9
S7-12 Pier Floorbeam Details			
N.A.	N.A.	+1.0	-1.8

* Effective stress range at outside web-flange weld.
† Not available.

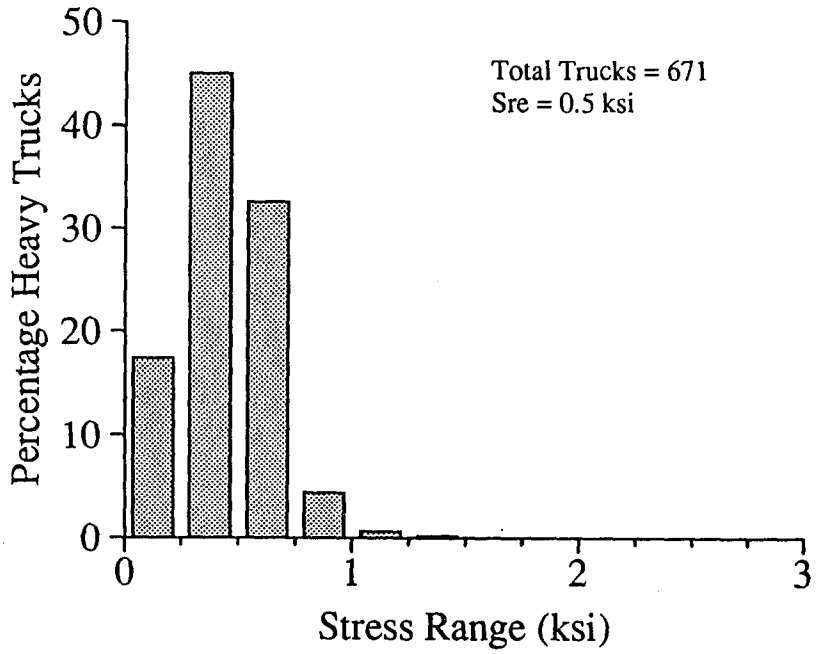

Figure 49. Histogram of Extrapolated Random Data at the End of the Inside Connection Plate Weld on Outside Girder of Pier S7-5 Before Retrofit

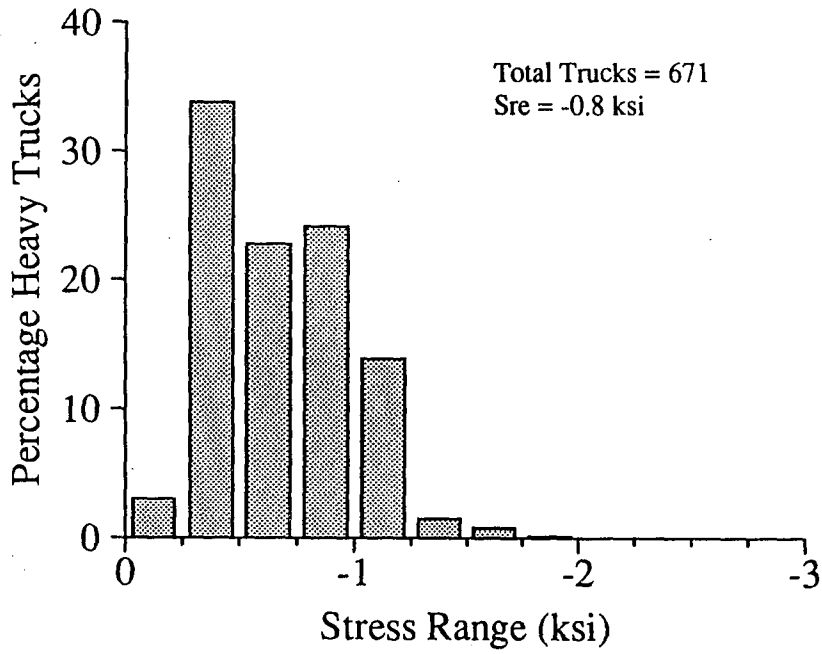

Figure 50. Histogram of Extrapolated Random Data at the Inside Web-Flange Weld Toe on Outside Girder of Pier S7-5 Before Retrofit

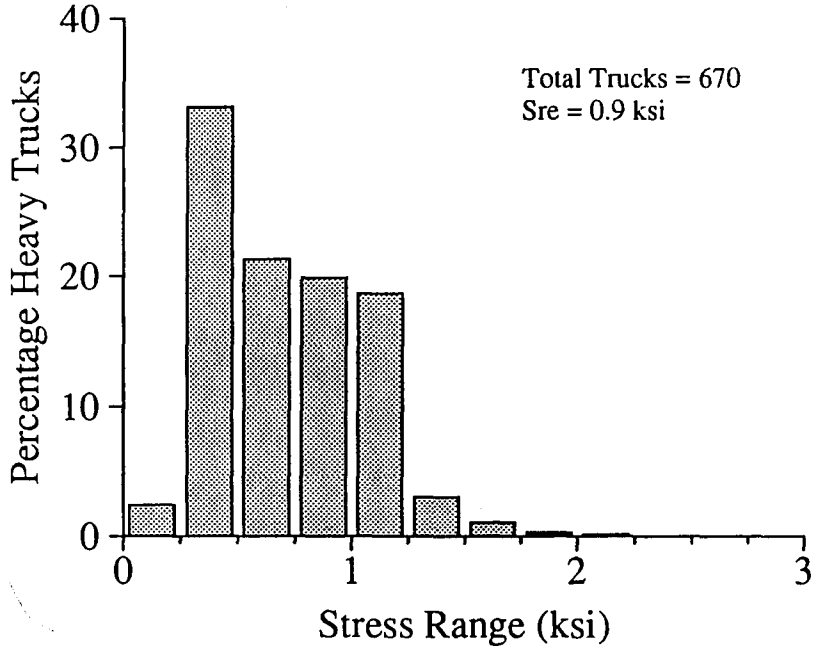

Figure 51. Histogram of Extrapolated Random Data at the Outside Web-Flange Weld Toe on Outside Girder of Pier S7-5 Before Retrofit

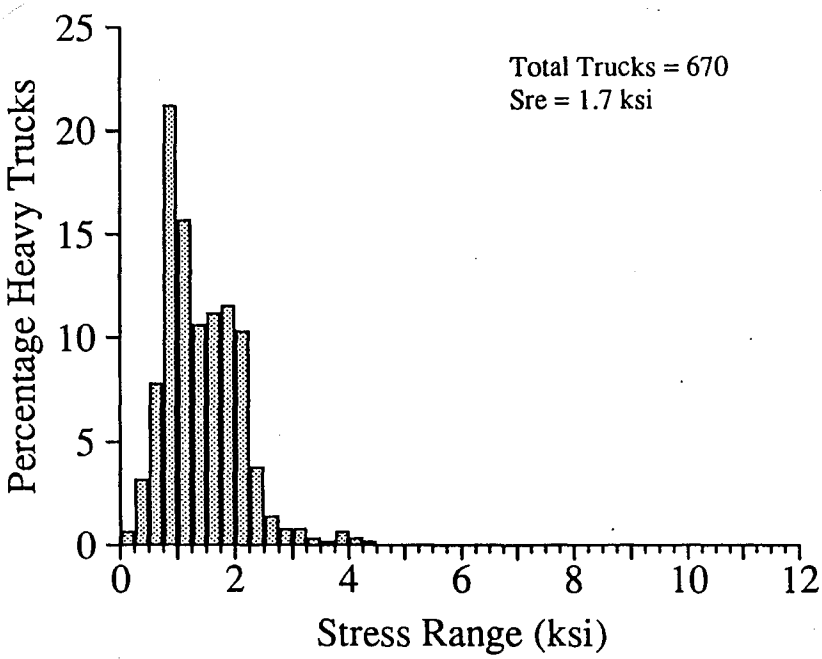

Figure 52. Histogram of Extrapolated Random Data at the End of the Inside Connection Plate Weld on Inside Girder of Pier S7-5 Before Retrofit

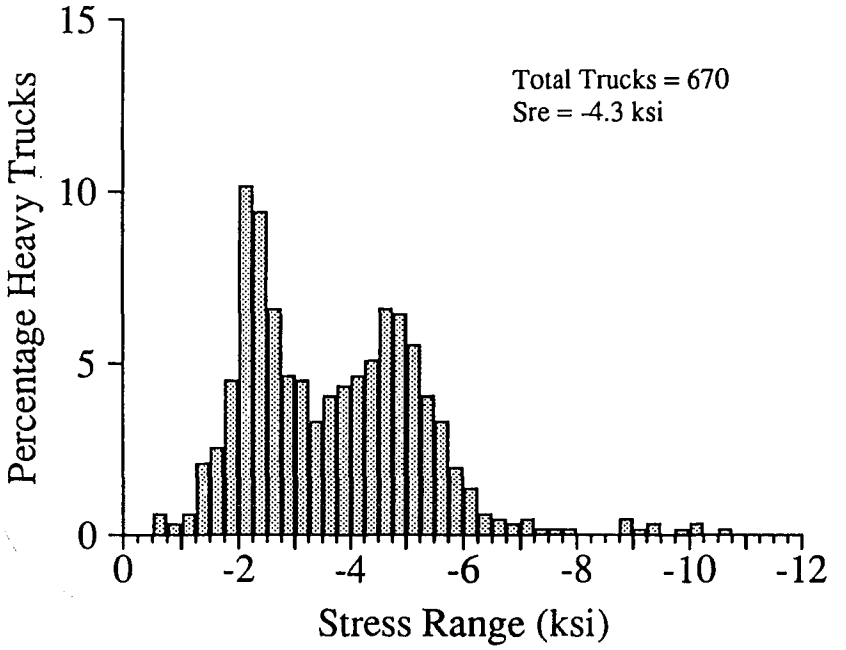

Figure 53. Histogram of Extrapolated Random Data at the Inside Web-Flange Weld Toe on Inside Girder of Pier S7-5 Before Retrofit

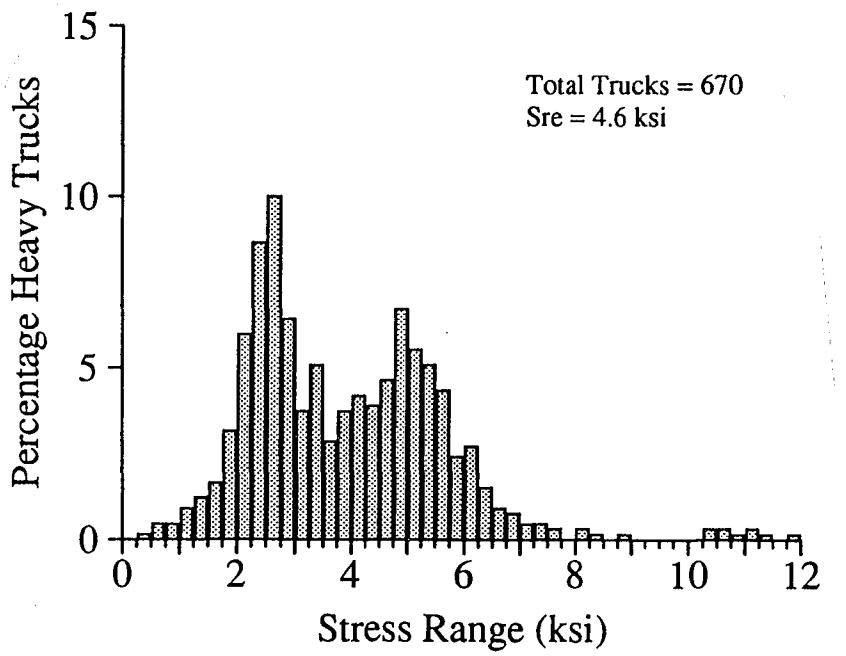

Figure 54. Histogram of Extrapolated Random Data at the Outside Web-Flange Weld Toe on Inside Girder of Pier S7-5 Before Retrofit

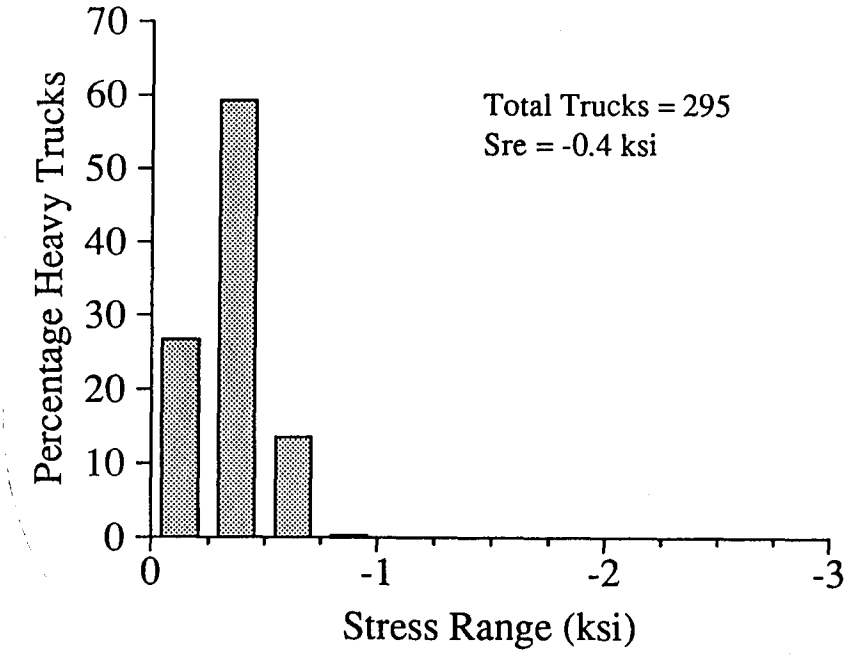

Figure 55. Histogram of Extrapolated Random Data at the End of the Inside Connection Plate Weld on Outside Girder of Pier S5-2 Before Retrofit

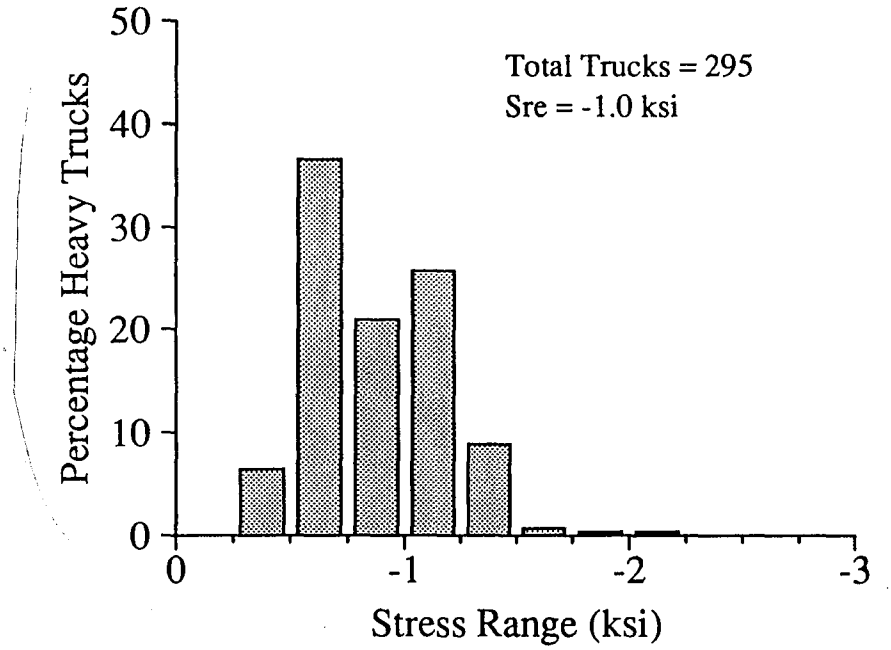

Figure 56. Histogram of Extrapolated Random Data at the Inside Web-Flange Weld Toe on Outside Girder of Pier S5-2 Before Retrofit

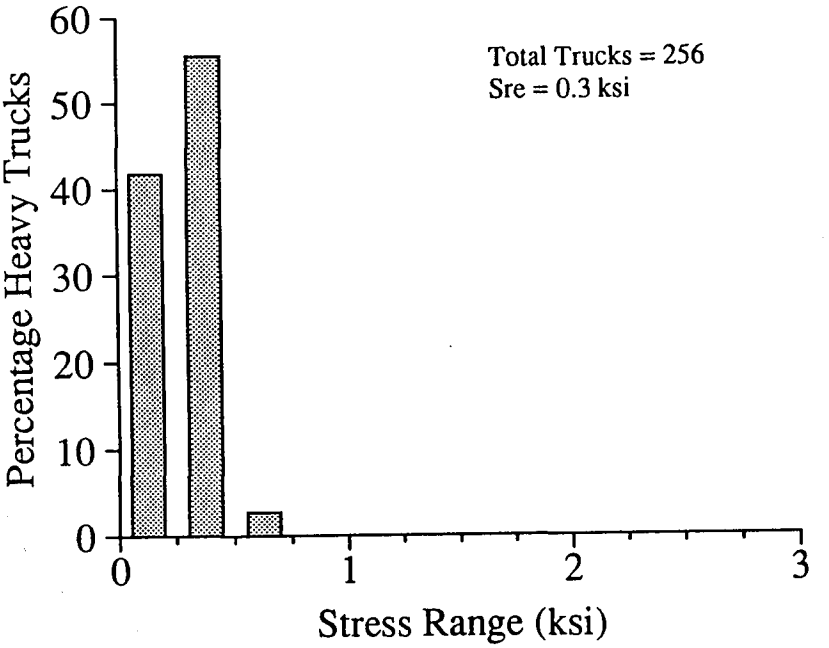

Figure 57. Histogram of Extrapolated Random Data at the End of the Inside Connection Plate Weld on Outside Girder of Pier S7-9 Before Retrofit

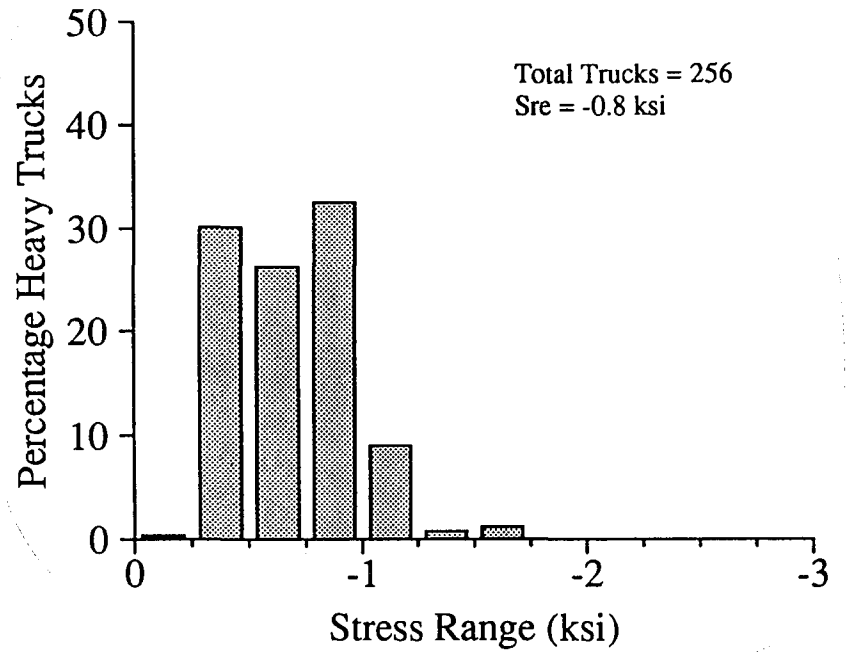

Figure 58. Histogram of Extrapolated Random Data at the Inside Web-Flange Weld Toe on Outside Girder of Pier S7-9 Before Retrofit

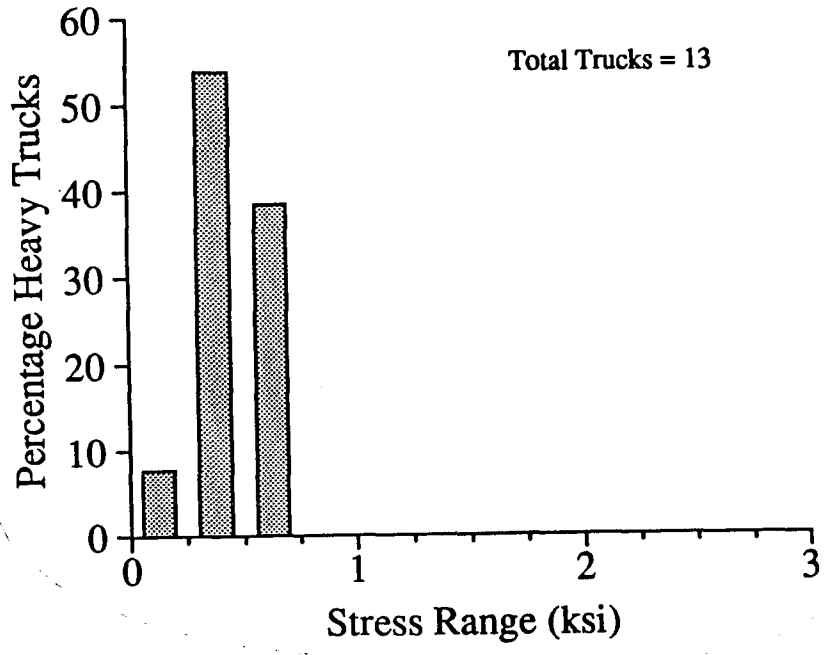

Figure 59. Histogram of Extrapolated Random Data at the Outside Web-Flange Weld Toe on Outside Girder of Pier S7-9 Before Retrofit

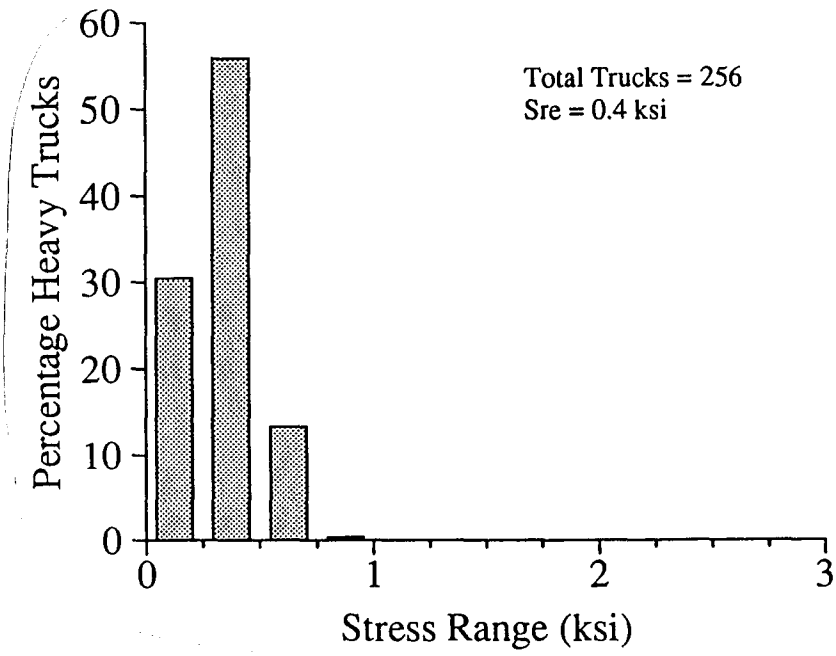

Figure 60. Histogram of Extrapolated Random Data at End of the Inside Connection Plate Weld on Inside Girder of Pier S7-9 Before Retrofit

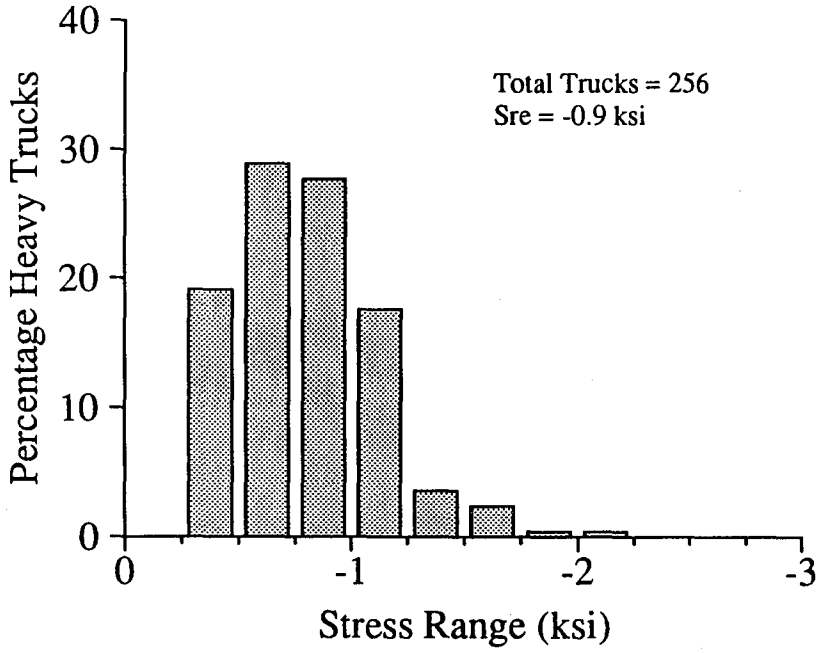

Figure 61. Histogram of Extrapolated Random Data at the Inside Web-Flange Weld Toe on Inside Girder of Pier S7-9 Before Retrofit

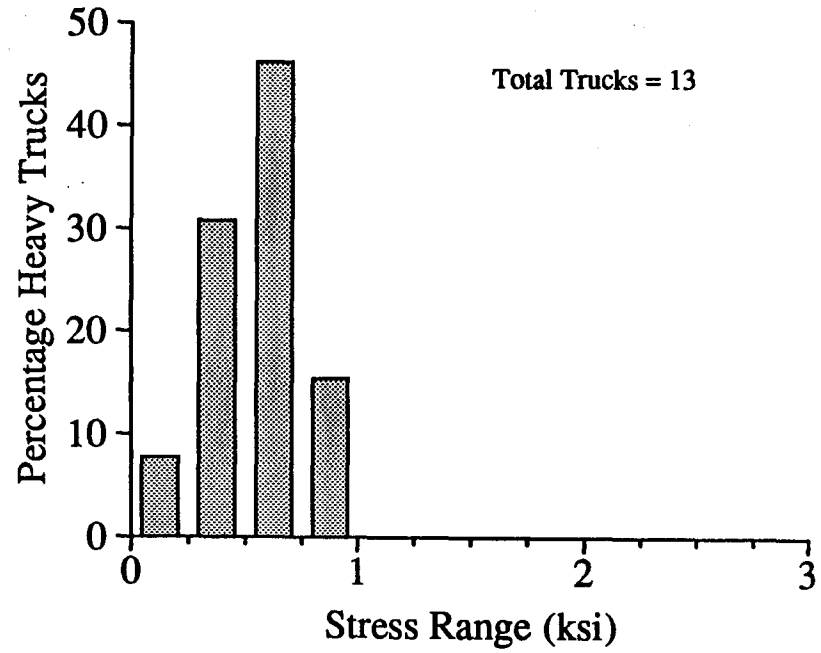

Figure 62. Histogram of Extrapolated Random Data at the Outside Web-Flange Weld Toe on Inside Girder of Pier S7-9 Before Retrofit

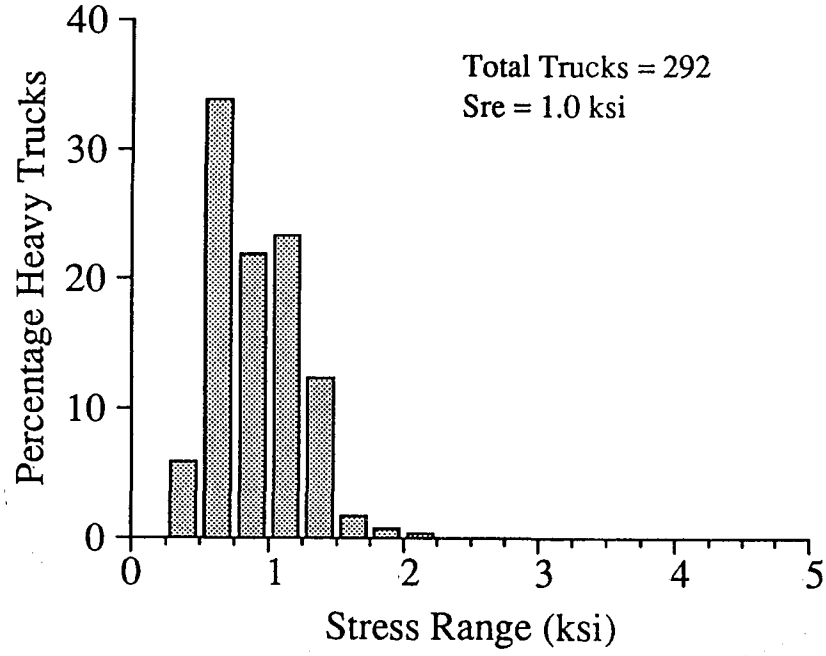

Figure 63. Histogram of Extrapolated Random Data at the End of the Inside Connection Plate Weld on Inside Girder of Pier S7-12 Before Retrofit

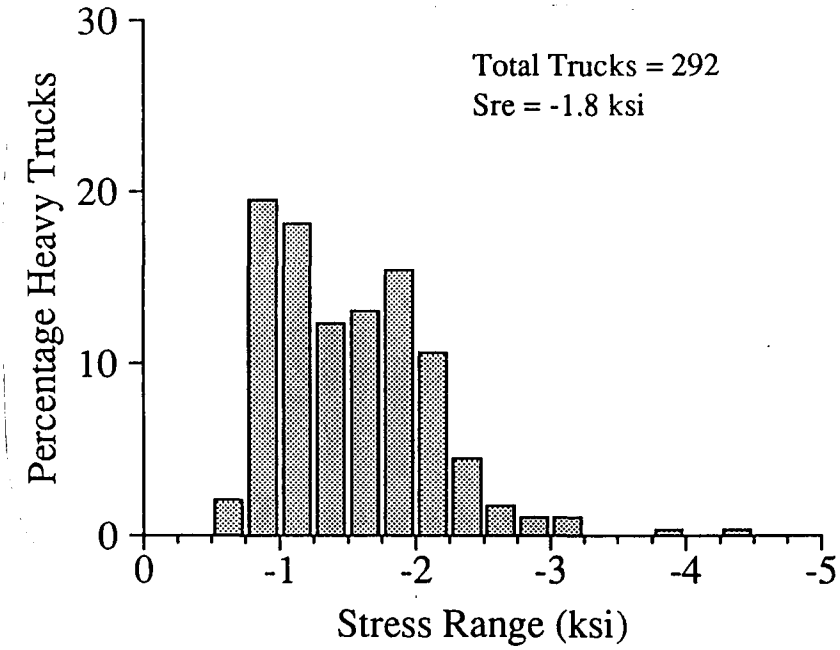

Figure 64. Histogram of Extrapolated Random Data at the Inside Web-Flange Weld Toe on Inside Girder of Pier S7-12 Before Retrofit

the Appendices. Histograms of stress ranges at the outside web-flange weld at both girders at Pier S7-5 are shown in Figures 51 and 54. The results in Table 19 indicate that the effective stress ranges at the inside girder at Pier S7-5 were significantly larger than those at the other locations.

The stress ranges obtained from the fast run calibration tests with the lowboy in test lanes B and C are shown in Table 20. Results are shown for the lowboy because the number and spacing of the axles for that test truck is believed to be most representative of the heavy trucks that normally cross the bridge. Also, the axle weights for the lowboy were consistently very near the legal limit for that truck type. The maximum stress ranges recorded due to a random truck crossing and the sum of the stress ranges from calibration tests in lanes B and C are also given in Table 20. The sum of the stress ranges from calibration tests in lanes B and C provide a good estimate of the stress range that would result from side-by-side truck crossings. This stress range is an approximate limit for the maximum stress range that can result from trucks hauling legal loads. In no case did the maximum stress range recorded from random truck traffic exceed that limit. Note that the sum of the stress ranges from calibration tests in lanes B and C for most cases is approximately twice as large as stress range for either lane.

The largest tensile stress range recorded from a random truck crossing was 12 ksi at the outside web-flange weld at

Table 20. Stress Ranges at Critical Locations Before Retrofit for Lowboy Test Truck Fast Runs

	Outside Girder		Inside Girder	
Test	Inside Conn. Plate Weld Sr (ksi)	Inside Web-Flange Weld Sr (ksi)	Inside Conn. Plate Weld Sr (ksi)	Inside Web-Flange Weld Sr (ksi)
S7-5 Pier Floorbeam Details				
Max. Random	+1.4	-1.9(2.2*)	+4.4	-10.7(12*)
Test Lane B	+0.8	-1.1(1.3*)	N.A.	N.A.
Test Lane C	N.A.†	N.A.	+1.3	-6.3(4.9*)
S5-2 Pier Floorbeam Details				
Max. Random	-0.9	-2.2	N.A.	N.A.
Test Lane B	-0.5	-1.4	N.A.	N.A.
Test Lane C	-0.5	-1.1	N.A.	N.A.
Lane B+C	-1.0	-2.5	N.A.	N.A.
S7-9 Pier Floorbeam Details				
Max. Random	+0.7	-1.7	+0.9	-2.2
Test Lane B	+0.6(0.7*)	-1.1	+0.7	-1.3(0.9*)
Test Lane C	+0.5(0.4*)	-0.8	+0.8	-1.8(1.2*)
Lane B+C	+1.1(1.1*)	-1.9	+1.5	-3.1(2.1*)
S7-12 Pier Floorbeam Details				
Max. Random	N.A.	N.A.	+2.2	-4.4
Test Lane B	N.A.	N.A.	+1.4	-2.3
Test Lane C	N.A.	N.A.	+1.8	-2.4
Lane B+C	N.A.	N.A.	+3.2	-4.7

* Stress range at outside web-flange weld.
† Not available.

the inside girder at Pier S7-5 as noted in parentheses in Table 20. Although this value can not be compared to the sum of the calibration test stress ranges for lanes B and C, it is suspected to be close to that unknown sum since it is over twice as large as the stress range recorded for the calibration test in lane C.

CHAPTER SEVEN
EVALUATION OF CRACKING AND REPAIR METHODS

CAUSE OF FATIGUE CRACK INITIATION

Fisher et al. (1990) investigated the initiation of fatigue cracks in web gaps at transverse connection plates due to cyclic out-of-plane distortions. They concluded that the fatigue resistance at the end of the connection plate to web weld was reasonably approximated by the AASHTO (1990) Category C fatigue resistance curve. Figure 65 shows the data collected by Fisher et al. (1990) for the number of cycles to crack initiation. The results are compared to the Category C fatigue resistance curve. As seen in the figure, the fatigue limit of the Category C curve is at a stress range of 10 ksi. Cracking did occur in some of the tests with constant amplitude stress ranges at the end of the connection plate weld between 7.5 ksi and 10 ksi. In most of the tests cracking first occurred at the end of the connection plate weld indicating that for the test specimen geometry the end of the connection plate weld was the most critical location. Fisher et al. noted that although cracking typically started at the end of the connection plate weld, the stress ranges at web-flange weld were generally higher. Stress ranges of 15 ksi were typically required at the web-flange weld to cause cracking.

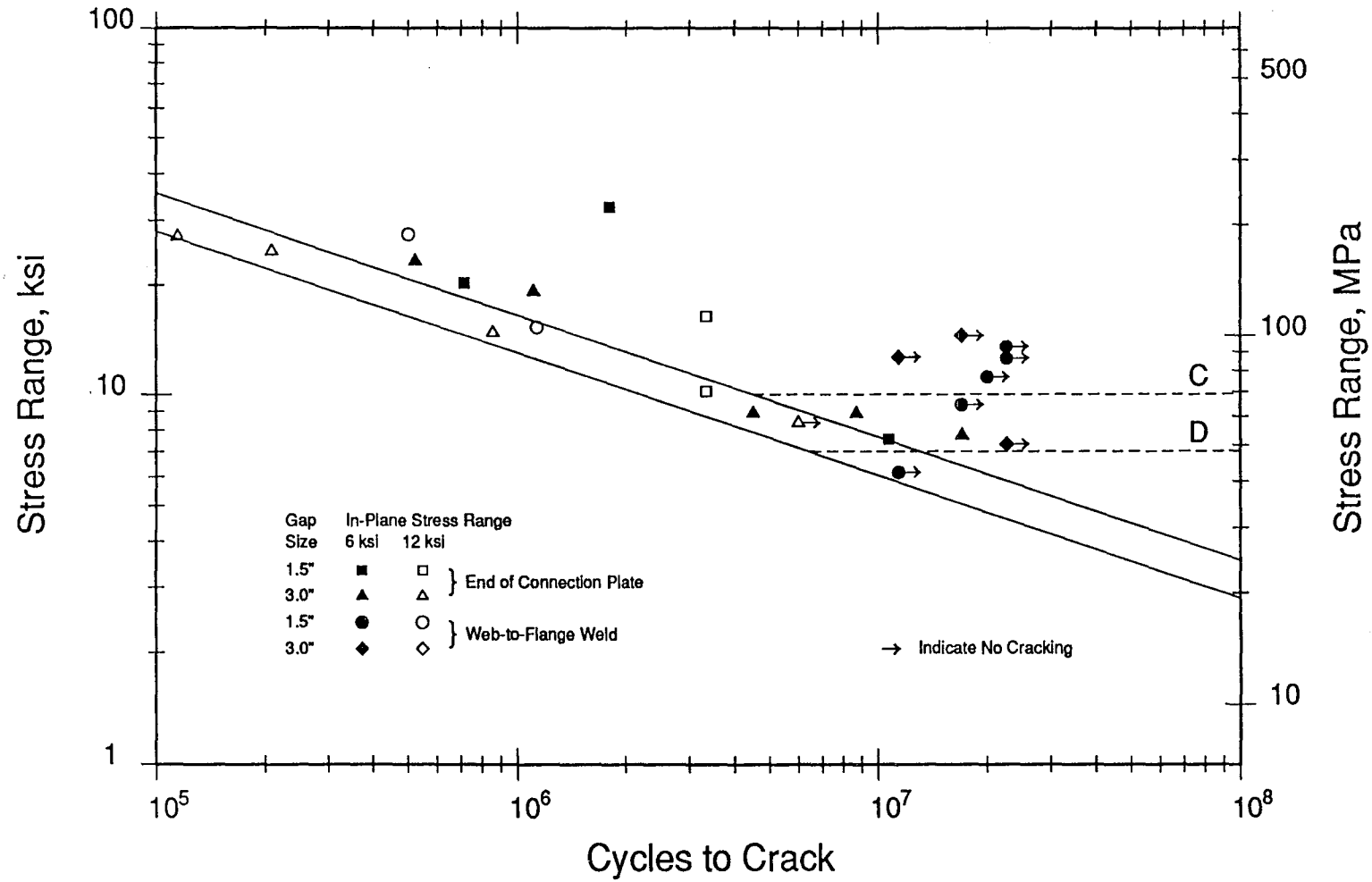

Figure 65. Fatigue Data Reported by Fisher et al. (1990) Illustrating the Fatigue Resistance of Connection Plate Details Subjected to Out-of-Plane Distortions

To evaluate the potential for fatigue cracking at the pier floorbeam-girder connections based on the measured stress ranges given in Chapter Six, fatigue limits of 10 ksi and 15 ksi will be used at the end of the connection plate weld and at the web-flange weld, respectively. For fatigue cracking to result from variable amplitude traffic loading, it is only necessary that a part of the applied stress ranges exceed the fatigue limit at one of the critical points in the connection. The maximum stress ranges that were recorded for trucks in the normal traffic stream will be used for comparison with the fatigue limits. These maximum stress ranges were observed over relatively short periods of time and can be expected to occur a significant number of times in the life of the bridge. The maximum recorded stress ranges do, however, require modification for stress concentration effects.

In the tests by Fisher et al. (1990), the web gap was large enough so that the web gap strain gages were placed along a vertical line matching the center of the connection plate. Because of this the stress ranges measured and extrapolated to the end of the connection plate weld and to the web-flange weld were good estimates of the maximum stress ranges occurring in the connection. The web gap strain gages used in the field tests reported in Chapter Six were shifted away from the centerline of the connection plate as shown in Figures 43 through 48. Finite element analyses performed by Reid (1991) as part of the project reported here indicate

that the maximum stress ranges in the pier floorbeam connections occur at the end of the connection plate and are approximately 1.8 times as large as the measured stress ranges extrapolated to the web-flange weld shown in Table 20, or 5 times as large as the measured stress ranges extrapolated to the end of the connection plate weld. Reid's results also indicate that the maximum stress range along the web-flange weld occurs at the centerline of the connection plate and is approximately 1.6 times larger than the measured stress ranges extrapolated to the web-flange weld in Table 20.

Multiplying the maximum stress ranges in Table 20 by the factors referenced above reveals that 2 of the 6 pier floorbeam connections listed in Table 20 experienced stress ranges large enough to cause fatigue cracking. These are the connection at the inside girder at pier S7-5 and the connection at the inside girder at pier S7-12. The maximum stress ranges at the inside girder at pier S7-5 are estimated to be 19 ksi (1.6 x 12 = 19) at the web-flange weld and 22 ksi (5 x 4.4 = 22, or 12 x 1.8 = 22) at the end of the connection plate. Each of these stress ranges exceed the fatigue limits. The maximum stress range at the end of the connection plate weld at the inside girder at pier S7-12 is estimated to be between 8 ksi (4.4 x 1.8 = 8) and 11 ksi (2.2 x 5 = 11). This stress range is also large enough to cause fatigue cracking. Cracking is not likely to occur at the other four connections listed in Table 20.

The above results are encouraging. The results indicate that cracking should not be expected at all pier locations in the future. However, the limited number of test results do not allow an accurate estimate of the percentage of the connections along the bridges that will experience cracking. Cracking can be expected in the future at both the inside and outside girders. This observation is based on the test results and the fact that cracking has already occurred at connections along both girders.

ASSESSMENT OF HOLE DRILLING AS A REPAIR METHOD

Past studies in the area of out-of-plane distortion induced fatigue cracking have resulted in guidelines for assessing the potential effectiveness of hole drilling as a repair method based on stress ranges for uncracked details. Fisher et al. (1990) concluded that hole drilling would effectively arrest fatigue cracks originating from the toe of a diaphragm-girder connection plate weld when the cyclic stress ranges were less than 15 ksi. This conclusion was based on lab tests conducted with a 6 ksi in-plane stress range which is characteristic of many simple span bridges where the critical web gap is at the bottom girder flange. Fisher et al. also indicated that based on past experience hole drilling is generally not effective as a permanent repair at floorbeam-girder connections of the type used in the Mobile Delta Crossing Bridges. However, based on the stress measurements at a short distance away from the connections shown in Table 20, it is likely that hole

drilling can be used effectively for a short term repair. Hole drilling should stop crack growth for a few years, but it is impossible to accurately estimate how long hole drilling will be effective.

An equation for calculating the hole size for use at crack tips was presented by Fisher et al. (1990) and is given as Equation 2 in Chapter Two. For the low in-plane stress ranges measured at the test locations, Equation 2 results in a very small hole diameter. A minimum hole diameter of one inch is recommended.

EFFECTIVENESS OF THE POSITIVE ATTACHMENT RETROFIT

Strain and displacement measurements were made at piers S7-5 and S7-9 before and after the positive attachment retrofit of Figure 4 and 5 was performed. The effectiveness of the positive attachment retrofit was judged on three indicators from the field tests: (1) the magnitudes of the strain and displacements measured during the calibration tests, (2) the average out-of-plane displacement of the web gap for random truck traffic data, and (3) the effective stress ranges at the number one gage on the outside girder web and the number two gage on the inside girder web.

Stress distribution plots for the static calibration tests illustrate the effects of the retrofit on the out-of-plane bending stresses in the web gap region. Figures 66 through 69 show the after retrofit stress distributions corresponding to the before retrofit stress distributions

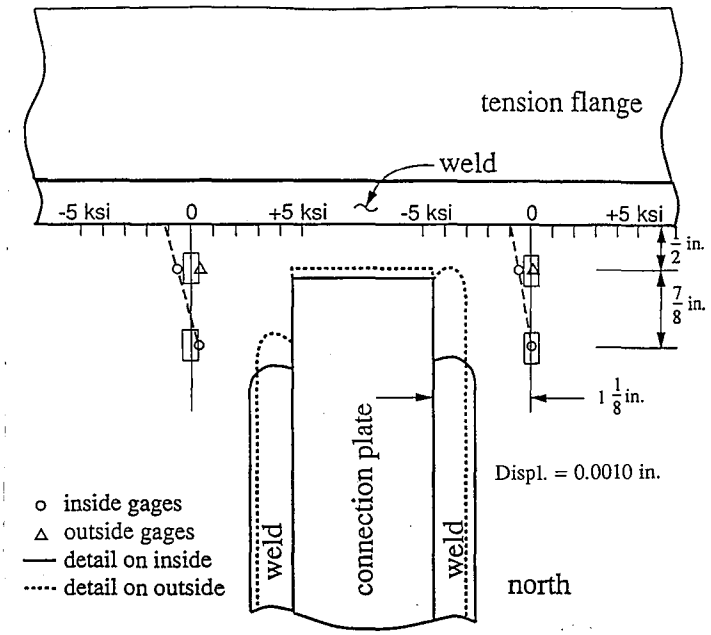

Figure 66. Static Stress Distribution on Outside Girder at Pier S7-5 (84 in. Girder) After Retrofit with Dump Truck in Outside Lane (Worst Case)

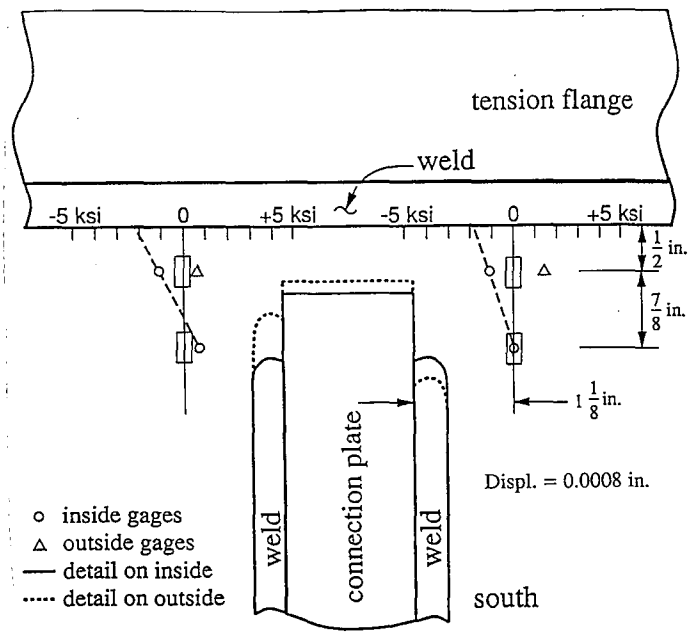

Figure 67. Static Stress Distribution on Inside Girder at Pier S7-5 (84 in. Girder) After Retrofit with Dump Truck in Outside Lane (Worst Case)

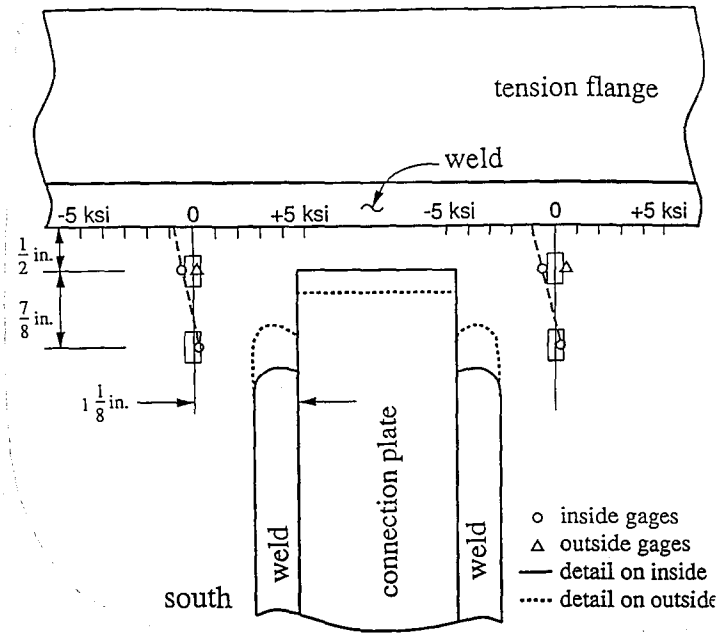

Figure 68. Static Stress Distribution on Outside Girder at Pier S7-9 (96 in. Girder) After Retrofit with Dump Truck in Outside Lane (Worst Case)

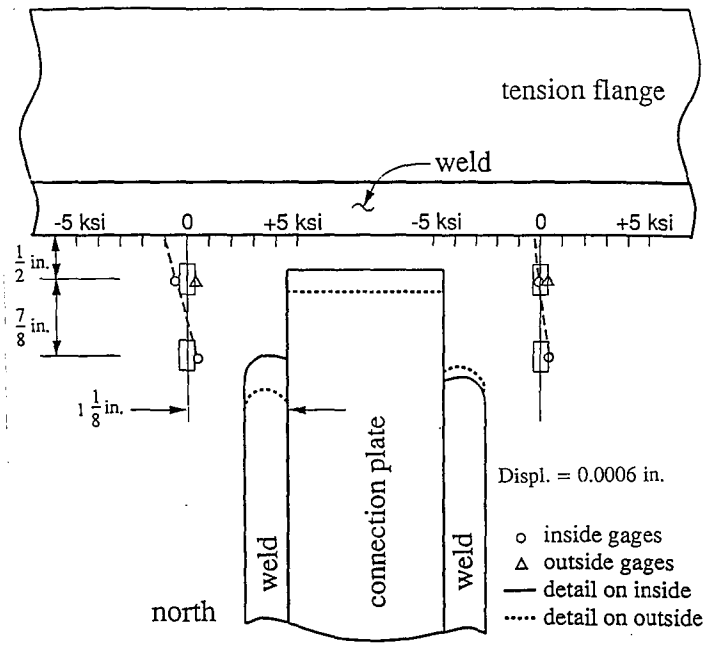

Figure 69. Static Stress Distribution on Inside Girder of Pier S7-9 (96 in Girder) After Retrofit with Dump Truck in Outside Lane (Worst Case)

shown in Figures 43, 44, 47 and 48. A comparison between these eight figures shows the effects of the retrofit under the controlled conditions of the static calibration tests. The greatest reduction in the stresses as a result of the retrofit occurred at the inside girder connection at pier S7-5. This observation is also illustrated by the summary of static calibration test results given in Table 21. At the inside girder at pier S7-5 the web gap stresses and displacement were reduced approximately 70%. The retrofit had only a small effect at the other three test locations where the stresses and displacements were initially small before the retrofit. In some cases the stresses and displacements appeared to increase after the retrofit. These changes are not significant and result primarily because the magnitude of the measurements were very small.

The plots of selected fast run calibration tests shown in Figures 70 through 73 graphically illustrate the effectiveness of the retrofit. In these figures, "B.R." after the gage name indicates the before retrofit response, and "A.R." indicates the after retrofit response. The zero strain levels of both responses were intentionally shifted in these plots so that each could be easily distinguished. Again, the plots illustrate that the retrofit had the greatest effect at the inside girder at pier S7-5 (Figure 71). Figures 72 and 73 show that the retrofit reduced the strains at the IN1 gages at pier S7-9 by approximately 50%.

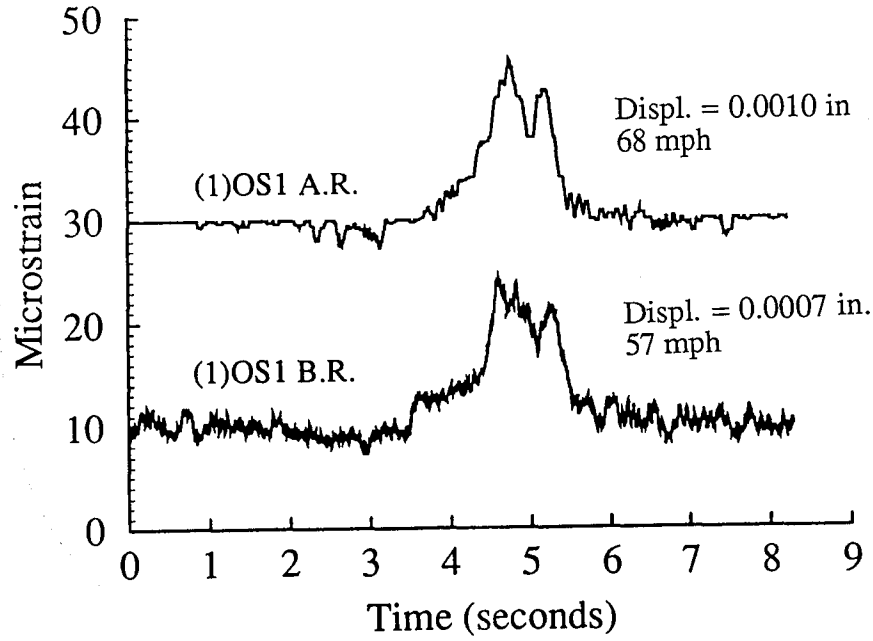

Figure 70. Before and After Retrofit Strain Responses for Gage OS1 on the Outside Girder of Pier S7-5 for the Lowboy Fast Run in the Outside Lane

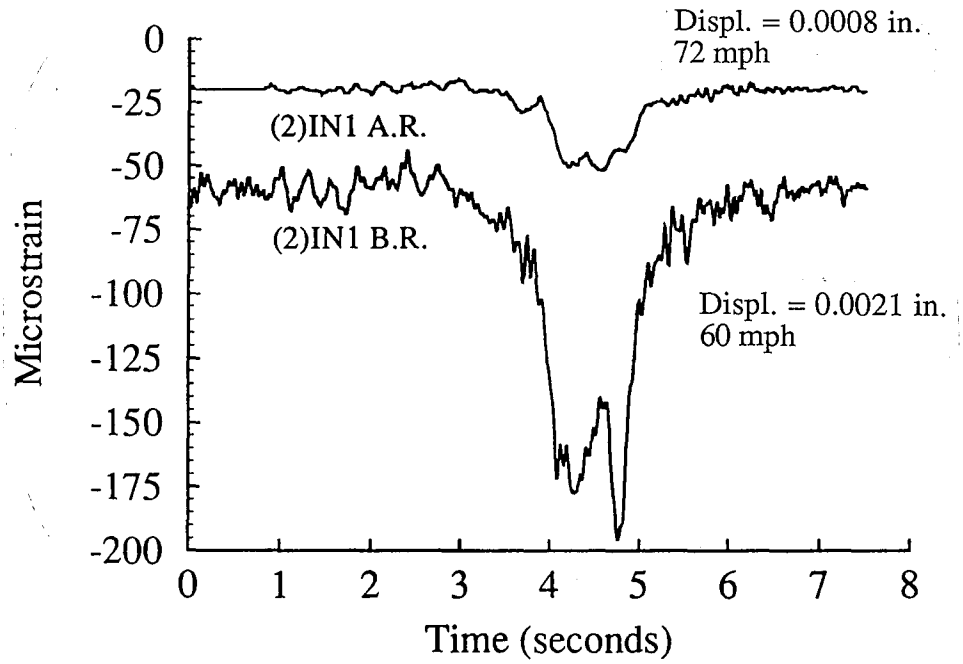

Figure 71. Before and After Retrofit Strain Responses for Gage IN1 on the Inside Girder of Pier S7-5 for the Lowboy Fast Run in the Inside Lane

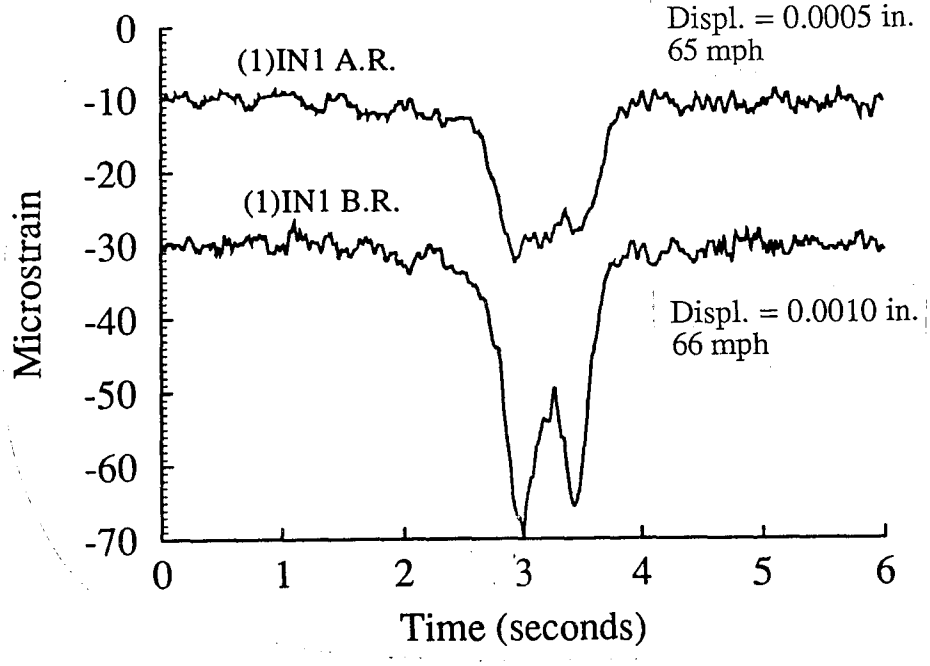

Figure 72. Before and After Retrofit Strain Responses for Gage IN1 on the Outside Girder of Pier S7-9 for the Lowboy Fast Run in the Outside Lane

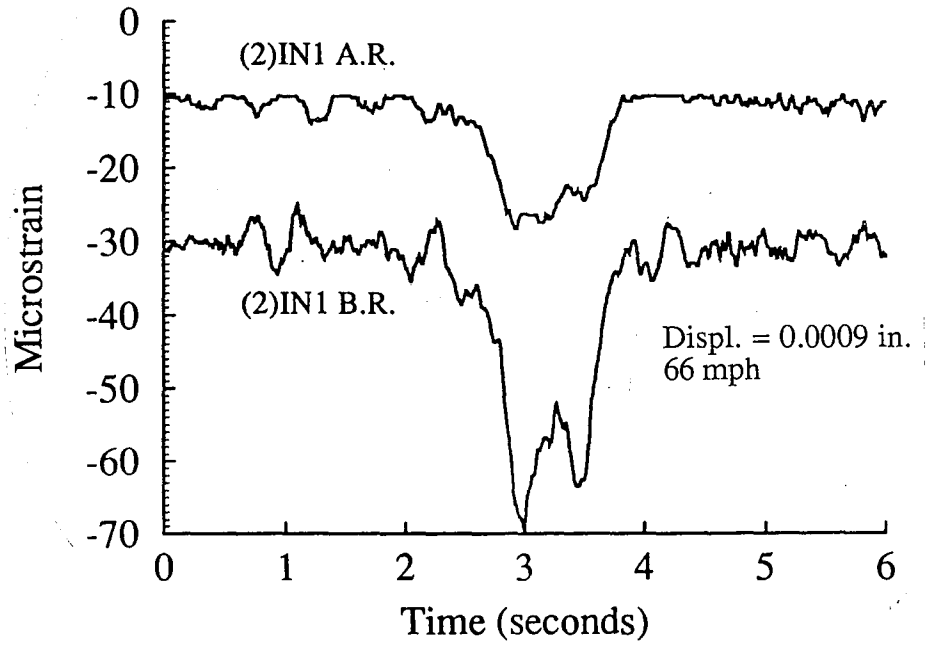

Figure 73. Before and After Retrofit Strain Responses for Gage IN1 on the Inside Girder of Pier S7-9 for the Lowboy Fast Run in the Outside Lane

Table 21. Static Calibration Test Results Before and After Positive Attachment Retrofit

Static Test			Outside Girder			Inside Girder		
Truck	Lane	Retrofit Status	IS1 ($\mu\epsilon$)	IS2 ($\mu\epsilon$)	LVDT (in.)	IS1 ($\mu\epsilon$)	IS2 ($\mu\epsilon$)	LVDT (in.)
S7-5 Pier Floorbeam Connections (84 in. Girders)								
lowboy	outside	before	-17	+12	0.0007	-103	+61	0.0025
lowboy	outside	after	-20	+8	0.0009	-34	-1	0.0007
lowboy	inside	before	-12	+9	0.0005	-115	+37	0.0023
lowboy	inside	after	-11	+7	0.0007	-32	+1	0.0009
dump trk	outside	before	-20	+13	0.0009	-135	+92	0.0035
dump trk	outside	after	-24	+7	0.0010	-40	-1	0.0008
dump trk	inside	before	-13	+13	0.0006	-127	+55	0.0029
dump trk	inside	after	-16	+8	0.0008	-34	+2	0.0010
S7-9 Pier Floorbeam Connections (96 in. Girders)								
lowboy	outside	before	-17	+6	0.0007	-14	+6	0.0008
lowboy	outside	after	-16	+8	N.A.*	+1	+11	0.0006
lowboy	inside	before	-11	+5	0.0007	-18	+8	0.0008
lowboy	inside	after	-12	+4	N.A.	+3	+10	0.0007
dump trk	outside	before	-13	+6	0.0008	-12	+8	0.0006
dump trk	outside	after	-18	+8	N.A.	-4	+13	0.0006
dump trk	inside	before	-11	+5	0.0007	-16	+9	0.0008
dump trk	inside	after	-14	+4	N.A.	+2	+13	0.0006

* Not available.

Table 22. Average and Standard Deviation of Out-of-Plane Displacements for Random Data at S7-5 Before and After the Positive Attachment Retrofit

Outside Girder		Inside Girder	
Average (in.)	Std. Dev. (in.)	Average (in.)	Std. Dev. (in.)
Pier S7-5 Before Retrofit			
+0.0005	+0.0002	+0.0017	+0.0007
Pier S7-5 After Retrofit			
+0.0006	+0.0002	+0.0005	+0.0002
Pier S7-9 Before Retrofit			
+0.0008	+0.0003	+0.0007	+0.0003
Pier S7-9 After Retrofit			
----	----	+0.0005	+0.0002

The connections at both girders at piers S7-5 and S7-9 were instrumented with LVDTs before and after the retrofit. The average and standard deviation of the measured out-of-plane displacements for the random data collected at each connection plate detail is listed in Table 22. Note that because of an equipment malfunction, displacement data is not available at the outside girder at S7-9 after retrofit. Figures 74 through 80 show histograms for each LVDT entry in Table 22. Inspection of the table and histograms illustrates that the inside girder web gap on S7-5 experienced significant reductions of approximately 70% in out-of-plane displacements as a result of the positive attachment retrofit.

Effective stress ranges based on linear extrapolation to the end of the connection plate and to the web-flange weld before and after the retrofit were not determined. More direct comparisons were made between the effective stress ranges both before and after the retrofit at the strain gage locations nearest the two critical locations. These locations were the number one gage on the outside of the girder web and the number two gage on the inside of the girder web. Table 23 lists the effective stress ranges at these gage locations for each floorbeam-girder connection detail. Histograms for each entry in Table 23 are shown in Figures 81 through 96. A comparison between the before and after retrofit data reveals significant reductions in the effective stress range on the inside girder at S7-5. The

Table 23. Effective Stress Ranges at Gages OS1 and IS2 for Random Data Before and After Retrofit

Outside Girder		Inside Girder	
OS1 (ksi)	IS2 (ksi)	OS1 (ksi)	IS2 (ksi)
Pier S7-5 Before Retrofit (670 Trucks)			
+0.4	+0.3	+2.0	+1.2
Pier S7-5 After Retrofit (318 Trucks)			
+0.3	+0.3	+0.9	+0.1
Pier S7-9 Before Retrofit (550 Trucks)			
+0.1	+0.2	+0.1	+0.2
Pier S7-9 After Retrofit (273 Trucks)			
+0.2	+0.2	+0.3	+0.3

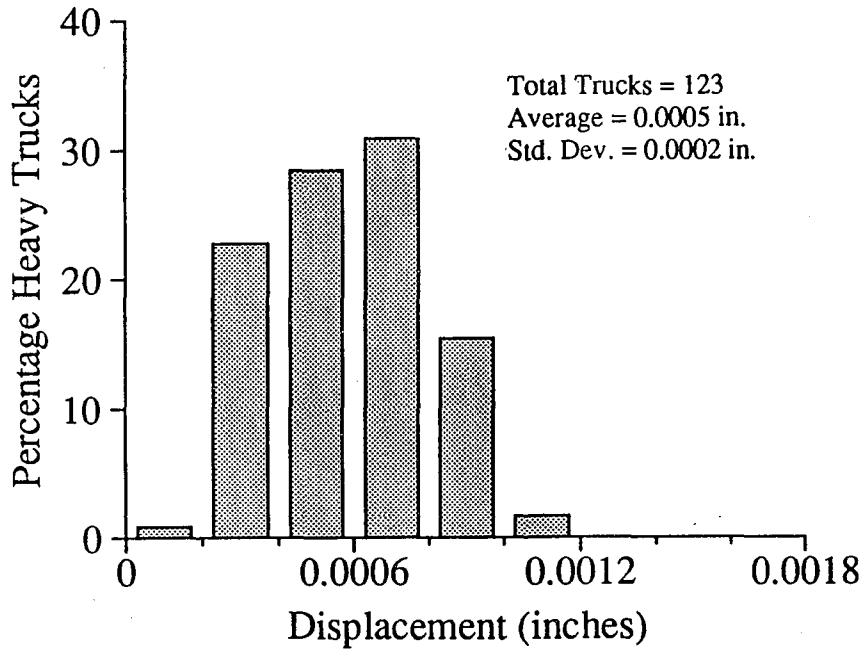

Figure 74. Histogram of Out-of-Plane Displacement of the Outside Girder Web Gap at Pier S7-5 Before Retrofit

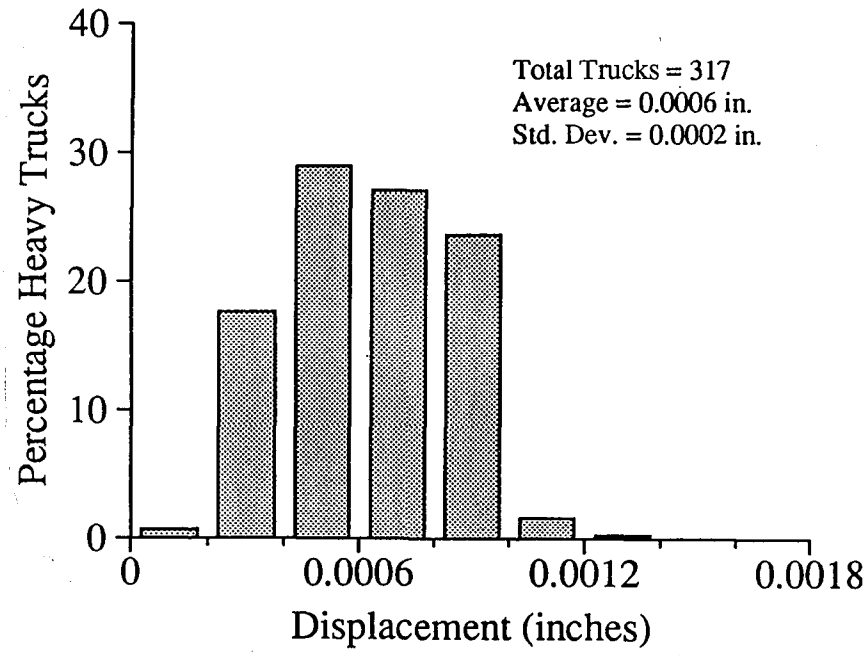

Figure 75. Histogram of Out-of-Plane Displacement of the Outside Girder Web Gap at Pier S7-5 After Retrofit

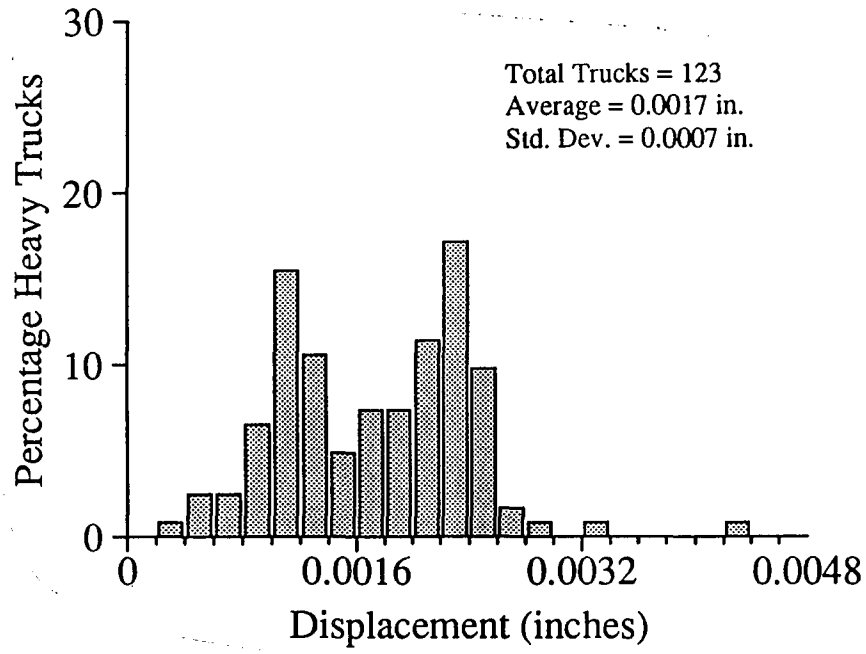

Figure 76. Histogram of Out-of-Plane Displacement of the Inside Girder Web Gap at Pier S7-5 Before Retrofit

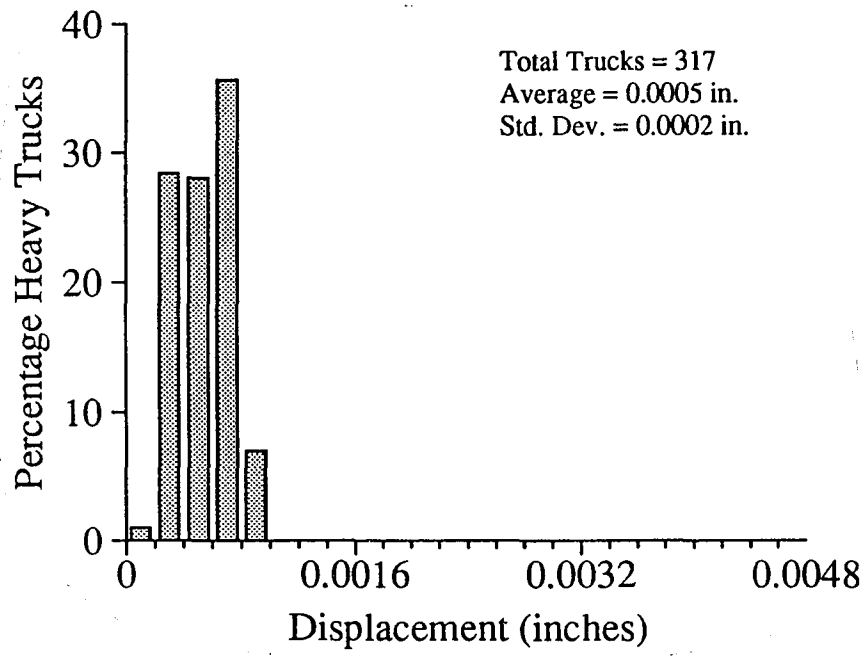

Figure 77. Histogram of Out-of-Plane Displacement of the Inside Girder Web Gap at Pier S7-5 After Retrofit

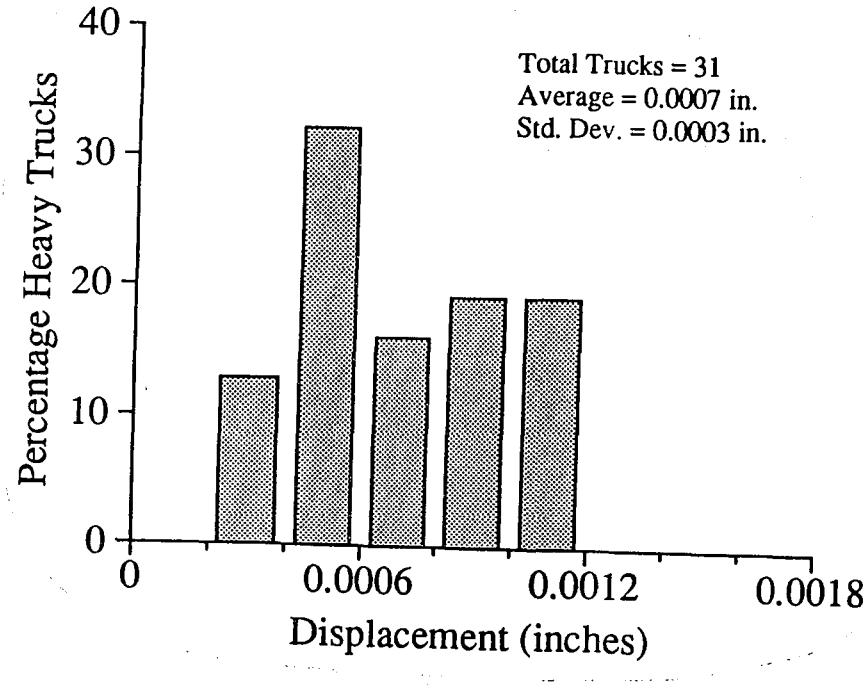

Figure 78. Histogram of Out-of-Plane Displacement of the Inside Girder Web Gap at Pier S7-9 Before Retrofit

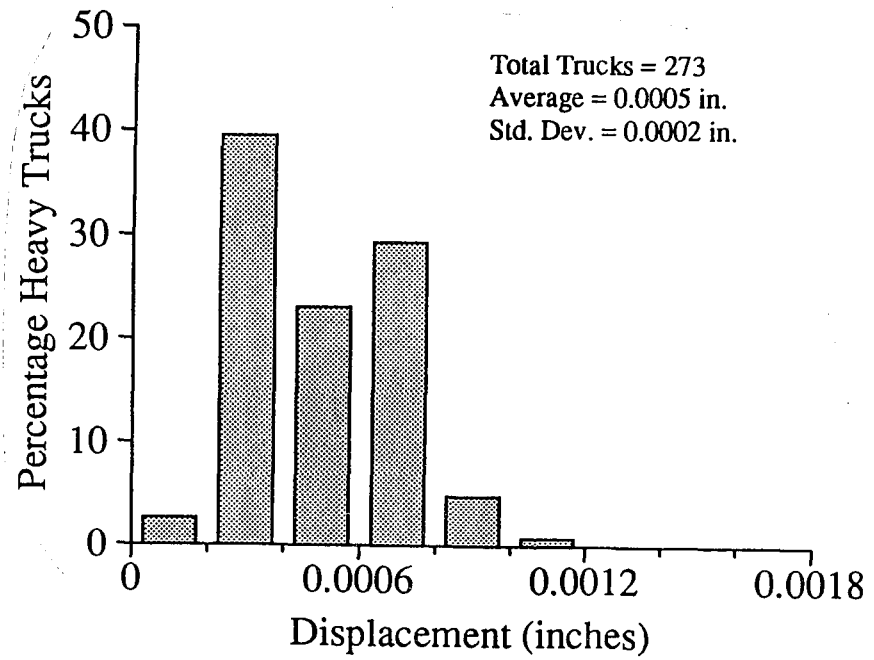

Figure 79. Histogram of Out-of-Plane Displacement of the Inside Girder Web Gap at Pier S7-9 After Retrofit

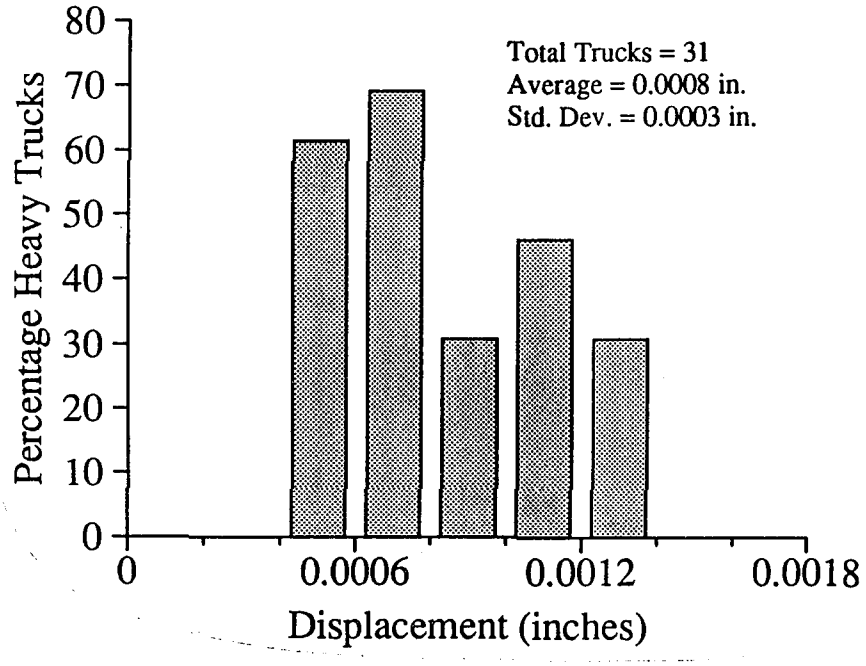

Figure 80. Histogram of Out-of-Plane Displacement of the Outside Girder Web Gap at Pier S7-9 Before Retrofit

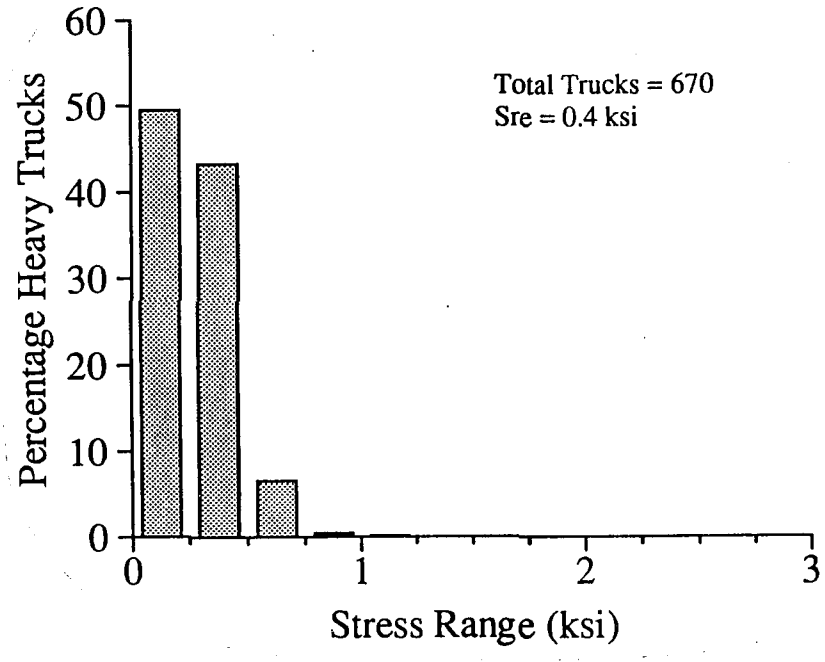

Figure 81. Histogram of the Random Data for Gage OS1 on the Outside Girder at S7-5 Before Retrofit

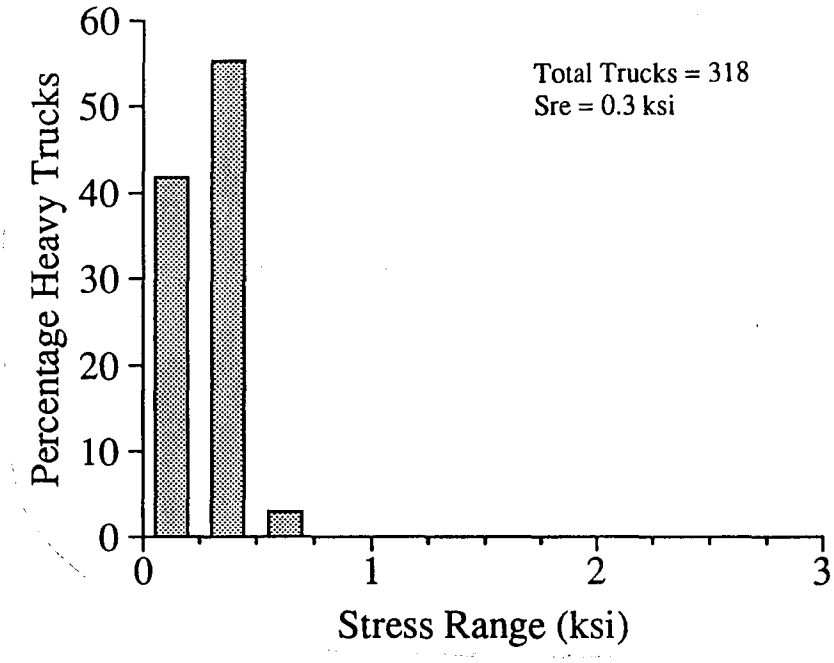

Figure 82. Histogram of the Random Data for Gage OS1 on the Outside Girder at S7-5 After Retrofit

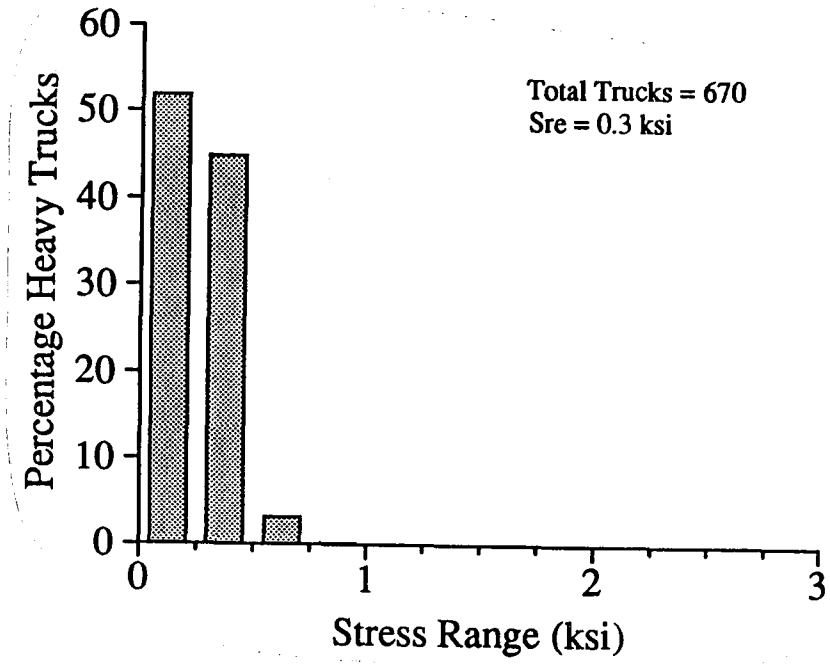

Figure 83. Histogram of the Random Data for Gage IS1 on the Outside Girder at S7-5 Before Retrofit

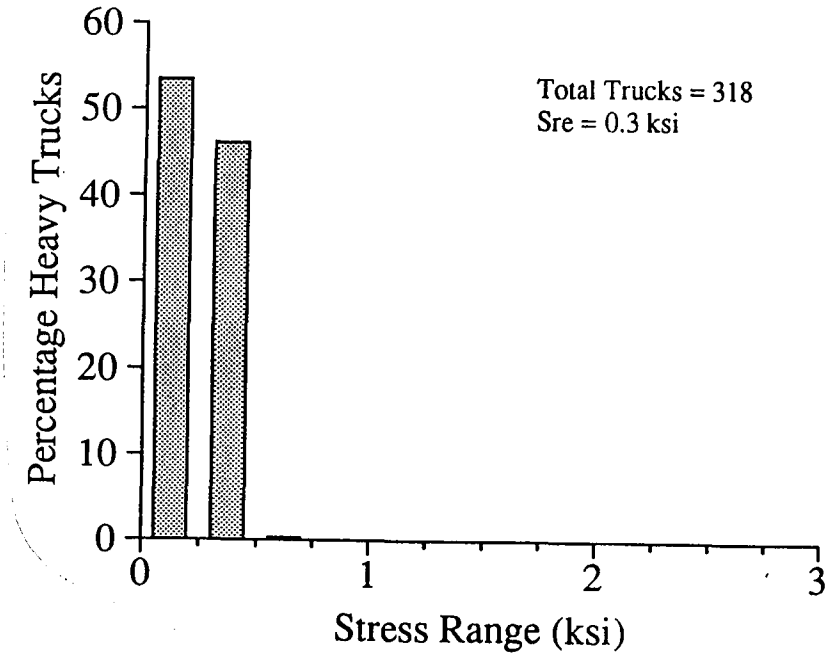

Figure 84. Histogram of the Random Data for Gage IS2 on the Outside Girder at S7-5 After Retrofit

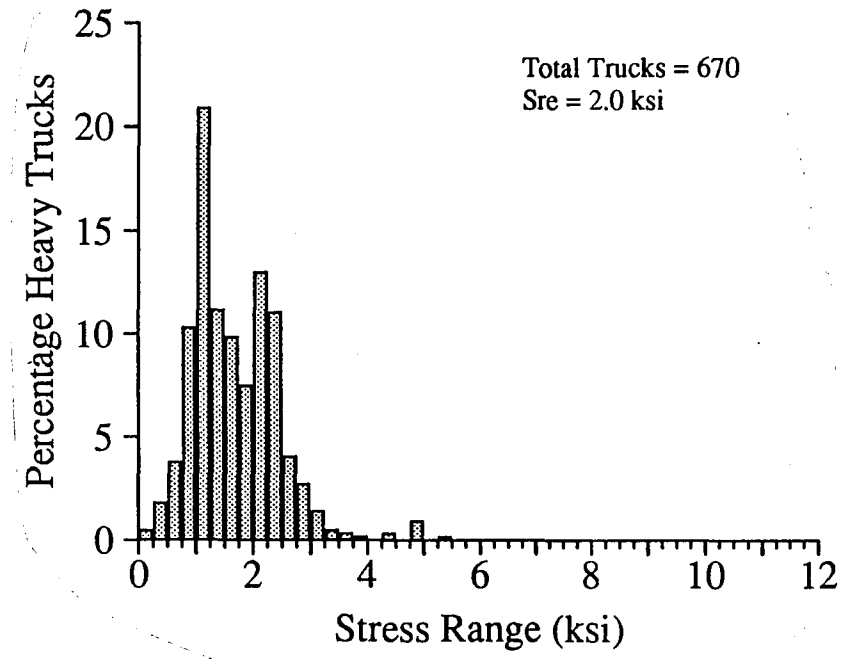

Figure 85. Histogram of the Random Data for Gage OS1 on the Inside Girder at S7-5 Before Retrofit

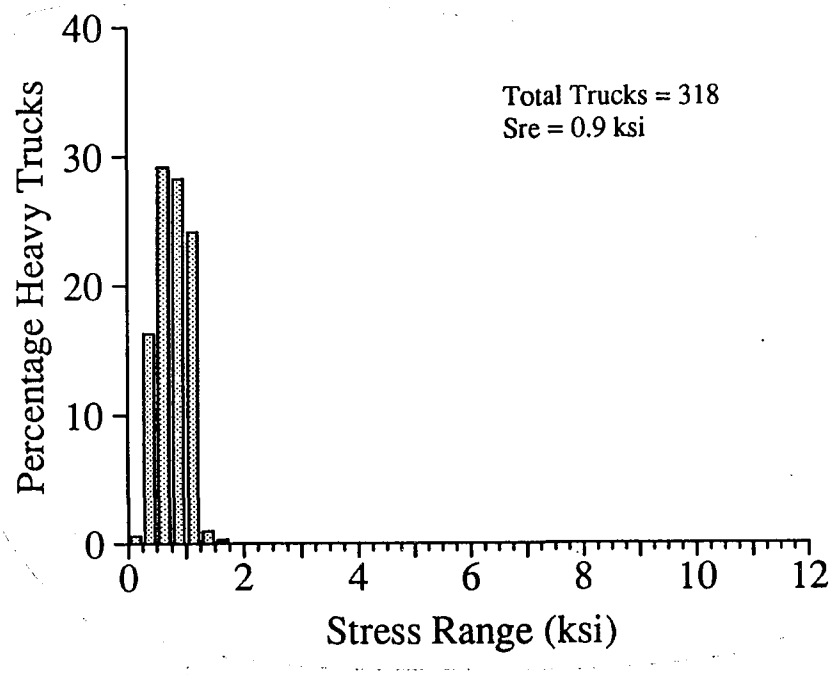

Figure 86. Histogram of the Random Data for Gage OS1 on the Inside Girder at S7-5 After Retrofit

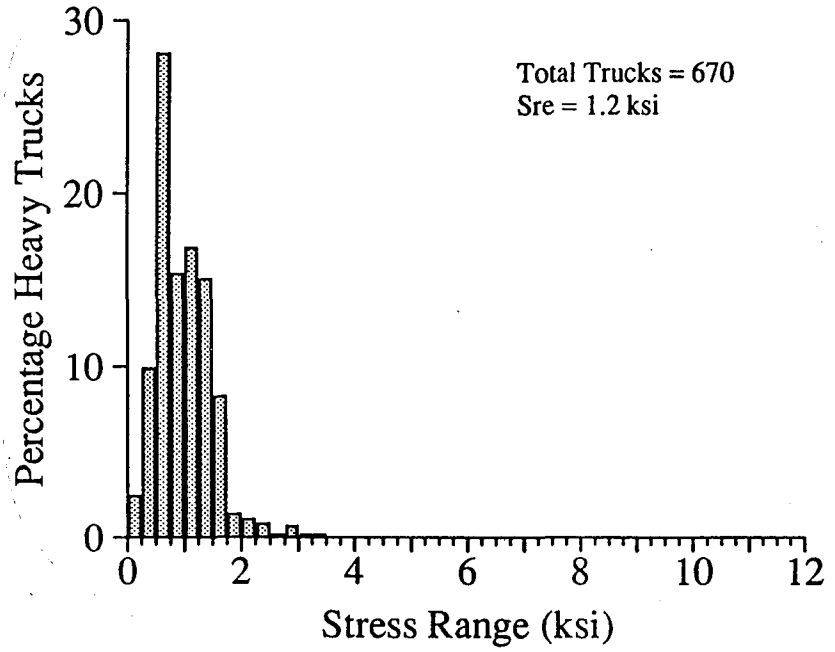

Figure 87. Histogram of the Random Data for Gage IS2 on the Inside Girder at S7-5 Before Retrofit

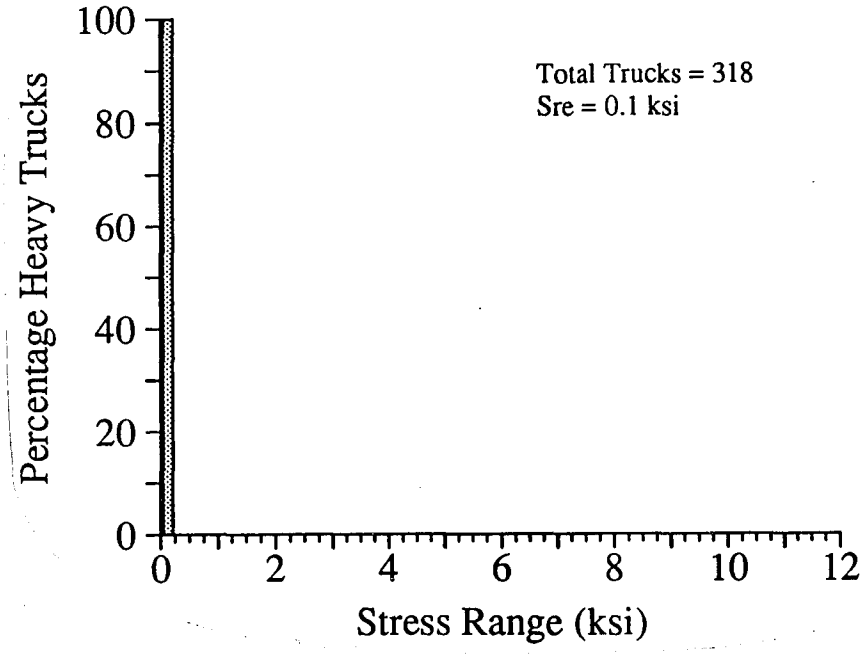

Figure 88. Histogram of the Random Data for Gage IS2 on the Inside Girder at S7-5 After Retrofit

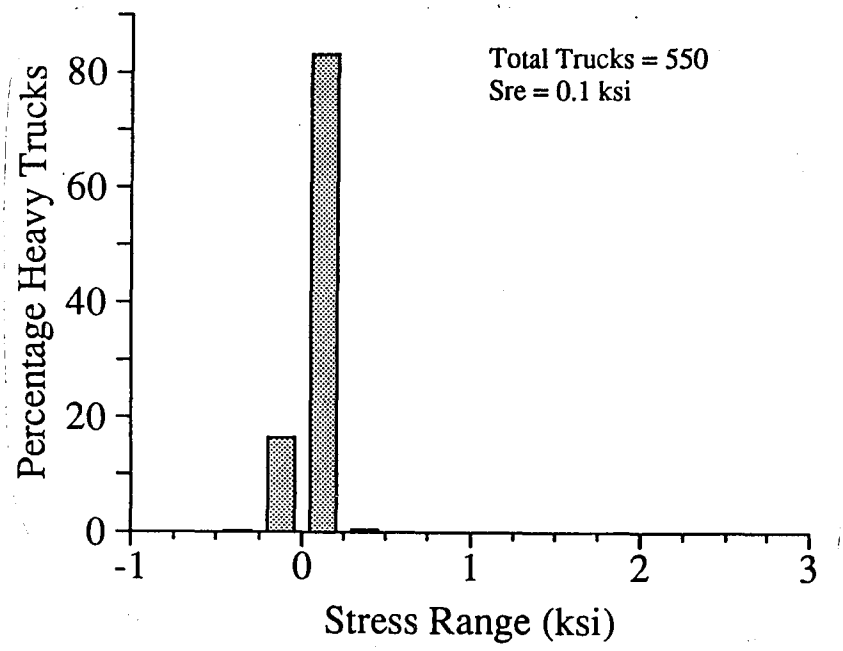

Figure 89. Histogram of the Random Data for Gage OS1 on the Outside Girder at S7-9 Before Retrofit

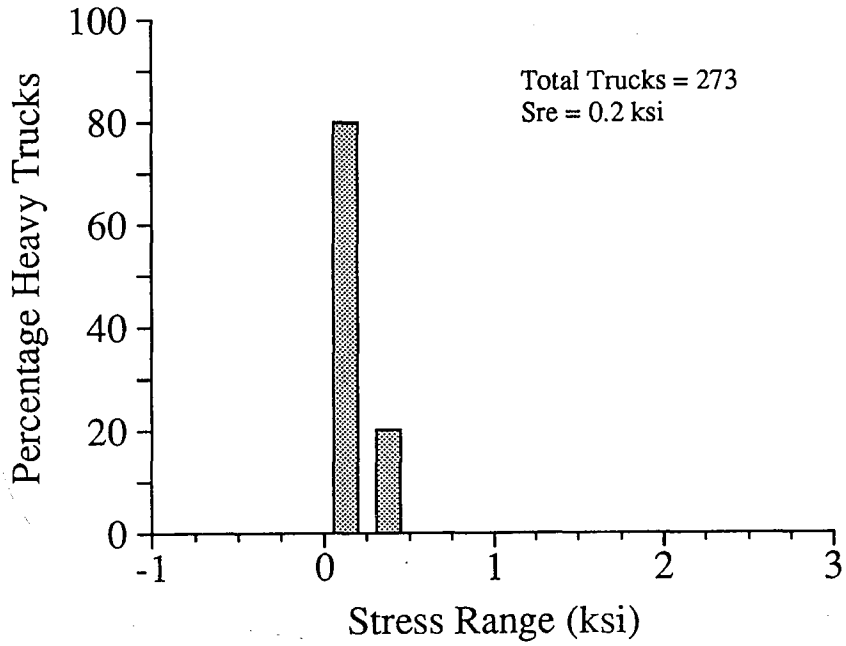

Figure 90. Histogram of the Random Data for Gage OS1 on the Outside Girder at S7-9 After Retrofit

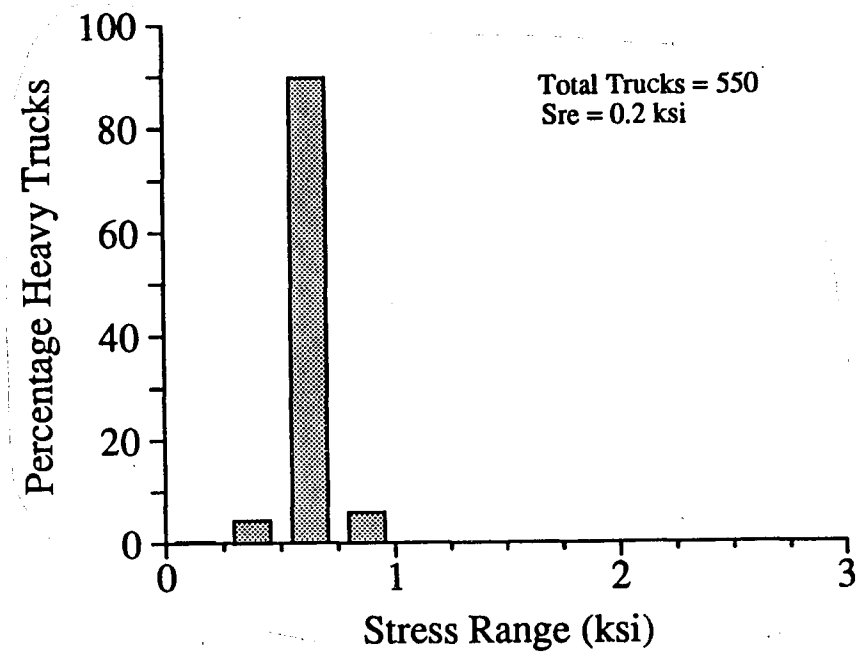

Figure 91. Histogram of the Random Data for Gage IS2 on the Outside Girder at S7-9 Before Retrofit

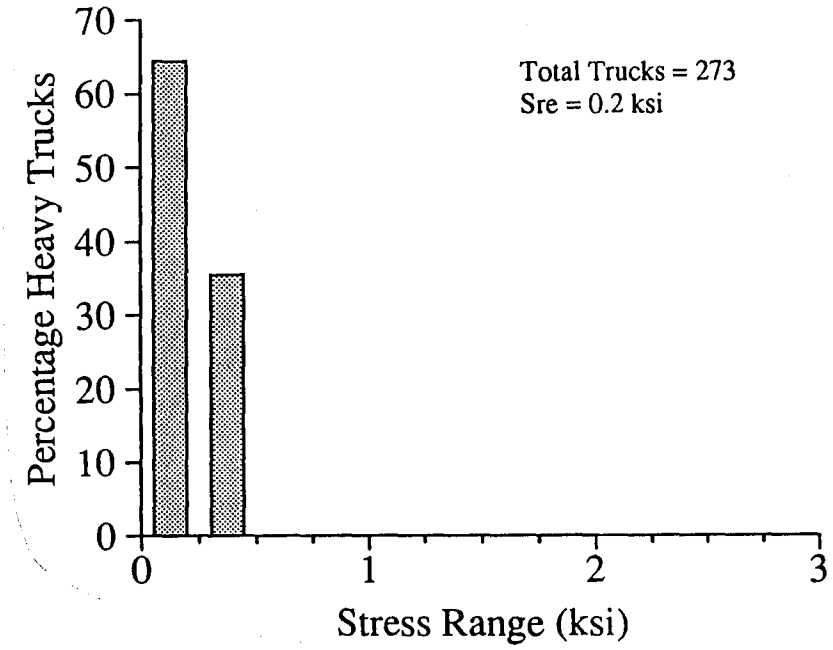

Figure 92. Histogram of the Random Data for Gage IS2 on the Outside Girder at S7-9 After Retrofit

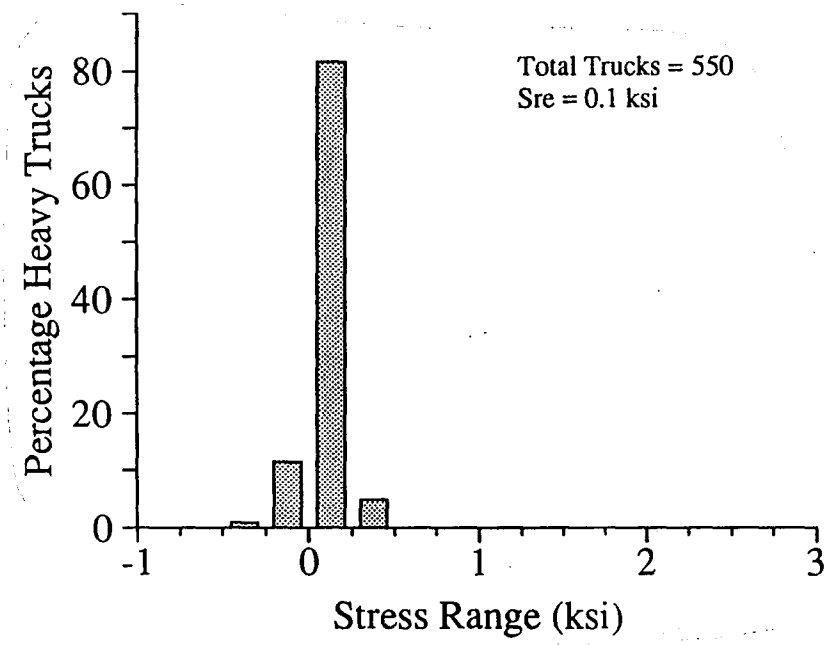

Figure 93. Histogram of the Random Data for Gage OS1 on the Inside Girder at S7-9 Before Retrofit

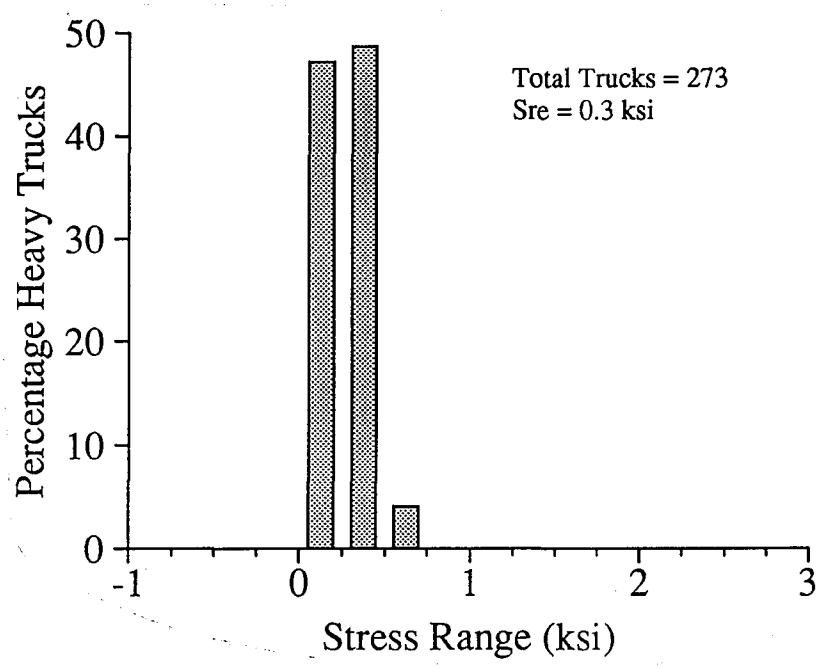

Figure 94. Histogram of the Random Data for Gage OS1 on the Inside Girder at S7-9 After Retrofit

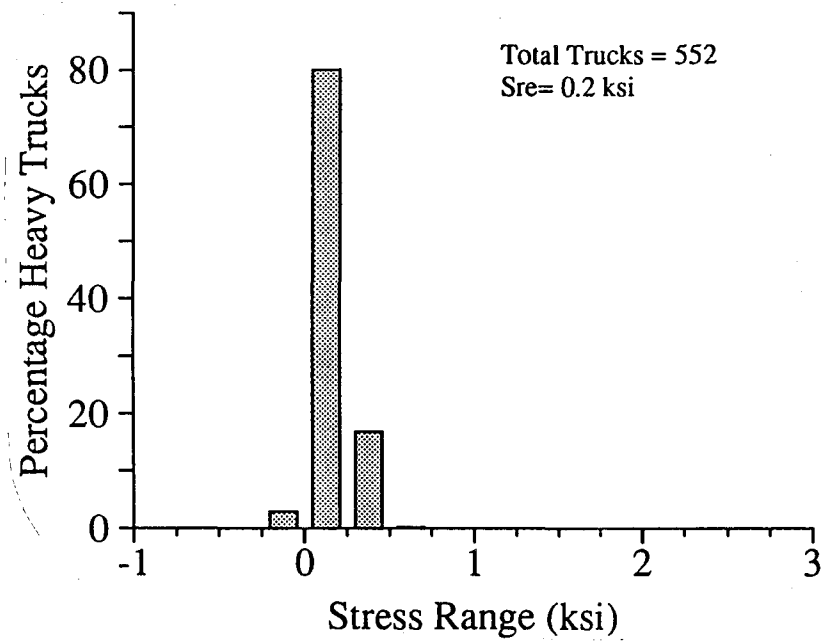

Figure 95. Histogram of the Random Data for Gage IS2 on the Inside Girder at S7-9 Before Retrofit

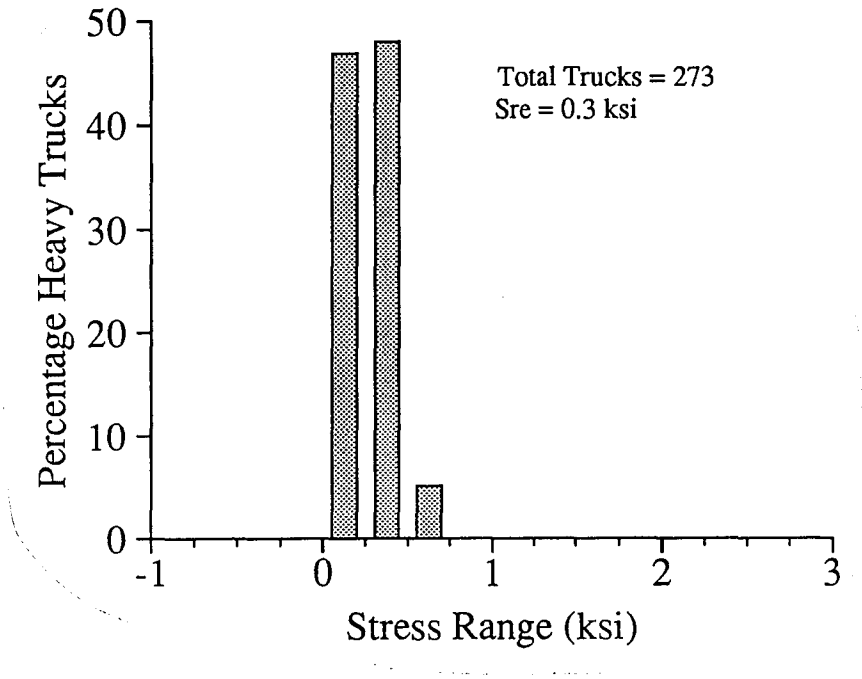

Figure 96. Histogram of the Random Data for Gage IS2 on the Inside Girder at S7-9 After Retrofit

retrofit had little effect at the other locations.

In summary, the positive attachment retrofit was found to be effective in reducing the out-of-plane displacements and bending stresses at the inside girder at pier S7-5. At that location reductions in stresses and displacements were approximately 70%. Results presented in Chapter Six indicate that the stresses before retrofit at the inside girder at pier S7-5 were large enough to cause fatigue cracking. The stresses at the critical locations for fatigue crack initiation are not large enough to cause cracking after the 70% reduction resulting from the retrofit. The retrofit when combined with hole drilling as suggested by Fisher et al. (1990) can also be expected to stop crack growth after distortion-induced cracking has occurred.

The positive attachment had a smaller effect at the other three locations where tests were performed. However, the stresses at these locations before retrofit were not large enough to cause cracking. These observations indicate that the positive attachment retrofit does not eliminate the out-of-plane displacement, but limits the magnitude. The test data indicates that out-of-plane displacements of up to 0.001 in. can be expected after the positive attachment is installed.

CHAPTER EIGHT
RESULTS AT FLOORBEAM CONNECTIONS AWAY FROM PIERS

An investigation of the potential for future cracking at floorbeam-girder connections away from the pier was based on the same methods used in Chapters Six and Seven. The potential for cracking was investigated at the first and second floorbeams away from piers S5-2 and S7-12. These locations are referred to here as floorbeams two and three. Field measurements were made at connections to the outside girder at S5-2 and at connections to the inside girder at S7-12.

RESULTS AT FLOORBEAM TWO

Calibration Test Results

Static stress distributions from calibration tests at floorbeam two connections are shown in Figures 97 and 98. These figures also illustrate the strain gage locations and geometry of the web gap region. Note that there were no connection plates on the outside face of the girder web at the floorbeam two and three locations. The stress distributions shown in Figures 97 and 98 are for the calibration test cases which produced the highest tension stresses in the web gap. These worst case stress distributions were produced by the dump truck positioned over floorbeam two in the outside lane. The largest tension stresses at each connection occur on the outside face of the

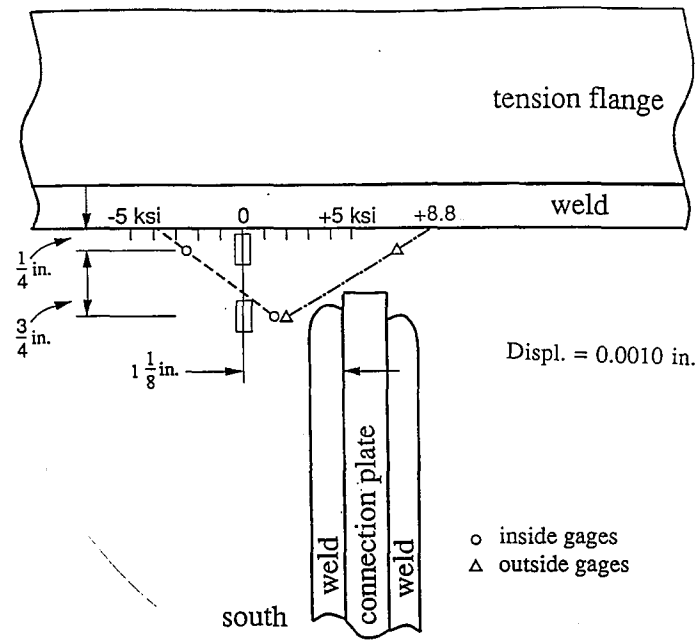

Figure 97. Static Stress Distribution for Outside Girder at Pier S5-2 Floorbeam Two with Dump Truck in Outside Lane (Worst Case)

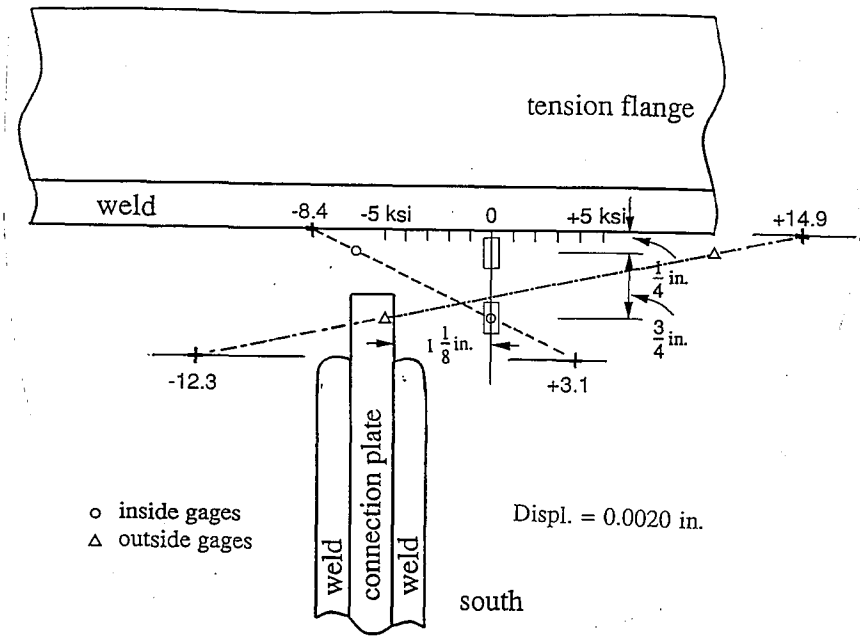

Figure 98. Static Stress Distribution for Inside Girder at Pier S7-12 Floorbeam Two with Dump Truck in Outside Lane (Worst Case)

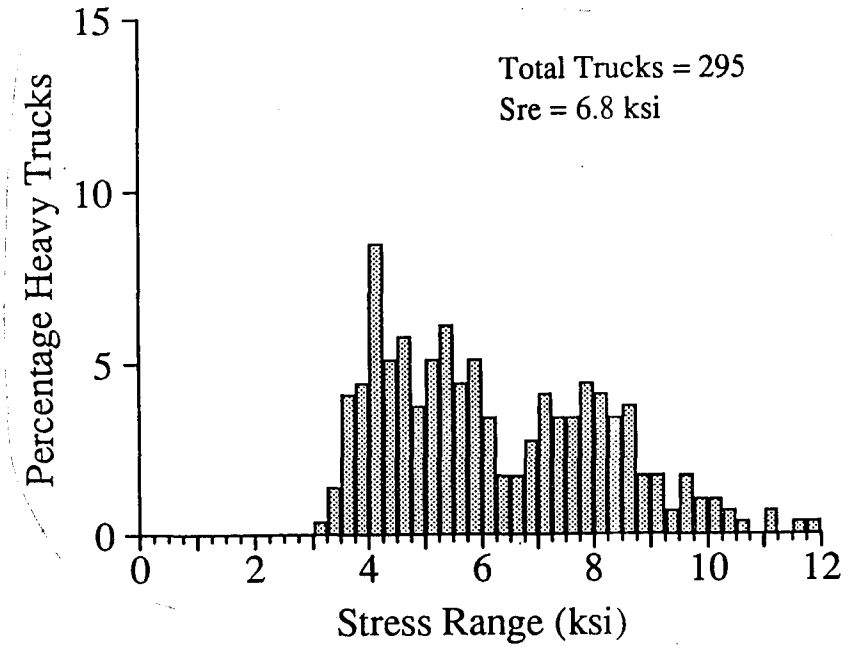

Figure 99. Histogram of Extrapolated Random Data at the Outside Web-Flange Weld on the Outside Girder at Pier S5-2 Floorbeam Two

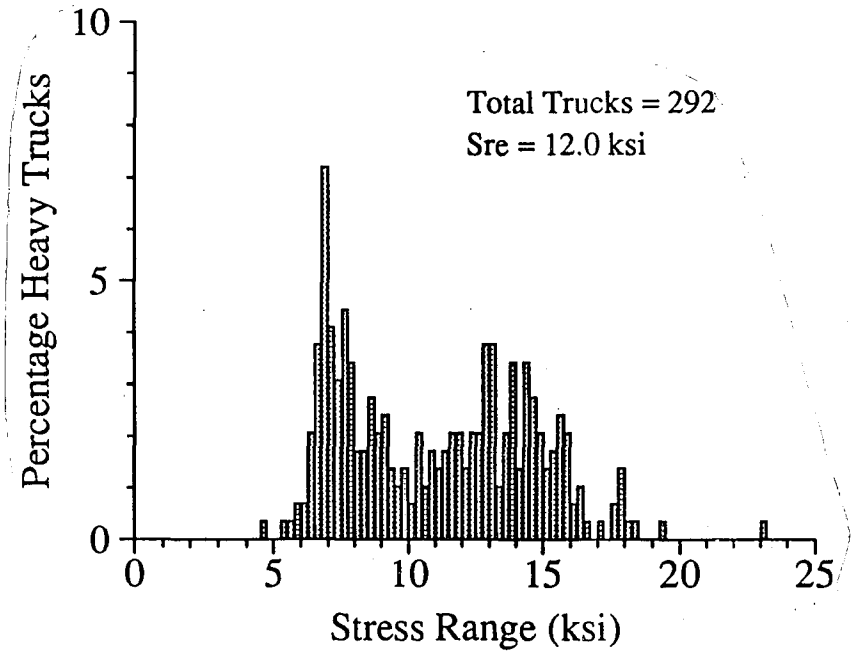

Figure 100. Histogram of Extrapolated Random Data at the Outside Web-Flange Weld Toe on the Inside Girder at Pier S7-12 Floorbeam Two

web at the web-flange weld. By linear extrapolation the maximum tension stress was found to be 8.8 ksi at S5-2 and 14.9 ksi at S7-12. A summary of the web gap strains and displacements recorded from the static calibration tests is given in Table 24.

Results from the fast run calibration tests with the lowboy test truck are shown in Table 25. The stress ranges shown in Table 25 were determined by linear extrapolation from stress ranges recorded at the strain gage locations. The stress ranges shown in the column "Outside Conn. Plate Weld" were extrapolated to the vertical location of the end of the inside connection plate using the stress ranges measured on the outside of the web. However, there is no connection plate on the outside. The stress ranges shown in Table 25 for the connection at S5-2 follow a pattern that is different from the results previously presented in this report. Note that the largest stress ranges were produced by the test truck in test lane C instead of test lane B. This results because the stress reversal created by the test truck moving from end-to-end of the continuous bridge span has a more significant effect on web gap stress range at floorbeams away from the piers.

Effective Stress Ranges from Truck Traffic

The calibration test results indicate that the highest tension stresses occur at the outside web-flange weld. Random truck crossing data were used to calculate Miner's effective stress ranges at this location. The effective stress range

Table 24. Static Calibration Test Results at Floorbeam Two for Test Trucks over Floorbeam Two

Static Test						
Truck	Lane	IS1 ($\mu\epsilon$)	IS2 ($\mu\epsilon$)	OS1 ($\mu\epsilon$)	OS2 ($\mu\epsilon$)	LVDT (in.)
S5-2 Floorbeam Two Connections (84 in. Girder)						
lowboy	outside	-61	+28	+155	+40	+0.0006
lowboy	inside	-65	+25	+151	+37	+0.0007
dump truck	outside	-93	+47	+245	+67	+0.0010
dump truck	inside	-94	+36	+220	+57	+0.0010
S7-12 Floorbeam Two Connections (96 in. Girder)						
lowboy	outside	-171	+4	+265	-143	+0.0016
lowboy	inside	-138	-12	+210	-87	+0.0011
dump truck	outside	-217	-1	+343	-169	+0.0020
dump truck	inside	-194	-9	+298	-130	+0.0016

Table 25. Stress Ranges at Critical Locations for Lowboy Test Truck

Test	Inside Conn. Plate Weld Sr (ksi)	Inside Web-Flange Weld Sr (ksi)	Outside Conn. Plate Weld Sr (ksi)	Outside Web-Flange Weld Sr (ksi)
S5-2 Floorbeam Two Connection (84 in. Girder)				
Max Random	N.A.†	N.A.	+4.7	+12
Test Lane B	+0.4	-5.1	+2.9	+9.6
Test Lane C	+0.5	-6.2	+3.4	+11.2
Lane B+C	+0.9	-11.3	+6.3	+20.8
S7-12 Floorbeam Two Connection (96 in. Girder)				
Max Random	N.A.	N.A.	-23.4	+23.2
Test Lane B	+5.1	-8.7	-13.1	+15.9
Test Lane C	+3.8	-9.3	-10.5	+13.6
Lane B+C	+8.9	-18.0	-23.5	+29.5

† Not available.

for S5-2 was 6.8 ksi, and for S7-12 the effective stress range was 12 ksi. Histograms of the data used for the effective stress range calculations are shown in Figures 99 and 100.

Only 24 random truck crossings were available for the inside gages from which stress ranges could be extrapolated to the end of the connection plate welds. These 24 truck records were used to correlate the stress at the end of the inside connection plate weld with the stress at the corresponding location on the outside face of the girder web. For each truck record, a ratio of the stress range at the end of the inside connection plate weld to the stress range at the corresponding location on the outside face of the girder web was determined. The average ratio was then used to estimate the stress range at the end of the inside connection plate weld from strain gage data for the outside face of the girder web. The results indicated that the stress range at the end of the inside connection plate weld at S5-2 was on the average 5.9 times lower (4.5 to 7.6) than the stress range at the corresponding location on the outside face of the girder web. The stress range at S7-12 on the inside was on the average 3.2 times lower (2.6 to 3.5) in magnitude than on the outside, and opposite in sign. By applying these ratios to the effective stress range calculation, the effective stress range at the inside connection plate weld was estimated to be +0.4 ksi at S5-2 and 4.3 ksi at S7-12. The effective stress ranges at all locations mentioned above

are shown in Table 26. Figures 101 and 102 show stress range histograms for the stress ranges at the location of the end of the connection plate weld on the outside face of the web.

Histograms of the out-of-plane displacements measured at S5-2 and S7-12 are shown in Figures 103 and 104. The average and standard deviation of the displacement measurements is also shown in the figures.

In-plane bending stresses were measured on the tension flange and on the girder web near the web gap at the floorbeam two test locations. The maximum stress range measured for approximately 300 truck crossings at each pier location was 0.5 ksi. The low in-plane stresses at the tension (top) flange match the behavior observed at the pier floorbeam connections.

Potential for Distortion-Induced Fatigue Cracking

The sum of the stress ranges measured during the lowboy fast run calibration tests in test lanes B and C provide a good estimate of the stress range that would result from side-by-side truck crossings. These stress ranges are shown in rows labeled "Lane B + C" in Table 25. These stress ranges provide an approximate limit on the stress ranges that can be expected to result from normal legal truck traffic. The maximum random stress ranges shown in Table 25 were measured for trucks in the normal traffic stream. Comparisons of the stress ranges shown in rows "Max. Random" and "Lane B + C" against the fatigue limits at the critical locations provide an indication of the potential for fatigue

Table 26. Effective Stress Ranges at Critical Locations at Floorbeam Two

Pier Location	Outside Web-Flange Weld Sre (ksi)	Outside Face at Location of Connection Plate Weld Sre (ksi)	Inside Connection Plate Weld Sre (ksi)
S5-2	+6.8	+2.1	+0.4*
S7-12	+12.0	-13.8	+4.3*

* Estimated from stress range at location of connection plate weld on outside face of web.

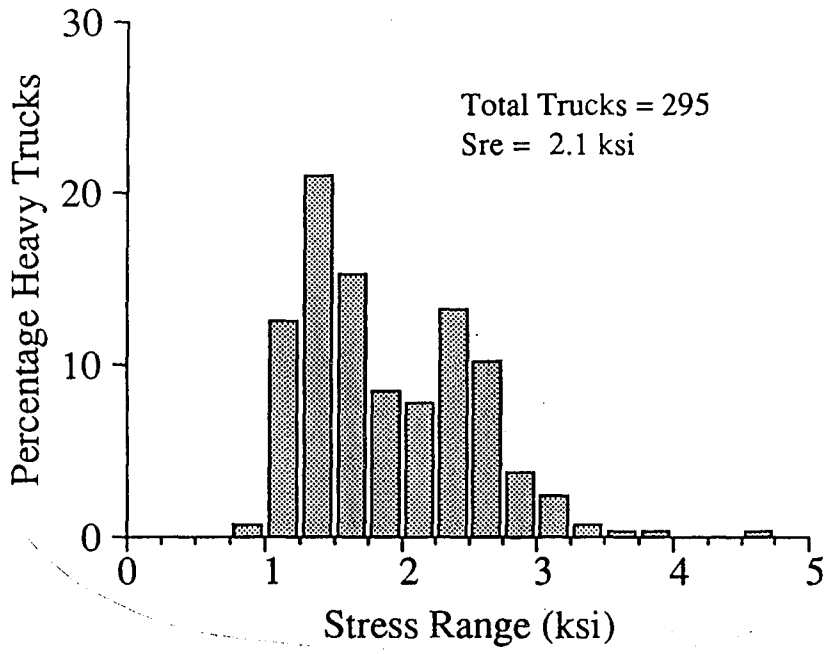

Figure 101. Histogram of Extrapolated Random Data at the Location of the Floorbeam Two Connection Plate Weld on the Outside Face of the Girder at S5-2

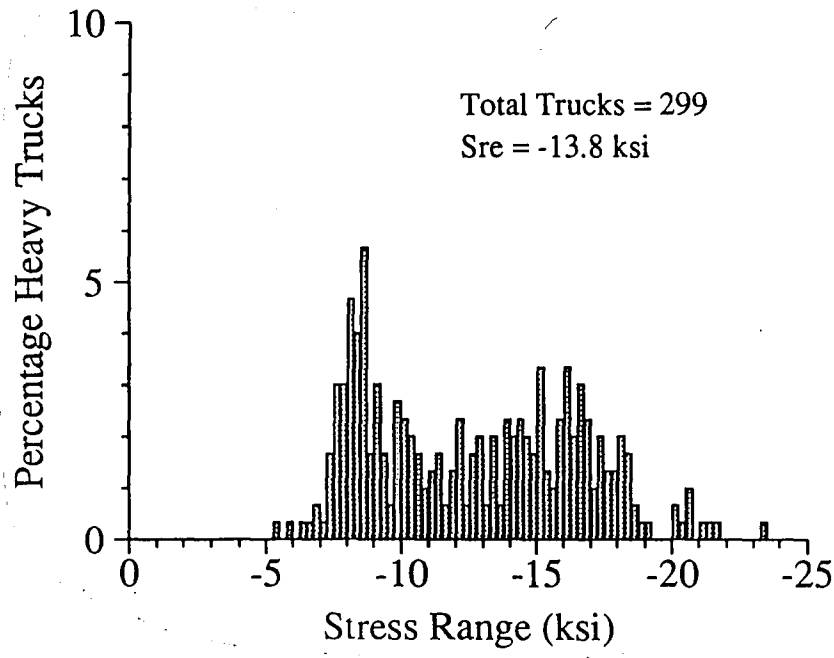

Figure 102. Histogram of Extrapolated Random Data at the Location of Floorbeam Two Connection Plate Weld on the Outside Face of the Girder at S7-12

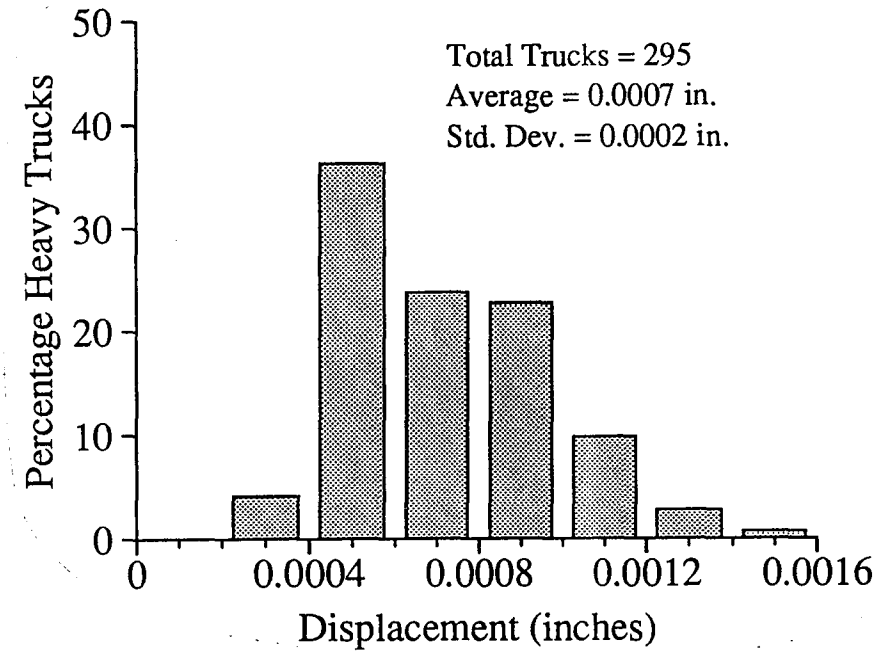

Figure 103. Histogram of the Out-of-Plane Displacements Recorded at Pier S5-2 Floorbeam Two

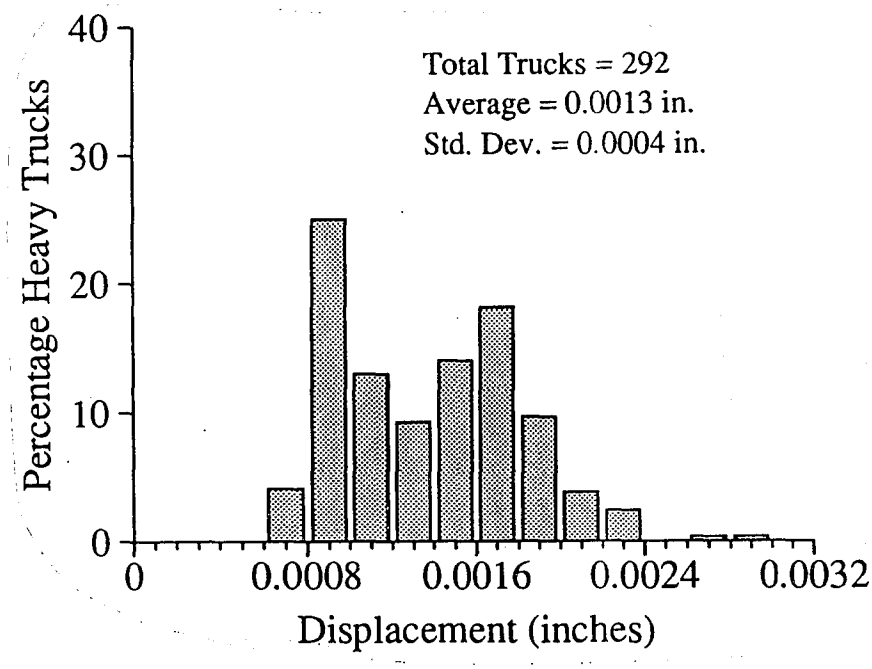

Figure 104. Histogram of the Out-of-Plane Displacements Recorded at Pier S7-12 Floorbeam Two

cracking in the web gap.

At the end of the inside connection plate weld, the fatigue limit is approximately 10 ksi (as discussed in Chapter Seven). Comparison with the stress ranges shown in Table 25 for S5-2 indicates that cracking is not likely to occur at the end of the connection plate. The stress range of 8.9 ksi for trucks in lanes B and C at S7-12 is close enough to the fatigue limit of 10 ksi to represent a significant possibility of future cracking. Finite element analyses of the floorbeam two connections performed by Reid (1992) indicate that the stress range along the centerline of the connection plate at the end of the connection plate weld is approximately equal to the stress range extrapolated from the strain gage locations to the web-flange weld. When the stress ranges at the end of the connection plate weld are assumed to be equal to the stress ranges shown in Table 25 at the web-flange weld, it is seen that fatigue cracking at both S5-2 and S7-12 is likely to occur.

The fatigue limit at the web-flange weld is approximately 15 ksi (as discussed in Chapter Seven). Comparison of this fatigue limit with stress ranges at the web-flange weld shown in Table 25 indicate that fatigue cracking is very likely to occur. Finite element analyses (Reid 1992) also indicate that the stress ranges at the web-flange weld at the centerline of the connection plate are approximately 50% larger than those shown in Table 25. Hence, the likelihood of cracking at the web-flange weld

appears even greater when the finite element analyses results are considered.

The above comparisons indicate that distortion-induced fatigue cracking is likely to occur in the web gaps at the floorbeam two locations. The low measured in-plane stress ranges at these locations indicate that the cracks are not likely to turn and propagate into the tension flange in a short period of time. Based on experiences cited by Fisher et al. (1990), a positive attachment retrofit of the type shown in Figures 4 and 5 is the only permanent method of repair. Short-term repairs can be made by hole drilling.

RESULTS AT FLOORBEAM THREE

The plate girder tension flange at the floorbeam three locations was the bottom flange, so the web gap of interest was near the bottom flange. Illustrations of the web gap geometry and strain gage locations at S5-2 and S7-12 are shown in Figures 105 and 106. Also shown are static stress distributions produced by the lowboy in the outside lane. Summaries of the strains and out-of-plane displacements recorded in the static calibration tests are given in Tables 27 and 28 for test trucks positioned over floorbeams two and three.

The end of the connection plate at S5-2 typically experienced very small inward displacements as a result of normal truck traffic. All the recorded stress ranges were small compressive stress ranges under 1 ksi which indicates that distortion induced cracking will not occur at this

Table 27. Static Calibration Test Results at Floorbeam Three for Test Trucks over Floorbeam Two

Static Test						
Truck	Lane	IS1 ($\mu\epsilon$)	IS2 ($\mu\epsilon$)	0S1 ($\mu\epsilon$)	0S2 ($\mu\epsilon$)	LVDT (in.)
S5-2 Floorbeam Three Connections (84 in. Girder)						
lowboy	outside	-3	-7	-13	-5	0.0000
lowboy	inside	-2	-5	-6	-3	0.0000
dump truck	outside	-4	-9	-17	-6	0.0000
dump truck	inside	-4	-6	-8	-4	0.0000
S7-12 Floorbeam Three Connections (96 in. Girder)						
lowboy	outside	-16	-7	+7	+12	+.0000
lowboy	inside	-24	-9	+2	+12	+.0002
dump truck	outside	-25	-8	+5	+17	+.0002
dump truck	inside	-24	-8	-2	+9	+.0003

Table 28. Static Calibration Test Results at Floorbeam Three for Test Trucks over Floorbeam Three

Static Test						
Truck	Lane	IS1 ($\mu\epsilon$)	IS2 ($\mu\epsilon$)	OS1 ($\mu\epsilon$)	OS2 ($\mu\epsilon$)	LVDT (in.)
S5-2 Floorbeam Three Connections (84 in. Girder)						
lowboy	outside	-9	-19	-28	-12	0.0000
lowboy	inside	-6	-10	-13	-6	0.0000
dump truck	outside	-9	-21	-31	-13	0.0000
dump truck	inside	-7	-10	-12	-5	0.0000
S7-12 Floorbeam Three Connections (96 in. Girder)						
lowboy	outside	-24	-19	+8	+12	-0.0002†
lowboy	inside	-27	-27	-1	+3	-0.0001
dump truck	outside	-11	-20	+9	+6	-0.0004
dump truck	inside	-17	-31	+2	-4	-0.0004

†Negative values indicate outward displacement at the end of connection plate.

location. A histogram of out-of-plane displacements recorded at S5-2 is shown in Figure 107. The average out-of-plane displacement was only 0.0001 in. which is equal to the smallest displacement that could be resolved with the LVDT that was used for the measurements. Hence, under normal traffic loading there was practically no measurable displacement.

The in-plane bending stresses at S5-2 floorbeam three were larger than those measured at the other test locations. The maximum in-plane stress range measured on the tension flange of the girder was 2.2 ksi.

The strain gages at S7-12 floorbeam three indicate that the web gap typically bent in single curvature. This is illustrated by the stress distributions shown in Figure 106. As shown in the figure, the stresses on the inside face of the web were compressive and very low in magnitude. The stresses on the outside were tensile and very low in magnitude. The same behavior was observed for trucks in the normal traffic stream. Based on the small stress ranges measured at this location, distortion-induced cracking will not occur.

The connection plate at S7-12 floorbeam three did experience out-of-plane displacements slightly larger than those at S5-12 floorbeam three. The connection plate moved both inward and outward with respect to the bottom flange for a single truck pass. The movement tended to be more outward than inward. Hence, the displacement ranges were recorded as

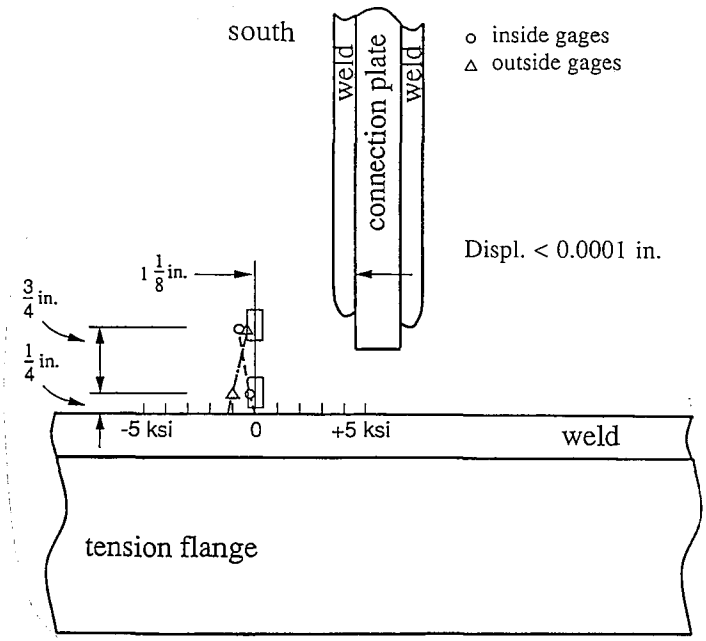

Figure 105. Static Stress Distribution for Outside Girder at Pier S5-2 Floorbeam Three with Lowboy in Outside Lane

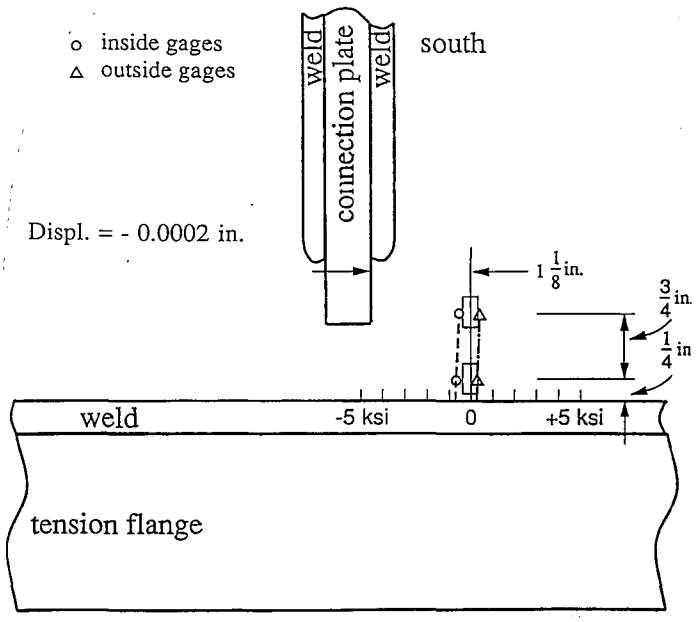

Figure 106. Static Stress Distribution for Inside Girder at Pier S7-12 Floorbeam Three with the Lowboy in the Outside Lane

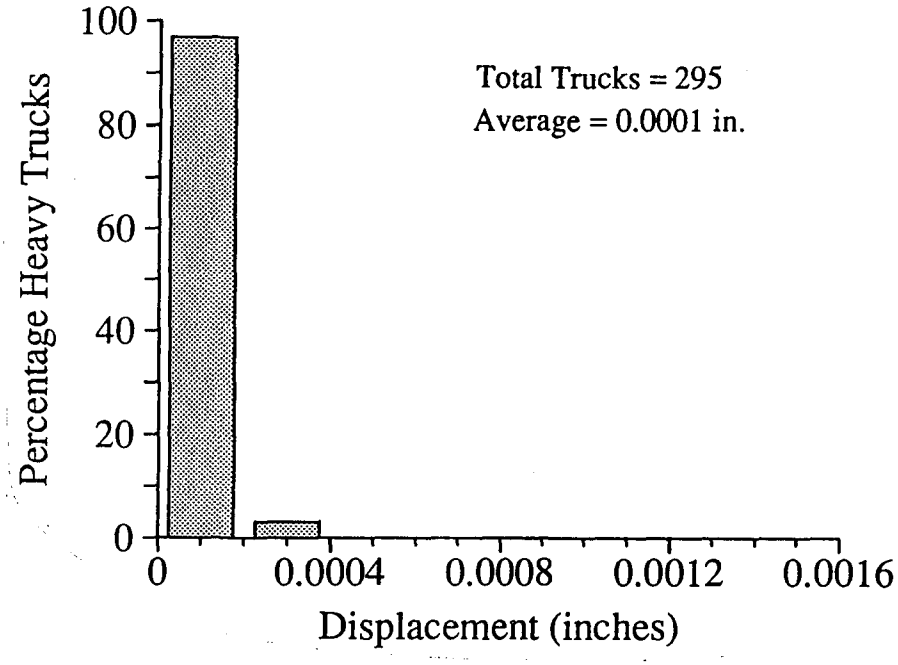

Figure 107. Histogram of the Out-of-Plane Displacements at Pier S5-2 Floorbeam Three

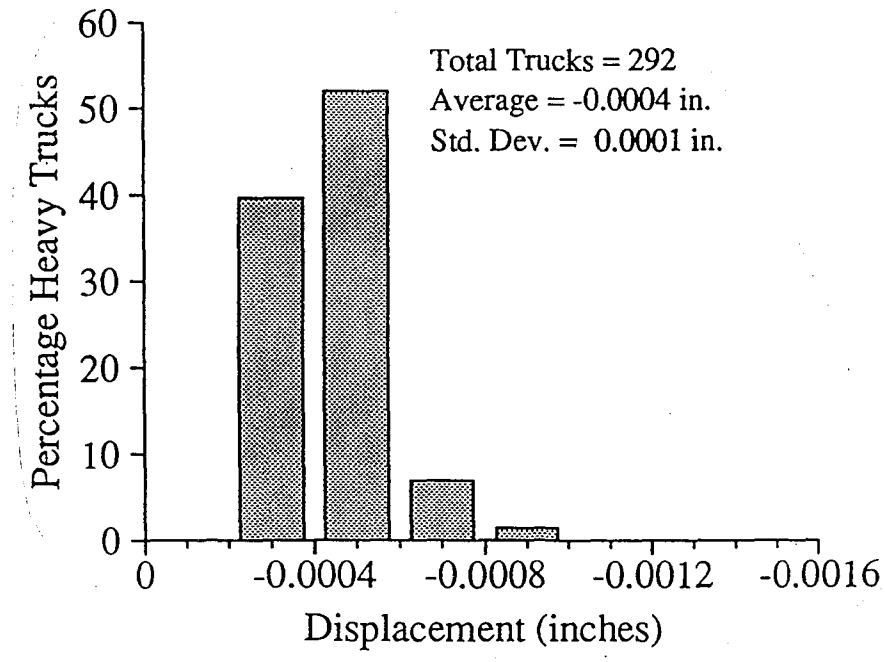

Figure 108. Histogram of the Out-of-Plane Displacements at Pier S7-12 Floorbeam Three

negative values. A histogram of the out-of-plane displacements is shown in Figure 108.

The in-plane stress ranges at S7-12 floorbeam three were not as large as those measured at S5-2 floorbeam three. The maximum in-plane stress range measured on the tension flange at floorbeam three was approximately 1.5 ksi, and the stress ranges were typically only 1.3 ksi.

The above results indicate that distortion-induced fatigue cracking will not occur at either of the floorbeam three locations where tests were performed. Distortion-induced cracking is very unlikely at any of the floorbeam three locations along the Mobile Delta Crossing bridges.

CHAPTER NINE
CONCLUSIONS AND RECOMMENDATIONS

SUMMARY AND CONCLUSIONS

One objective of the research project was to evaluate the stress conditions and potential for future fatigue cracking at the floorbeam-girder connections of the I-65 Mobile Delta Crossing bridges through field testing. Field measurements of stresses and displacements were made at a total of ten connection plate details at two different girder depths. At each girder depth, field measurements were made at five floorbeam connection plate details. These five details include three connections at pier floorbeams, one connection at the first floorbeam away from the pier, and one connection at the second floorbeam away from the pier.

The test data indicated that two of the six connection plate details tested at pier floorbeam locations experienced distortion-induced stress ranges large enough to cause fatigue cracking. One of the connections was at an 84 in. deep girder, and one was at a 96 in. deep girder. Given the fact that cracks have been detected at the piers at four locations along 84 in. girders and one location along 96 in. girders, and that low stress conditions were found at four of the connections tested, it appears that significantly different stress conditions exist at the pier floorbeam connections along the bridges. No pattern was identified that clearly indicates which locations along the bridges are

most likely to experience cracking in the future. The test results do indicate that cracking is not likely to occur at all pier floorbeam locations. The small number of connections chosen for field tests does not allow an accurate estimate of percentage of connections at which cracking will occur. However, it appears that cracking should be expected at approximately one-third of the pier floorbeam connections.

Both of the connection plate details tested at the first floorbeam away from pier supports had high distortion-induced stresses. The stress ranges occurring at both connections were large enough to cause fatigue cracking. Cracking can be expected in the future at other connections at the first floorbeam away from the pier.

The connection plate details tested at the second floorbeam away from the pier had very small distortion-induced stresses. Fatigue cracking is very unlikely to occur at any of these locations in the future.

Since the plate girders of a two girder system are considered fracture critical members, the possibility of the web cracks turning up into the tension flange is of interest. The field measurements indicate that for all the details tested, the in-plane stress ranges in the tension flange were very small (below 1.0 ksi) at the piers and first floorbeams away from the piers. Therefore, the initiation and propagation of a web gap crack into the tension flange is not likely to occur in a period of time shorter than the normal two year inspection interval.

Another objective of the project was to evaluate the effectiveness of the positive attachment retrofit designed by the Alabama Highway Department for use in repairing floorbeam-girder connections with distortion-induced cracking. The evaluation was performed by comparing distortion-induced stress ranges and displacements in uncracked connections before and after the retrofit was performed. The comparisons indicated that the positive attachment retrofit is an effective repair method. The retrofit was installed at one of the pier locations where test data indicated that fatigue cracking would occur. The retrofit reduced the out-of-plane displacement of the connection plate and distortion-induced stresses by approximately 70%. This was a large enough reduction in distortion-induced stresses to conclude that cracking will not occur at that location in the future. The positive attachment retrofit will also be effective in arresting fatigue crack growth when used after cracking has occurred.

RECOMMENDATIONS

Due to the low in-plane stress ranges measured in the tension flanges at all the test locations, web gap cracking resulting from out-of-plane bending at the floorbeam-girder connections does not pose as great an emergency as once suspected. Furthermore, the distortion-induced stress conditions at the various piers were shown to vary significantly. These findings indicate that performing the positive attachment retrofit on all 192 details on the

bridges at the present time is unwarranted. Instead, the results of this project indicate that floorbeam-girder connections with web gap cracking should be repaired on an as needed basis. The normal two year inspection cycle will be sufficient for identifying new occurrences of web gap cracks. When cracks are found as a result of inspection, the crack tips should be removed by drilling a one inch diameter hole at each crack to temporarily arrest the growth of the cracks, and, in most cases, crack growth will be stopped for a few years. This period of arrest should allow all the connections with web gap cracking found in two consecutive inspections to be repaired by positive attachment at the same time. However, it is not recommended that hole drilling be used to delay positive attachment for more than three years.

REFERENCES

American Association of State Highway and Transportation Officials. (1990). Guide Specifications for Fatigue Evaluation of Existing Steel Bridges, Washington D.C.

Bowers, D.G. (1973). "Loading History of Span 10 on Yellow Mill Pond Viaduct," HRB, Highway Research Record, 428, 64-71.

Christiano, P.O. and Goodman, L.E. (1972). "Bridge Stress Range History," HRB, Highway Research Record, 382, 1-12.

Deen, R.C. and Havens, J.H. (1976). "Fatigue Analysis from Strain Gage Data and Probability Analysis," TRB, Transportation Research Record, 579, 82-102.

Douglas, T.R., (1972). "Fatigue Life of Bridges Under Repeated Highway Loadings," HRB, Highway Research Record, 382, 13-20.

Douglas, T.R. and Karsh, J.B. (1971). "Fatigue Life of Bridges Under Repeated Highway Loading," HPR, Alabama Highway Research, 54, 1-48.

Downing, S. and Socie, D.F. (1982). "Simple Rainflow Counting Algorithms," International Journal of Fatigue, Jan., 31-40.

Fisher, J.W. (1978). "Fatigue Cracking in Bridges from Out-of-Plane Displacements," Canadian Journal of Civil Engineering, 5(4), 542-556.

Fisher, J.W. Bathelemy, B.M., Mertz, D.R., and Edinger, J.A. (1980). "Fatigue Behavior of Full-Scale Welded Bridge Attachments," TRB, Transportaion Research Board, NCHRP No. 227, November.

Fisher, J.W., Fisher, T.A., and Kostem, C.N. (1979). "Displacement Induced Fatigue Cracks," Engineering Structures, Oct., 252-257.

Fisher, J.W., Hausammann, H., Sullivan, M.D., and Pense, A.W. (1979b). "Detection and Repair of Fatigue Damage in Welded Highway Bridges," Technical Report, NCHRP No. 206, TRB, Washington D.C., June.

Fisher, J.W., Jin, J., Wagner, D.C., and Yen, B.T. (1990). "Distortion Induced Cracking in Steel Bridge Members," Final Report. ATLSS No. 90-07. NCHRP No. 12-28(6).

Fisher, J.W., Yen, B.T., and Wagner, D. (1987). "Review of Field Measurements for Distortion-Induced Fatigue Cracking in Steel Bridges," TRB, Transportation Research Record, 1118, 49-55.

Fisher, J. W., Yen, B.T., and Wang, D. (1989). "Fatigue of Bridge Structures- A Commentary and Guide for Design, Evaluation,and Investigation of Cracking," ATLSS, Advanced Technology for Large Scale Structural Systems, Lehigh University, July, 89-02.

Galambos, C.F. and Heins,. C.P. (1971). "Loading History of Highway Bridges, Comparison of Stress Range Histograms," HRB, Highway Research Record, 354, 1-13.

Goodpasture, D.W., Burdette, E.G., Patrick, Jr. P.C., and Snider, J.N. (1976). "Prediction of Bridge Girder Stress Histograms from Truck Type Distribution," TRB, Transportation Research Record, 579, 72-81.

Hayes, J.E. (1965). Fatigue Analysis and Fail-Safe Design in Analysis and Design of Flight Vehicle Structures, Cincinnati, Ohio: Tristate Offset Co, pp. C13-1 to C13-42.

Heins, Jr. C.P. and Khosa, R.L. (1972). "Comparisons Between Induced Girder Stresses and Corresponding Vehicle Weights," HRB, Highway Research Record, 382, 21-26.

Keating, P.B. and Fisher, J.W. (1987). "Fatigue Behavior of Variable Loaded Bridge Details Near the Fatigue Limit," TRB, Transportation Research Record, 1118, 56-64.

Lee, J.J., Castiglioni, C., Fisher, J.W., Kostem, C.N., and Yen, B.T. (1986). Displacement Induced Stresses in Multigirder Steel Bridges, Fritz Eng. Lab. Rept., Lehigh University, Oct.

Peter, J., King, C., and Csagoly, P.F. (1976). "Field Testing of Aquasabon River Bridge in Ontario," TRB, Transportation Research Record, 579, 48-60.

Reid, Charles B. (1992). "Out-of-Plane Displacement Induced Stresses in Floorbeam-to-Girder Connections," thesis presented to Auburn University, in partial fulfillment of the requirements for the degree of Master of Science.

Schijve, J. (1963). "The Analysis of Random Load Time Histories with Relation to Fatigue Tests and Life Calculation," Fatigue of Aircraft Structures, (Barrois, W., Ripley, E.L. eds), Macmillian, New York, 115-149.

Socie, D.F., Schifflet, G., and Berns, H. (1979). "A Field Recording System with Applications to Fatigue Analysis," International Journal of Fatigue, April, 1(2), 103-111.

Technical Manual for the MEGADAC Series 2000: Release 3.2. (1988). Optim Corporation, Germantown, Maryland.

Wetzel, R.M. (1971). A Method of Fatigue Damage Analysis, Ph.D. Thesis. University of Waterloo (Dept. of Civil Eng.), Ontario, Canada.

Wetzel, R.M., ed. (1977). Fatigue Under Complex Loading: Analysis and Experiments, Warrendale, Pennsylvania: Society of Automotive Engineers, Inc. pp. 145-62.

Woodward, H.M. and Fisher, J.W. (1980). Prediction of Fatigue Failure in Steel Bridges, Lehigh University, Technical Report 2, Aug., 386-12(80).

Yamada, K. and Albrecht, P. (1976). "Fatigue Design of Welded Bridge Details for Service Stresses," TRB, Transportation Research Record, 607, 25-30.

APPENDICES

APPENDIX A

S7-5 TABULATED RANDOM TRUCK HISTOGRAM DATA

GAGE: IS1
OUTSIDE GIRDER
BEFORE RETROFIT

STRESS RANGE (ksi)	NUMBER OF TRUCKS
0.00 to -0.249	236
-0.25 to -0.499	346
-0.50 to -0.749	81
-0.75 to -0.999	8

Miner's Sre = 0.4
Total Trucks = 671

GAGE: IS1
OUTSIDE GIRDER
AFTER RETROFIT

STRESS RANGE (ksi)	NUMBER OF TRUCKS
0.00 to -0.249	0
-0.25 to -0.499	16
-0.50 to -0.749	10
-0.75 to -0.999	0

Miner's Sre = N/A
Total Trucks = 26

GAGE: IS2
OUTSIDE GIRDER
BEFORE RETROFIT

STRESS RANGE (ksi)	NUMBER OF TRUCKS
0.00 to -0.249	348
-0.25 to -0.499	301
-0.50 to -0.749	21
-0.75 to -0.999	1

Miner's Sre = -0.3
Total Trucks = 671

GAGE: IS2
OUTSIDE GIRDER
AFTER RETROFIT

STRESS RANGE (ksi)	NUMBER OF TRUCKS
0.00 to -0.249	170
-0.25 to -0.499	147
-0.50 to -0.749	1
-0.75 to -0.999	0

Miner's Sre = -0.3
Total Trucks = 318

GAGE: OS1
OUTSIDE GIRDER
BEFORE RETROFIT

STRESS RANGE (ksi)	NUMBER OF TRUCKS
0.00 to 0.249	332
0.25 to 0.499	290
0.50 to 0.749	44
0.75 to 0.999	3
1.00 to 1.249	1

Miner's Sre = 0.4
Total Trucks = 670

GAGE: OS1
OUTSIDE GIRDER
AFTER RETROFIT

STRESS RANGE (ksi)	NUMBER OF TRUCKS
0.00 to 0.249	133
0.25 to 0.499	176
0.50 to 0.749	9
0.75 to 0.999	0
1.00 to 1.249	0

Miner's Sre = 0.3
Total Trucks = 670

GAGE: OS2
OUTSIDE GIRDER
BEFORE RETROFIT

STRESS RANGE (ksi)	NUMBER OF TRUCKS
0.00 to -0.249	63
-0.25 to -0.499	331
-0.50 to -0.749	249
-0.75 to -0.999	24
-1.00 to -1.249	3

Miner's Sre = -0.5
Total Trucks = 670

GAGE: IN2
OUTSIDE GIRDER
BEFORE RETROFIT

STRESS RANGE (ksi)	NUMBER OF TRUCKS
-0.50 to -0.251	1
-0.25 to -0.001	31
0.00 to 0.249	497
0.25 to 0.499	123
0.50 to 0.749	2
0.75 to 0.999	0
1.00 to 1.249	0

Miner's Sre = 0.2
Total Trucks = 670

EXTRAPOLATED TO:
END OF THE INSIDE
CONNECTION PLATE WELD
OUTSIDE GIRDER
BEFORE RETROFIT

STRESS RANGE (ksi)	NUMBER OF TRUCKS
0.00 to 0.249	117
0.25 to 0.499	302
0.50 to 0.749	218
0.75 to 0.999	29
1.00 to 1.249	4
1.25 to 1.499	1

Miner's Sre = 0.5
Total Trucks = 671

EXTRAPOLATED TO:
END OF THE INSIDE
CONNECTION PLATE WELD
OUTSIDE GIRDER
AFTER RETROFIT

STRESS RANGE (ksi)	NUMBER OF TRUCKS
0.00 to 0.249	0
0.25 to 0.499	22
0.50 to 0.749	4
0.75 to 0.999	0
1.00 to 1.249	0
1.25 to 1.499	0

Miner's Sre = N/A
Total Trucks = 26

EXTRAPOLATED TO:
OUTSIDE WEB-TO-FLANGE
WELD TOE
OUTSIDE GIRDER
BEFORE RETROFIT

STRESS RANGE (ksi)	NUMBER OF TRUCKS
0.00 to 0.249	16
0.25 to 0.499	222
0.50 to 0.749	143
0.75 to 0.999	133
1.00 to 1.249	125
1.25 to 1.499	20
1.50 to 1.749	7
1.75 to 1.999	22
2.00 to 2.249	1
2.25 to 2.499	0
2.50 to 2.749	0
2.75 to 2.999	0
3.00 to 3.249	1

Miner's Sre = 0.9
Total Trucks = 670

EXTRAPOLATED TO:
LOCATION OF THE
INSIDE CONNECTION PLATE
WELD ON OUTSIDE WEB
OUTSIDE GIRDER
BEFORE RETROFIT

STRESS RANGE (ksi)	NUMBER OF TRUCKS
0.00 to -0.249	20
-0.25 to -0.499	227
-0.50 to -0.749	153
-0.75 to -0.999	162
-1.00 to -1.249	93
-1.25 to -1.499	10
-1.50 to -1.749	5
-1.75 to -1.999	1

Miner's Sre = -0.8
Total Trucks = 671

EXTRAPOLATED TO:
LOCATION OF THE
INSIDE CONNECTION PLATE
WELD ON OUTSIDE WEB
OUTSIDE GIRDER
AFTER RETROFIT

STRESS RANGE (ksi)	NUMBER OF TRUCKS
0.00 to -0.249	0
-0.25 to -0.499	1
-0.50 to -0.749	8
-0.75 to -0.999	11
-1.00 to -1.249	6
-1.25 to -1.499	0
-1.50 to -1.749	0
-1.75 to -1.999	0

Miner's Sre = N/A
Total Trucks = 26

LVDT
OUTSIDE GIRDER
BEFORE RETROFIT

DISPLACEMENT (in.)	NUMBER OF TRUCKS
0.0000 to 0.00019	1
0.0002 to 0.00039	28
0.0004 to 0.00059	35
0.0006 to 0.00079	38
0.0008 to 0.00099	19
0.0010 to 0.00119	2
0.0012 to 0.00139	0

Average = 0.0005
Std. Dev. = 0.0002
Total Trucks = 123

LVDT
OUTSIDE GIRDER
AFTER RETROFIT

DISPLACEMENT (in.)	NUMBER OF TRUCKS
0.0000 to 0.00019	2
0.0002 to 0.00039	56
0.0004 to 0.00059	92
0.0006 to 0.00079	86
0.0008 to 0.00099	75
0.0010 to 0.00119	5
0.0012 to 0.00139	1

Average = 0.0006
Std. Dev. = 0.0002
Total Trucks = 123

GAGE: IS1
INSIDE GIRDER
BEFORE RETROFIT

STRESS RANGE (ksi)	NUMBER OF TRUCKS
0.00 to -0.249	0
-0.25 to -0.499	5
-0.50 to -0.749	12
-0.75 to -0.999	32
-1.00 to -1.249	103
-1.25 to -1.499	103
-1.50 to -1.749	63
-1.75 to -1.999	26
-2.00 to -2.249	63
-2.25 to -2.499	72
-2.50 to -2.749	64
-2.75 to -2.999	60
-3.00 to -3.249	34
-3.25 to -3.499	14
-3.50 to -3.749	2
-3.75 to -3.999	4
-4.00 to -4.249	0
-4.25 to -4.499	4
-4.50 to -4.749	1
-4.75 to -4.999	4
-5.00 to -5.249	0
-5.25 to -5.499	2
-5.50 to -5.749	1
-5.75 to -5.999	1

Miner's Sre = -2.3
Total Trucks = 670

GAGE: IS1
INSIDE GIRDER
AFTER RETROFIT

STRESS RANGE (ksi)	NUMBER OF TRUCKS
0.00 to -0.249	0
-0.25 to -0.499	4
-0.50 to -0.749	4
-0.75 to -0.999	10
-1.00 to -1.249	8
-1.25 to -1.499	0
-1.50 to -1.749	0
-1.75 to -1.999	0
-2.00 to -2.249	0
-2.25 to -2.499	0
-2.50 to -2.749	0
-2.75 to -2.999	0
-3.00 to -3.249	0
-3.25 to -3.499	0
-3.50 to -3.749	0
-3.75 to -3.999	0
-4.00 to -4.249	0
-4.25 to -4.499	0
-4.50 to -4.749	0
-4.75 to -4.999	0
-5.00 to -5.249	0
-5.25 to -5.499	0
-5.50 to -5.749	0
-5.75 to -5.999	0

Miner's Sre = N/A
Total Trucks = 26

GAGE: IS2
INSIDE GIRDER
BEFORE RETROFIT

STRESS RANGE (ksi)	NUMBER OF TRUCKS
0.00 to -0.249	16
-0.25 to -0.499	66
-0.50 to -0.749	188
-0.75 to -0.999	103
-1.00 to -1.249	113
-1.25 to -1.499	101
-1.50 to -1.749	55
-1.75 to -1.999	9
-2.00 to -2.249	7
-2.25 to -2.499	5
-2.50 to -2.749	1
-2.75 to -2.999	4
-3.00 to -3.249	1
-3.25 to -3.499	1

Miner's Sre = -1.2
Total Trucks = 670

GAGE: IS2
INSIDE GIRDER
AFTER RETROFIT

STRESS RANGE (ksi)	NUMBER OF TRUCKS
0.00 to -0.249	318
-0.25 to -0.499	0
-0.50 to -0.749	0
-0.75 to -0.999	0
-1.00 to -1.249	0
-1.25 to -1.499	0
-1.50 to -1.749	0
-1.75 to -1.999	0
-2.00 to -2.249	0
-2.25 to -2.499	0
-2.50 to -2.749	0
-2.75 to -2.999	0
-3.00 to -3.249	0
-3.25 to -3.499	0

Miner's Sre = -0.1
Total Trucks = 318

GAGE: OS1
INSIDE GIRDER
BEFORE RETROFIT

STRESS RANGE (ksi)	NUMBER OF TRUCKS
0.00 to 0.249	3
0.25 to 0.499	12
0.50 to 0.749	25
0.75 to 0.999	69
1.00 to 1.249	140
1.25 to 1.499	75
1.50 to 1.749	66
1.75 to 1.999	50
2.00 to 2.249	87
2.25 to 2.499	74
2.50 to 2.749	27
2.75 to 2.999	18
3.00 to 3.249	9
3.25 to 3.499	3
3.50 to 3.749	2
3.75 to 3.999	1
4.00 to 4.249	0
4.25 to 4.499	2
4.50 to 4.749	0
4.75 to 4.999	6
5.00 to 5.249	0
5.25 to 5.499	1

Miner's Sre = 2.0
Total Trucks = 670

GAGE: OS1
INSIDE GIRDER
AFTER RETROFIT

STRESS RANGE (ksi)	NUMBER OF TRUCKS
0.00 to 0.249	2
0.25 to 0.499	52
0.50 to 0.749	93
0.75 to 0.999	90
1.00 to 1.249	77
1.25 to 1.499	3
1.50 to 1.749	1
1.75 to 1.999	0
2.00 to 2.249	0
2.25 to 2.499	0
2.50 to 2.749	0
2.75 to 2.999	0
3.00 to 3.249	0
3.25 to 3.499	0
3.50 to 3.749	0
3.75 to 3.999	0
4.00 to 4.249	0
4.25 to 4.499	0
4.50 to 4.749	0
4.75 to 4.999	0
5.00 to 5.249	0
5.25 to 5.499	0

Miner's Sre = 0.9
Total Trucks = 318

GAGE: OS2
INSIDE GIRDER
BEFORE RETROFIT

STRESS RANGE (ksi)	NUMBER OF TRUCKS
0.00 to -0.249	0
-0.25 to -0.499	4
-0.50 to -0.749	4
-0.75 to -0.999	16
-1.00 to -1.249	49
-1.25 to -1.499	107
-1.50 to -1.749	87
-1.75 to -1.999	39
-2.00 to -2.249	36
-2.25 to -2.499	63
-2.50 to -2.749	45
-2.75 to -2.999	77
-3.00 to -3.249	59
-3.25 to -3.499	40
-3.50 to -3.749	13
-3.75 to -3.999	11
-4.00 to -4.249	2
-4.25 to -4.499	6
-4.50 to -4.749	2
-4.75 to -4.999	1
-5.00 to -5.249	0
-5.25 to -5.499	1
-5.50 to -5.749	1
-5.75 to -5.999	2
-6.00 to -6.249	4
-6.25 to -6.499	1

Miner's Sre = -2.6
Total Trucks = 670

GAGE: IN2
INSIDE GIRDER
BEFORE RETROFIT

STRESS RANGE (ksi)	NUMBER OF TRUCKS
0.00 to 0.249	6
0.25 to 0.499	29
0.50 to 0.749	82
0.75 to 0.999	132
1.00 to 1.249	120
1.25 to 1.499	74
1.50 to 1.749	104
1.75 to 1.999	52
2.00 to 2.249	43
2.25 to 2.499	12
2.50 to 2.749	2
2.75 to 2.999	3
3.00 to 3.249	1
3.25 to 3.499	1
3.50 to 3.749	0
3.75 to 3.999	1
4.00 to 4.249	4
4.25 to 4.499	3
4.50 to 4.749	1

Miner's Sre = 1.6
Total Trucks = 670

EXTRAPOLATED TO:
END OF THE INSIDE
CONNECTION PLATE WELD
INSIDE GIRDER
BEFORE RETROFIT

STRESS RANGE (ksi)	NUMBER OF TRUCKS
0.00 to 0.249	4
0.25 to 0.499	21
0.50 to 0.749	52
0.75 to 0.999	142
1.00 to 1.249	105
1.25 to 1.499	71
1.50 to 1.749	75
1.75 to 1.999	77
2.00 to 2.249	69
2.25 to 2.499	25
2.50 to 2.749	9
2.75 to 2.999	5
3.00 to 3.249	5
3.25 to 3.499	2
3.50 to 3.749	1
3.75 to 3.999	4
4.00 to 4.249	2
4.25 to 4.499	1

Miner's Sre = 0.5
Total Trucks = 671

EXTRAPOLATED TO:
END OF THE INSIDE
CONNECTION PLATE WELD
INSIDE GIRDER
AFTER RETROFIT

STRESS RANGE (ksi)	NUMBER OF TRUCKS
0.00 to 0.249	24
0.25 to 0.499	2
0.50 to 0.749	0
0.75 to 0.999	0
1.00 to 1.249	0
1.25 to 1.499	0
1.50 to 1.749	0
1.75 to 1.999	0
2.00 to 2.249	0
2.25 to 2.499	0
2.50 to 2.749	0
2.75 to 2.999	0
3.00 to 3.249	0
3.25 to 3.499	0
3.50 to 3.749	0
3.75 to 3.999	0
4.00 to 4.249	0
4.25 to 4.499	0

Miner's Sre = N/A
Total Trucks = 26

EXTRAPOLATED TO:
OUTSIDE WEB-TO-FLANGE
WELD TOE
INSIDE GIRDER
BEFORE RETROFIT

STRESS RANGE (ksi)	NUMBER OF TRUCKS
0.00 to 0.249	0
0.25 to 0.499	1
0.50 to 0.749	3
0.75 to 0.999	3
1.00 to 1.249	6
1.25 to 1.499	8
1.50 to 1.749	11
1.75 to 1.999	21
2.00 to 2.249	40
2.25 to 2.499	58
2.50 to 2.749	67
2.75 to 2.999	43
3.00 to 3.249	25
3.25 to 3.499	34
3.50 to 3.749	19
3.75 to 3.999	25
4.00 to 4.249	28
4.25 to 4.499	26
4.50 to 4.749	31
4.75 to 4.999	45
5.00 to 5.249	37
5.25 to 5.499	34
5.50 to 5.749	29
5.75 to 5.999	16
6.00 to 6.249	18
6.25 to 6.499	10

6.50	to	6.749	6
6.75	to	6.999	5
7.00	to	7.249	3
7.25	to	7.499	3
7.50	to	7.749	2
7.75	to	7.999	0
8.00	to	8.249	2
8.25	to	8.499	1
8.50	to	8.749	0
8.75	to	8.999	1
9.00	to	9.249	0
9.25	to	9.499	0
9.50	to	9.749	0
9.75	to	9.999	0
10.00	to	10.249	0
10.25	to	10.499	2
10.50	to	10.749	2
10.75	to	10.999	1
11.00	to	11.249	2
11.25	to	11.499	1
11.50	to	11.749	0
11.75	to	11.999	1

Miner's Sre = 4.6
Total Trucks = 670

EXTRAPOLATED TO:
LOCATION OF THE
INSIDE CONNECTION PLATE
WELD ON OUTSIDE WEB
INSIDE GIRDER
BEFORE RETROFIT

STRESS RANGE (ksi)			NUMBER OF TRUCKS
0.00	to	-0.249	0
-0.25	to	-0.499	0
-0.50	to	-0.749	4
-0.75	to	-0.999	2
-1.00	to	-1.249	4
-1.25	to	-1.499	14
-1.50	to	-1.749	17
-1.75	to	-1.999	30
-2.00	to	-2.249	68
-2.25	to	-2.499	63
-2.50	to	-2.749	44
-2.75	to	-2.999	31
-3.00	to	-3.249	30
-3.25	to	-3.499	22
-3.50	to	-3.749	27
-3.75	to	-3.999	29
-4.00	to	-4.249	31
-4.25	to	-4.499	34
-4.50	to	-4.749	44
-4.75	to	-4.999	43
-5.00	to	-5.249	37
-5.25	to	-5.499	27
-5.50	to	-5.749	22
-5.75	to	-5.999	13
-6.00	to	-6.249	9
-6.25	to	-6.499	4
-6.50	to	-6.749	3
-6.75	to	-6.999	2
-7.00	to	-7.249	3
-7.25	to	-7.499	1
-7.50	to	-7.749	1
-7.75	to	-7.999	1
-8.00	to	-8.249	0
-8.25	to	-8.499	0
-8.50	to	-8.749	0
-8.75	to	-8.999	3
-9.00	to	-9.249	1
-9.25	to	-9.499	2
-9.50	to	-9.749	0
-9.75	to	-9.999	1
-10.00	to	-10.249	2
-10.25	to	-10.499	0
-10.50	to	-10.749	1
-10.75	to	-10.999	0

Miner's Sre = -4.3
Total Trucks = 670

EXTRAPOLATED TO:
LOCATION OF THE
INSIDE CONNECTION PLATE
WELD ON OUTSIDE WEB
INSIDE GIRDER
AFTER RETROFIT

STRESS RANGE (ksi)			NUMBER OF TRUCKS
0.00	to	-0.249	0
-0.25	to	-0.499	0
-0.50	to	-0.749	4
-0.75	to	-0.999	3
-1.00	to	-1.249	5
-1.25	to	-1.499	4
-1.50	to	-1.749	6
-1.75	to	-1.999	4
-2.00	to	-2.249	0
-2.25	to	-2.499	0
-2.50	to	-2.749	0
-2.75	to	-2.999	0
-3.00	to	-3.249	0
-3.25	to	-3.499	0
-3.50	to	-3.749	0
-3.75	to	-3.999	0
-4.00	to	-4.249	0
-4.25	to	-4.499	0
-4.50	to	-4.749	0
-4.75	to	-4.999	0
-5.00	to	-5.249	0
-5.25	to	-5.499	0
-5.50	to	-5.749	0
-5.75	to	-5.999	0
-6.00	to	-6.249	0
-6.25	to	-6.499	0
-6.50	to	-6.749	0
-6.75	to	-6.999	0
-7.00	to	-7.249	0
-7.25	to	-7.499	0
-7.50	to	-7.749	0
-7.75	to	-7.999	0
-8.00	to	-8.249	0
-8.25	to	-8.499	0
-8.50	to	-8.749	0
-8.75	to	-8.999	0
-9.00	to	-9.249	0
-9.25	to	-9.499	0
-9.50	to	-9.749	0
-9.75	to	-9.999	0
-10.00	to	-10.249	0
-10.25	to	-10.499	0
-10.50	to	-10.749	0
-10.75	to	-10.999	0

Miner's Sre = N/A
Total Trucks = 26

LVDT
INSIDE GIRDER
BEFORE RETROFIT

DISPLACEMENT (in.)			NUMBER OF TRUCKS
0.0000	to	0.00019	0
0.0002	to	0.00039	1
0.0004	to	0.00059	3
0.0006	to	0.00079	3
0.0008	to	0.00099	8
0.0010	to	0.00119	19
0.0012	to	0.00139	13
0.0014	to	0.00159	6
0.0016	to	0.00179	9
0.0018	to	0.00199	9
0.0020	to	0.00219	14
0.0022	to	0.00239	21
0.0024	to	0.00259	12
0.0026	to	0.00279	2
0.0028	to	0.00299	1
0.0030	to	0.00319	0
0.0032	to	0.00339	1
0.0034	to	0.00359	0
0.0036	to	0.00379	0
0.0038	to	0.00399	0
0.0040	to	0.00419	0
0.0042	to	0.00439	1

Average = 0.0017
Std. Dev. = 0.0007
Total Trucks = 123

LVDT
INSIDE GIRDER
AFTER RETROFIT

DISPLACEMENT (in.)			NUMBER OF TRUCKS
0.0000	to	0.00019	3
0.0002	to	0.00039	90
0.0004	to	0.00059	89
0.0006	to	0.00079	113
0.0008	to	0.00099	22
0.0010	to	0.00119	0
0.0012	to	0.00139	0
0.0014	to	0.00159	0
0.0016	to	0.00179	0
0.0018	to	0.00199	0
0.0020	to	0.00219	0
0.0022	to	0.00239	0
0.0024	to	0.00259	0
0.0026	to	0.00279	0
0.0028	to	0.00299	0
0.0030	to	0.00319	0
0.0032	to	0.00339	0
0.0034	to	0.00359	0
0.0036	to	0.00379	0
0.0038	to	0.00399	0
0.0040	to	0.00419	0
0.0042	to	0.00439	0

Average = 0.0005
Std. Dev. = 0.0002
Total Trucks = 317

APPENDIX B

S7-9 TABULATED RANDOM TRUCK HISTOGRAM DATA

GAGE: IS1
OUTSIDE GIRDER
BEFORE RETROFIT

STRESS RANGE (ksi)	NUMBER OF TRUCKS
0.00 to -0.249	49
-0.25 to -0.499	151
-0.50 to -0.749	52
-0.75 to -0.999	4

Miner's Sre = 0.4
Total Trucks = 256

GAGE: IS1
OUTSIDE GIRDER
AFTER RETROFIT

STRESS RANGE (ksi)	NUMBER OF TRUCKS
0.00 to -0.249	2
-0.25 to -0.499	14
-0.50 to -0.749	9
-0.75 to -0.999	1

Miner's Sre = N/A
Total Trucks = 26

GAGE: IS2
OUTSIDE GIRDER
BEFORE RETROFIT

STRESS RANGE (ksi)	NUMBER OF TRUCKS
-0.25 to -0.001	1
0.00 to 0.249	24
0.25 to 0.499	496
0.50 to 0.749	32

Miner's Sre = 0.2
Total Trucks = 553

GAGE: IS2
OUTSIDE GIRDER
AFTER RETROFIT

STRESS RANGE (ksi)	NUMBER OF TRUCKS
-0.25 to -0.001	0
0.00 to 0.249	176
0.25 to 0.499	97
0.50 to 0.749	0

Miner's Sre = 0.2
Total Trucks = 273

GAGE: OS1
OUTSIDE GIRDER
BEFORE RETROFIT

STRESS RANGE (ksi)	NUMBER OF TRUCKS
-0.50 to -0.251	1
-0.25 to -0.001	90
0.00 to 0.249	457
0.25 to 0.499	2

Miner's Sre = 0.1
Total Trucks = 550

GAGE: OS1
OUTSIDE GIRDER
AFTER RETROFIT

STRESS RANGE (ksi)	NUMBER OF TRUCKS
-0.50 to -0.251	0
-0.25 to -0.001	0
0.00 to 0.249	218
0.25 to 0.499	55

Miner's Sre = 0.2
Total Trucks = 273

GAGE: OS2
OUTSIDE GIRDER
BEFORE RETROFIT

STRESS RANGE (ksi)	NUMBER OF TRUCKS
0.00 to -0.249	0
-0.25 to -0.499	7
-0.50 to -0.749	5
-0.75 to -0.999	1

Miner's Sre = N/A
Total Trucks = 13

GAGE: IN2
OUTSIDE GIRDER
BEFORE RETROFIT

STRESS RANGE (ksi)	NUMBER OF TRUCKS
0.00 to 0.249	413
0.25 to 0.499	135
0.50 to 0.749	4

Miner's Sre = 0.2
Total Trucks = 552

EXTRAPOLATED TO:
END OF THE INSIDE
CONNECTION PLATE WELD
OUTSIDE GIRDER
BEFORE RETROFIT

STRESS RANGE (ksi)	NUMBER OF TRUCKS
0.00 to 0.249	107
0.25 to 0.499	142
0.50 to 0.749	7

Miner's Sre = 0.3
Total Trucks = 256

EXTRAPOLATED TO:
END OF THE INSIDE
CONNECTION PLATE WELD
OUTSIDE GIRDER
AFTER RETROFIT

STRESS RANGE (ksi)	NUMBER OF TRUCKS
0.00 to 0.249	6
0.25 to 0.499	12
0.50 to 0.749	8

Miner's Sre = N/A
Total Trucks = 26

EXTRAPOLATED TO:
OUTSIDE WEB-TO-FLANGE
WELD TOE
OUTSIDE GIRDER
BEFORE RETROFIT

STRESS RANGE (ksi)	NUMBER OF TRUCKS
0.00 to 0.249	1
0.25 to 0.499	7
0.50 to 0.749	5

Miner's Sre = N/A
Total Trucks = 13

EXTRAPOLATED TO:
LOCATION OF THE
INSIDE CONNECTION PLATE
WELD ON OUTSIDE WEB
OUTSIDE GIRDER
BEFORE RETROFIT

STRESS RANGE (ksi)	NUMBER OF TRUCKS
0.00 to -0.249	1
-0.25 to -0.499	77
-0.50 to -0.749	67
-0.75 to -0.999	83
-1.00 to -1.249	23
-1.25 to -1.499	2
-1.50 to -1.749	3

Miner's Sre = -0.8
Total Trucks = 256

EXTRAPOLATED TO:
LOCATION OF THE
INSIDE CONNECTION PLATE
WELD ON OUTSIDE WEB
OUTSIDE GIRDER
AFTER RETROFIT

STRESS RANGE (ksi)	NUMBER OF TRUCKS
0.00 to -0.249	0
-0.25 to -0.499	5
-0.50 to -0.749	7
-0.75 to -0.999	6
-1.00 to -1.249	7
-1.25 to -1.499	0
-1.50 to -1.749	1

Miner's Sre = N/A
Total Trucks = 26

LVDT
OUTSIDE GIRDER
BEFORE RETROFIT

DISPLACEMENT (in.)	NUMBER OF TRUCKS
0.0000 to 0.00019	0
0.0002 to 0.00039	0
0.0004 to 0.00059	8
0.0006 to 0.00079	9
0.0008 to 0.00099	4
0.0010 to 0.00119	6
0.0012 to 0.00139	4

Average = 0.0008
Std. Dev. = 0.0003
Total Trucks = 31

GAGE: IS1
INSIDE GIRDER
BEFORE RETROFIT

STRESS RANGE (ksi)	NUMBER OF TRUCKS
0.50 to 0.251	0
0.25 to 0.001	0
0.00 to -0.249	33
-0.25 to -0.499	145
-0.50 to -0.749	66
-0.75 to -0.999	10
-1.00 to -1.249	2

Miner's Sre = -0.5
Total Trucks = 256

GAGE: IS1
INSIDE GIRDER
AFTER RETROFIT

STRESS RANGE (ksi)	NUMBER OF TRUCKS
0.50 to 0.251	24
0.25 to 0.001	2
0.00 to -0.249	0
-0.25 to -0.499	0
-0.50 to -0.749	0
-0.75 to -0.999	0
-1.00 to -1.249	0

Miner's Sre = N/A
Total Trucks = 26

GAGE: IS2
INSIDE GIRDER
BEFORE RETROFIT

STRESS RANGE (ksi)	NUMBER OF TRUCKS
-0.25 to -0.001	16
0.00 to 0.249	442
0.25 to 0.499	93
0.50 to 0.749	1

Miner's Sre = 0.2
Total Trucks = 552

GAGE: IS2
INSIDE GIRDER
AFTER RETROFIT

STRESS RANGE (ksi)	NUMBER OF TRUCKS
-0.25 to -0.001	128
0.00 to 0.249	131
0.25 to 0.499	14
0.50 to 0.749	0

Miner's Sre = 0.3
Total Trucks = 273

GAGE: OS1
INSIDE GIRDER
BEFORE RETROFIT

STRESS RANGE (ksi)	NUMBER OF TRUCKS
-0.50 to -0.251	5
-0.25 to -0.001	63
0.00 to 0.249	456
0.25 to 0.499	26
0.50 to 0.749	0

Miner's Sre = 0.1
Total Trucks = 550

GAGE: OS1
INSIDE GIRDER
AFTER RETROFIT

STRESS RANGE (ksi)	NUMBER OF TRUCKS
-0.50 to -0.251	0
-0.25 to -0.001	0
0.00 to 0.249	129
0.25 to 0.499	133
0.50 to 0.749	11

Miner's Sre = 0.3
Total Trucks = 273

GAGE: OS2
INSIDE GIRDER
BEFORE RETROFIT

STRESS RANGE (ksi)	NUMBER OF TRUCKS
0.00 to -0.249	0
-0.25 to -0.499	4
-0.50 to -0.749	3
-0.75 to -0.999	6

Miner's Sre = N/A
Total Trucks = 13

GAGE: IN2
INSIDE GIRDER
BEFORE RETROFIT

STRESS RANGE (ksi)	NUMBER OF TRUCKS
0.00 to 0.249	194
0.25 to 0.499	291
0.50 to 0.749	61
0.75 to 0.999	5
1.00 to 1.249	2

Miner's Sre = 0.4
Total Trucks = 553

EXTRAPOLATED TO:
END OF THE INSIDE
CONNECTION PLATE WELD
INSIDE GIRDER
BEFORE RETROFIT

STRESS RANGE (ksi)	NUMBER OF TRUCKS
0.00 to 0.249	78
0.25 to 0.499	143
0.50 to 0.749	34
0.75 to 0.999	1

Miner's Sre = 0.4
Total Trucks = 256

EXTRAPOLATED TO:
END OF THE INSIDE
CONNECTION PLATE WELD
INSIDE GIRDER
AFTER RETROFIT

STRESS RANGE (ksi)	NUMBER OF TRUCKS
0.00 to 0.249	12
0.25 to 0.499	12
0.50 to 0.749	2
0.75 to 0.999	0

Miner's Sre = N/A
Total Trucks = 26

EXTRAPOLATED TO:
OUTSIDE WEB-TO-FLANGE
WELD TOE
INSIDE GIRDER
BEFORE RETROFIT

STRESS RANGE (ksi)	NUMBER OF TRUCKS
0.00 to 0.249	1
0.25 to 0.499	4
0.50 to 0.749	6
0.75 to 0.999	2

Miner's Sre = N/A
Total Trucks = 13

EXTRAPOLATED TO:
LOCATION OF THE
INSIDE CONNECTION PLATE
WELD ON OUTSIDE WEB
INSIDE GIRDER
BEFORE RETROFIT

STRESS RANGE (ksi)			NUMBER OF TRUCKS
0.00	to	-0.249	0
-0.25	to	-0.499	49
-0.50	to	-0.749	74
-0.75	to	-0.999	71
-1.00	to	-1.249	45
-1.25	to	-1.499	9
-1.50	to	-1.749	6
-1.75	to	-1.999	1
-2.00	to	-2.249	1

Miner's Sre = -0.9
Total Trucks = 256

EXTRAPOLATED TO:
LOCATION OF THE
INSIDE CONNECTION PLATE
WELD ON OUTSIDE WEB
INSIDE GIRDER
AFTER RETROFIT

STRESS RANGE (ksi)			NUMBER OF TRUCKS
0.00	to	-0.249	26
-0.25	to	-0.499	0
-0.50	to	-0.749	0
-0.75	to	-0.999	0
-1.00	to	-1.249	0
-1.25	to	-1.499	0
-1.50	to	-1.749	0
-1.75	to	-1.999	0
-2.00	to	-2.249	0

Miner's Sre = N/A
Total Trucks = 26

LVDT
INSIDE GIRDER
BEFORE RETROFIT

DISPLACEMENT (in.)			NUMBER OF TRUCKS
0.0000	to	0.00019	0
0.0002	to	0.00039	4
0.0004	to	0.00059	10
0.0006	to	0.00079	5
0.0008	to	0.00099	6
0.0010	to	0.00119	6
0.0012	to	0.00139	0

Average = 0.0007
Std. Dev. = 0.0003
Total Trucks = 31

LVDT
INSIDE GIRDER
AFTER RETROFIT

DISPLACEMENT (in.)			NUMBER OF TRUCKS
0.0000	to	0.00019	7
0.0002	to	0.00039	108
0.0004	to	0.00059	63
0.0006	to	0.00079	80
0.0008	to	0.00099	13
0.0010	to	0.00119	2
0.0012	to	0.00139	0

Average = 0.0005
Std. Dev. = 0.0002
Total Trucks = 273

APPENDIX C

S5-2 TABULATED RANDOM TRUCK HISTOGRAM DATA

GAGE: IS1
OUTSIDE GIRDER
FLOORBEAM ONE

STRESS RANGE (ksi)	NUMBER OF TRUCKS
0.00 to -0.249	8
-0.25 to -0.499	175
-0.50 to -0.749	105
-0.75 to -0.999	6
-1.00 to -1.249	1

Miner's Sre = 0.5
Total Trucks = 295

GAGE: IS2
OUTSIDE GIRDER
FLOORBEAM ONE

STRESS RANGE (ksi)	NUMBER OF TRUCKS
0.00 to 0.249	156
0.25 to 0.499	135
0.50 to 0.749	3
0.75 to 0.999	1
1.00 to 1.249	0

Miner's Sre = 0.3
Total Trucks = 295

GAGE: OS1
OUTSIDE GIRDER
FLOORBEAM TWO

STRESS RANGE (ksi)	NUMBER OF TRUCKS
0.00 to 0.249	0
0.25 to 0.499	0
0.50 to 0.749	0
0.75 to 0.999	0
1.00 to 1.249	0
1.25 to 1.499	0
1.50 to 1.749	0
1.75 to 1.999	0
2.00 to 2.249	0
2.25 to 2.499	0
2.50 to 2.749	5
2.75 to 2.999	12
3.00 to 3.249	19
3.25 to 3.499	27
3.50 to 3.749	22
3.75 to 3.999	12
4.00 to 4.249	24
4.25 to 4.499	15
4.50 to 4.749	17
4.75 to 4.999	16
5.00 to 5.249	6
5.25 to 5.499	6
5.50 to 5.749	14
5.75 to 5.999	13
6.00 to 6.249	12
6.25 to 6.499	19
6.50 to 6.749	13
6.75 to 6.999	13
7.00 to 7.249	6
7.25 to 7.499	4
7.50 to 7.749	7
7.75 to 7.999	3
8.00 to 8.249	4
8.25 to 8.499	2
8.50 to 8.749	0
8.75 to 8.999	0
9.00 to 9.249	1
9.25 to 9.499	2
9.50 to 9.749	1

Miner's Sre = 5.5
Total Trucks = 295

GAGE: OS2
OUTSIDE GIRDER
FLOORBEAM TWO

STRESS RANGE (ksi)	NUMBER OF TRUCKS
0.00 to 0.249	0
0.25 to 0.499	0
0.50 to 0.749	15
0.75 to 0.999	87
1.00 to 1.249	56
1.25 to 1.499	42
1.50 to 1.749	53
1.75 to 1.999	26
2.00 to 2.249	12
2.25 to 2.499	2
2.50 to 2.749	1
2.75 to 2.999	1

Miner's Sre = 1.4
Total Trucks = 295

GAGE: IS1
OUTSIDE GIRDER
FLOORBEAM THREE

STRESS RANGE (ksi)	NUMBER OF TRUCKS
0.00 to -0.249	5
-0.25 to -0.499	16
-0.50 to -0.749	3
-0.75 to -0.999	1

Miner's Sre = N/A
Total Trucks = 25

GAGE: IS2
OUTSIDE GIRDER
FLOORBEAM THREE

STRESS RANGE (ksi)	NUMBER OF TRUCKS
0.00 to -0.249	0
-0.25 to -0.499	8
-0.50 to -0.749	6
-0.75 to -0.999	7
-1.00 to -1.249	3
-1.25 to -1.499	1

Miner's Sre = N/A
Total Trucks = 25

EXTRAPOLATED TO:
END OF THE INSIDE
CONNECTION PLATE WELD
OUTSIDE GIRDER
FLOORBEAM ONE

STRESS RANGE (ksi)	NUMBER OF TRUCKS
0.00 to -0.249	79
-0.25 to -0.499	175
-0.50 to -0.749	40
-0.75 to -0.999	1

Miner's Sre = -0.4
Total Trucks = 295

EXTRAPOLATED TO:
INSIDE WEB-TO-FLANGE
WELD TOE
OUTSIDE GIRDER
FLOORBEAM ONE

STRESS RANGE (ksi)	NUMBER OF TRUCKS
0.00 to -0.249	0
-0.25 to -0.499	19
-0.50 to -0.749	108
-0.75 to -0.999	62
-1.00 to -1.249	76
-1.25 to -1.499	26
-1.50 to -1.749	2
-1.75 to -1.999	1
-2.00 to -2.249	1

Miner's Sre = -1.0
Total Trucks = 295

EXTRAPOLATED TO:
OUTSIDE WEB-TO-FLANGE
WEL TOE
OUTSIDE GIRDER
FLOORBEAM TWO

STRESS RANGE (ksi)			NUMBER OF TRUCKS
0.00	to	0.249	0
0.25	to	0.499	0
0.50	to	0.749	0
0.75	to	0.999	0
1.00	to	1.249	0
1.25	to	1.499	0
1.50	to	1.749	0
1.75	to	1.999	0
2.00	to	2.249	0
2.25	to	2.499	0
2.50	to	2.749	0
2.75	to	2.999	0
3.00	to	3.249	1
3.25	to	3.499	4
3.50	to	3.749	12
3.75	to	3.999	13
4.00	to	4.249	25
4.25	to	4.499	15
4.50	to	4.749	17
4.75	to	4.999	11
5.00	to	5.249	15
5.25	to	5.499	18
5.50	to	5.749	13
5.75	to	5.999	15
6.00	to	6.249	10
6.25	to	6.499	5
6.50	to	6.749	5
6.75	to	6.999	8
7.00	to	7.249	12
7.25	to	7.499	10
7.50	to	7.749	10
7.75	to	7.999	13
8.00	to	8.249	12
8.25	to	8.499	10
8.50	to	8.749	11
8.75	to	8.999	5
9.00	to	9.249	5
9.25	to	9.499	2
9.50	to	9.749	5
9.75	to	9.999	3
10.00	to	10.249	3
10.25	to	10.499	2
10.50	to	10.749	1
10.75	to	10.999	0
11.00	to	11.249	2
11.25	to	11.499	0
11.50	to	11.749	1
11.75	to	11.999	1

Miner's Sre = 6.8
Total Trucks = 295

EXTRAPOLATED TO:
LOCATION OF THE
INSIDE CONNECTION PLATE
WELD ON OUTSIDE WEB
OUTSIDE GIRDER
FLOORBEAM TWO

STRESS RANGE (ksi)			NUMBER OF TRUCKS
0.00	to	0.249	0
0.25	to	0.499	0
0.50	to	0.749	0
0.75	to	0.999	2
1.00	to	1.249	36
1.25	to	1.499	65
1.50	to	1.749	46
1.75	to	1.999	26
2.00	to	2.249	25
2.25	to	2.499	40
2.50	to	2.749	32
2.75	to	2.999	11
3.00	to	3.249	7
3.25	to	3.499	2
3.50	to	3.749	1
3.75	to	3.999	1
4.00	to	4.249	0
4.25	to	4.499	0
4.50	to	4.749	1

Miner's Sre = 2.1
Total Trucks = 295

EXTRAPOLATED TO:
OUTSIDE WEB-TO-FLANGE
WELD TOE
OUTSIDE GIRDER
FLOORBEAM THREE

STRESS RANGE (ksi)	NUMBER OF TRUCKS
0.00 to -0.249	13
-0.25 to -0.499	11
-0.50 to -0.749	1

Miner's Sre = N/A
Total Trucks = 25

EXTRAPOLATED TO:
LOCATION OF THE
INSIDE CONNECTION PLATE
WELD ON OUTSIDE WEB
OUTSIDE GIRDER
FLOORBEAM THREE

STRESS RANGE (ksi)	NUMBER OF TRUCKS
0.00 to -0.249	0
-0.25 to -0.499	6
-0.50 to -0.749	7
-0.75 to -0.999	3
-1.00 to -1.249	8
-1.25 to -1.499	0
-1.50 to -1.749	1

Miner's Sre = N/A
Total Trucks = 25

LVDT
INSIDE GIRDER
FLOORBEAM ONE

DISPLACEMENT (in.)	NUMBER OF TRUCKS
0.0000 to 0.00019	12
0.0002 to 0.00039	130
0.0004 to 0.00059	110
0.0006 to 0.00079	40
0.0008 to 0.00099	3
0.0010 to 0.00119	0
0.0012 to 0.00139	0
0.0014 to 0.00159	0

Average = 0.0004
Std. Dev. = 0.0002
Total Trucks = 295

LVDT
INSIDE GIRDER
FLOORBEAM TWO

DISPLACEMENT (in.)	NUMBER OF TRUCKS
0.0000 to 0.00019	0
0.0002 to 0.00039	12
0.0004 to 0.00059	107
0.0006 to 0.00079	70
0.0008 to 0.00099	67
0.0010 to 0.00119	29
0.0012 to 0.00139	8
0.0014 to 0.00159	2

Average = 0.0007
Std. Dev. = 0.0002
Total Trucks = 295

LVDT
OUTSIDE GIRDER
FLOORBEAM THREE

DISPLACEMENT (in.)	NUMBER OF TRUCKS
0.0000 to 0.00019	286
0.0002 to 0.00039	9

Average = 0.0001
Std. Dev. = 0.00003
Total Trucks = 295

APPENDIX D

S7-12 TABULATED RANDOM TRUCK HISTOGRAM DATA

GAGE: IS1
INSIDE GIRDER
FLOORBEAM ONE

STRESS RANGE (ksi)	NUMBER OF TRUCKS
0.00 to -0.249	0
-0.25 to -0.499	39
-0.50 to -0.749	94
-0.75 to -0.999	70
-1.00 to -1.249	66
-1.25 to -1.499	14
-1.50 to -1.749	4
-1.75 to -1.999	3
-2.00 to -2.249	1
-2.25 to -2.499	1

Miner's Sre = -1.0
Total Trucks = 292

GAGE: IS2
INSIDE GIRDER
FLOORBEAM ONE

STRESS RANGE (ksi)	NUMBER OF TRUCKS
0.00 to 0.249	64
0.25 to 0.499	178
0.50 to 0.749	45
0.75 to 0.999	5

Miner's Sre = 0.4
Total Trucks = 292

GAGE: OS1
INSIDE GIRDER
FLOORBEAM TWO

STRESS RANGE (ksi)	NUMBER OF TRUCKS
0.00 to 0.249	0
0.25 to 0.499	0
0.50 to 0.749	0
0.75 to 0.999	0
1.00 to 1.249	0
1.25 to 1.499	0
1.50 to 1.749	0
1.75 to 1.999	0
2.00 to 2.249	0
2.25 to 2.499	0
2.50 to 2.749	0
2.75 to 2.999	0
3.00 to 3.249	0
3.25 to 3.499	1
3.50 to 3.749	2
3.75 to 3.999	2
4.00 to 4.249	2
4.25 to 4.499	19
4.50 to 4.749	25
4.75 to 4.999	15
5.00 to 5.249	19
5.25 to 5.499	9
5.50 to 5.749	12
5.75 to 5.999	7
6.00 to 6.249	9
6.25 to 6.499	6
6.50 to 6.749	4
6.75 to 6.999	7
7.00 to 7.249	5
7.25 to 7.499	6
7.50 to 7.749	10
7.75 to 7.999	7

GAGE: OS2
INSIDE GIRDER
FLOORBEAM TWO

STRESS RANGE (ksi)	NUMBER OF TRUCKS
0.00 to -0.249	0
-0.25 to -0.499	0
-0.50 to -0.749	0
-0.75 to -0.999	0
-1.00 to -1.249	0
-1.25 to -1.499	0
-1.50 to -1.749	2
-1.75 to -1.999	5
-2.00 to -2.249	18
-2.25 to -2.499	43
-2.50 to -2.749	25
-2.75 to -2.999	20
-3.00 to -3.249	15
-3.25 to -3.499	13
-3.50 to -3.749	14
-3.75 to -3.999	19
-4.00 to -4.249	17
-4.25 to -4.499	23
-4.50 to -4.749	27
-4.75 to -4.999	22
-5.00 to -5.249	15
-5.25 to -5.499	3
-5.50 to -5.749	3
-5.75 to -5.999	5
-6.00 to -6.249	1
-6.25 to -6.499	1
-6.50 to -6.749	0
-6.75 to -6.999	1

Miner's Sre = -3.9
Total Trucks = 292

8.00	to	8.249	10
8.25	to	8.499	8
8.50	to	8.749	14
8.75	to	8.999	9
9.00	to	9.249	11
9.25	to	9.499	9
9.50	to	9.749	15
9.75	to	9.999	10
10.00	to	10.249	7
10.25	to	10.499	6
10.50	to	10.749	10
10.75	to	10.999	3
11.00	to	11.249	2
11.25	to	11.499	1
11.50	to	11.749	2
11.75	to	11.999	2
12.00	to	12.249	4
12.25	to	12.499	0
12.50	to	12.749	0
12.75	to	12.999	1
13.00	to	13.249	0
13.25	to	13.499	0
13.50	to	13.749	0
13.75	to	13.999	0
14.00	to	14.249	0
14.25	to	14.499	0
14.50	to	14.749	0
14.75	to	14.999	0
15.00	to	15.249	0
15.25	to	15.499	0
15.50	to	15.749	1

Miner's Sre = 8.0
Total Trucks = 292

GAGE: IS1
INSIDE GIRDER
FLOORBEAM THREE

STRESS RANGE (ksi)			NUMBER OF TRUCKS
0.00	to	-0.249	0
-0.25	to	-0.499	0
-0.50	to	-0.749	8
-0.75	to	-0.999	72
-1.00	to	-1.249	48
-1.25	to	-1.499	40
-1.50	to	-1.749	40
-1.75	to	-1.999	44
-2.00	to	-2.249	27
-2.25	to	-2.499	8
-2.50	to	-2.749	3
-2.75	to	-2.999	1
-3.00	to	-3.249	0
-3.25	to	-3.499	1

Miner's Sre = 1.6
Total Trucks = 292

GAGE: IS2
INSIDE GIRDER
FLOORBEAM THREE

STRESS RANGE (ksi)			NUMBER OF TRUCKS
0.00	to	-0.249	0
-0.25	to	-0.499	76
-0.50	to	-0.749	73
-0.75	to	-0.999	66
-1.00	to	-1.249	63
-1.25	to	-1.499	12
-1.50	to	-1.749	1
-1.75	to	-1.999	1

Miner's Sre = -0.9
Total Trucks = 292

EXTRAPOLATED TO:
END OF THE INSIDE
CONNECTION PLATE WELD
INSIDE GIRDER
FLOORBEAM ONE

STRESS RANGE (ksi)		NUMBER OF TRUCKS
0.00 to	0.249	0
0.25 to	0.499	17
0.50 to	0.749	99
0.75 to	0.999	64
1.00 to	1.249	68
1.25 to	1.499	36
1.50 to	1.749	5
1.75 to	1.999	2
2.00 to	2.249	1

Miner's Sre = 1.0
Total Trucks = 292

EXTRAPOLATED TO:
INSIDE WEB-TO-FLANGE
WELD TOE
INSIDE GIRDER
FLOORBEAM ONE

STRESS RANGE (ksi)		NUMBER OF TRUCKS
0.00 to	-0.249	0
-0.25 to	-0.499	0
-0.50 to	-0.749	6
-0.75 to	-0.999	57
-1.00 to	-1.249	53
-1.25 to	-1.499	36
-1.50 to	-1.749	38
-1.75 to	-1.999	45
-2.00 to	-2.249	31
-2.25 to	-2.499	13
-2.50 to	-2.749	5
-2.75 to	-2.999	3
-3.00 to	-3.249	3
-3.25 to	-3.499	0
-3.50 to	-3.749	0
-3.75 to	-3.999	1
-4.00 to	-4.249	0
-4.25 to	-4.499	1

Miner's Sre = -1.7
Total Trucks = 292

EXTRAPOLATED TO:
OUTSIDE WEB-TO-FLANGE
WELD TOE
INSIDE GIRDER
FLOORBEAM TWO

STRESS RANGE (ksi)		NUMBER OF TRUCKS
4.00 to	4.249	0
4.25 to	4.499	0
4.50 to	4.749	1
4.75 to	4.999	0
5.00 to	5.249	0
5.25 to	5.499	1
5.50 to	5.749	1
5.75 to	5.999	2
6.00 to	6.249	2
6.25 to	6.499	6
6.50 to	6.749	11
6.75 to	6.999	21
7.00 to	7.249	12
7.25 to	7.499	9
7.50 to	7.749	13
7.75 to	7.999	10
8.00 to	8.249	5
8.25 to	8.499	5
8.50 to	8.749	8

EXTRAPOLATED TO:
LOCATION OF THE
INSIDE CONNECTION PLATE
WELD ON OUTSIDE WEB
INSIDE GIRDER
FLOORBEAM TWO

STRESS RANGE (ksi)		NUMBER OF TRUCKS
4.00 to	4.249	0
4.25 to	4.499	0
4.50 to	4.749	0
4.75 to	4.999	0
5.00 to	5.249	0
5.25 to	5.499	1
5.50 to	5.749	0
5.75 to	5.999	1
6.00 to	6.249	0
6.25 to	6.499	1
6.50 to	6.749	1
6.75 to	6.999	2
7.00 to	7.249	1
7.25 to	7.499	5
7.50 to	7.749	9
7.75 to	7.999	9
8.00 to	8.249	14
8.25 to	8.499	12
8.50 to	8.749	17

8.75	to	8.999	6	8.75	to	8.999	5
9.00	to	9.249	7	9.00	to	9.249	9
9.25	to	9.499	4	9.25	to	9.499	5
9.50	to	9.749	3	9.50	to	9.749	2
9.75	to	9.999	4	9.75	to	9.999	8
10.00	to	10.249	2	10.00	to	10.249	7
10.25	to	10.499	6	10.25	to	10.499	6
10.50	to	10.749	3	10.50	to	10.749	5
10.75	to	10.999	5	10.75	to	10.999	3
11.00	to	11.249	4	11.00	to	11.249	4
11.25	to	11.499	5	11.25	to	11.499	5
11.50	to	11.749	6	11.50	to	11.749	2
11.75	to	11.999	6	11.75	to	11.999	4
12.00	to	12.249	4	12.00	to	12.249	7
12.25	to	12.499	6	12.25	to	12.499	2
12.50	to	12.749	6	12.50	to	12.749	5
12.75	to	12.999	11	12.75	to	12.999	6
13.00	to	13.249	11	13.00	to	13.249	2
13.25	to	13.499	3	13.25	to	13.499	6
13.50	to	13.749	6	13.50	to	13.749	2
13.75	to	13.999	10	13.75	to	13.999	7
14.00	to	14.249	4	14.00	to	14.249	6
14.25	to	14.499	10	14.25	to	14.499	7
14.50	to	14.749	8	14.50	to	14.749	6
14.75	to	14.999	6	14.75	to	14.999	5
15.00	to	15.249	4	15.00	to	15.249	10
15.25	to	15.499	5	15.25	to	15.499	14
15.50	to	15.749	7	15.50	to	15.749	3
15.75	to	15.999	6	15.75	to	15.999	7
16.00	to	16.249	2	16.00	to	16.249	10
16.25	to	16.499	3	16.25	to	16.499	6
16.50	to	16.749	1	16.50	to	16.749	9
16.75	to	16.999	0	16.75	to	16.999	7
17.00	to	17.249	1	17.00	to	17.249	3
17.25	to	17.499	0	17.25	to	17.499	6
17.50	to	17.749	2	17.50	to	17.749	4
17.75	to	17.999	4	17.75	to	17.999	4
18.00	to	18.249	1	18.00	to	18.249	6
18.25	to	18.499	1	18.25	to	18.499	5
18.50	to	18.749	0	18.50	to	18.749	2
18.75	to	18.999	0	18.75	to	18.999	1
19.00	to	19.249	0	19.00	to	19.249	1
19.25	to	19.499	1	19.25	to	19.499	0
19.50	to	19.749	0	19.50	to	19.749	0
19.75	to	19.999	0	19.75	to	19.999	0
20.00	to	20.249	0	20.00	to	20.249	2
20.25	to	20.499	0	20.25	to	20.499	1
20.50	to	20.749	0	20.50	to	20.749	3
20.75	to	20.999	0	20.75	to	20.999	0
21.00	to	21.249	0	21.00	to	21.249	1
21.25	to	21.499	0	21.25	to	21.499	1
21.50	to	21.749	0	21.50	to	21.749	1
21.75	to	21.999	0	21.75	to	21.999	0
22.00	to	22.249	0	22.00	to	22.249	0
22.25	to	22.499	0	29.25	to	29.499	0
22.50	to	22.749	0	22.50	to	22.749	0
22.75	to	22.999	0	22.75	to	22.999	0
23.00	to	23.249	1	23.00	to	23.249	0
				23.25	to	23.499	1

Miner's Sre = 12.0
Total Trucks = 292

Miner's Sre = -13.8
Total Trucks = 299

EXTRAPOLATED TO:
OUTSIDE WEB-TO-FLANGE
WELD TOE
INSIDE GIRDER
FLOORBEAM THREE

STRESS RANGE (ksi)	NUMBER OF TRUCKS
0.00 to -0.249	0
-0.25 to -0.499	0
-0.50 to -0.749	3
-0.75 to -0.999	28
-1.00 to -1.249	69
-1.25 to -1.499	34
-1.50 to -1.749	40
-1.75 to -1.999	33
-2.00 to -2.249	41
-2.25 to -2.499	29
-2.50 to -2.749	6
-2.75 to -2.999	5
-3.00 to -3.249	3
-3.25 to -3.499	0
-3.50 to -3.749	0
-3.75 to -3.999	1

Miner's Sre = 1.8
Total Trucks = 292

EXTRAPOLATED TO:
LOCATION OF THE
INSIDE CONNECTION PLATE
WELD ON OUTSIDE WEB
INSIDE GIRDER
FLOORBEAM THREE

STRESS RANGE (ksi)	NUMBER OF TRUCKS
-1.00 to -0.751	6
-0.75 to -0.501	21
-0.50 to -0.251	89
-0.25 to -0.001	146
0.00 to -0.249	29
0.25 to -0.499	1
0.50 to -0.749	0
0.75 to -0.999	0

Miner's Sre = -0.4
Total Trucks = 292

LVDT
INSIDE GIRDER
FLOORBEAM ONE

DISPLACEMENT (in.)	NUMBER OF TRUCKS
0.0000 to 0.00019	0
0.0002 to 0.00039	0
0.0004 to 0.00059	0
0.0006 to 0.00079	1
0.0008 to 0.00099	30
0.0010 to 0.00119	50
0.0012 to 0.00139	37
0.0014 to 0.00159	26
0.0016 to 0.00179	25
0.0018 to 0.00199	39
0.0020 to 0.00219	39
0.0022 to 0.00239	28
0.0024 to 0.00259	7
0.0026 to 0.00279	5
0.0028 to 0.00299	2
0.0030 to 0.00319	1
0.0032 to 0.00339	1
0.0034 to 0.00359	0
0.0036 to 0.00379	0
0.0038 to 0.00399	1

Average = 0.0016
Std. Dev. = 0.0005
Total Trucks = 292

LVDT
INSIDE GIRDER
FLOORBEAM TWO

DISPLACEMENT (in.)	NUMBER OF TRUCKS
0.0000 to 0.00019	0
0.0002 to 0.00039	0
0.0004 to 0.00059	0
0.0006 to 0.00079	12
0.0008 to 0.00099	73
0.0010 to 0.00119	38
0.0012 to 0.00139	27
0.0014 to 0.00159	41
0.0016 to 0.00179	53
0.0018 to 0.00199	28
0.0020 to 0.00219	11
0.0022 to 0.00239	7
0.0024 to 0.00259	0
0.0026 to 0.00279	1
0.0028 to 0.00299	1

Average = 0.0013
Std. Dev. = 0.0004
Total Trucks = 292

LVDT
INSIDE GIRDER
FLOORBEAM THREE

DISPLACEMENT (in.)	NUMBER OF TRUCKS
0.0000 to -0.00019	0
-0.0002 to -0.00039	116
-0.0004 to -0.00059	152
-0.0006 to -0.00079	20
-0.0008 to -0.00099	4

Average = -0.0004
Std. Dev. = -0.0001
Total Trucks = 295